Summer 2014

Implementation of Analytical Fatigue Models Into Opensim to Predict the Effects of Fatigue on Anterior Cruciate Ligament Loading

Michael A. Samann
Old Dominion University

IMPLEMENTATION OF ANALYTICAL FATIGUE MODELS INTO OPENSIM TO PREDICT THE EFFECTS OF FATIGUE ON ANTERIOR CRUCIATE LIGAMENT LOADING

by

Michael A. Samaan
B.S. May 2008, Rutgers University
M.S. December 2009, University of Texas at San Antonio

A Dissertation Submitted to the Faculty of
Old Dominion University in Partial Fulfillment of the
Requirements for the Degree of

DOCTOR OF PHILOSOPHY

MECHANICAL AND AEROSPACE ENGINEERING

OLD DOMINION UNIVERSITY
August 2014

Approved by:

Stacie I. Ringleb (Advisor)

Sebastian Y. Bawab (Co-Advisor)

Joshua T. Weinhandl (Member)

Gene Hou (Member)

ABSTRACT

IMPLEMENTATION OF ANALYTICAL FATIGUE MODELS INTO OPENSIM TO PREDICT THE EFFECTS OF FATIGUE ON ANTERIOR CRUCIATE LIGAMENT LOADING

Michael A. Samaan
Old Dominion University, 2014
Director: Stacie I. Ringleb
Co-Director: Sebastian Y. Bawab

The anterior cruciate ligament (ACL) provides stability to the knee joint while performing activities such as a side step cut. Neuromuscular fatigue, a reduction in muscle force producing capabilities, alters lower extremity mechanics while performing a side step cut and may increase the risk of ACL injury, particularly in females. Musculoskeletal modeling allows for the measurement of muscle forces, which are difficult to measure *in-vivo*. Therefore, musculoskeletal modeling, may improve our understanding of the effects of neuromuscular fatigue on muscle force production and loading of the ACL. Therefore, the purpose of this study was to develop a musculoskeletal model which incorporated two analytical fatigue models by Tang *et al* (2005) and Xia *et al* (2008). These fatigue models were used to determine the effects of neuromuscular fatigue on muscle force production and ACL loading at various levels of fatigue (i.e. 10%, 25%, 50%, 75% and 90%) and were validated by comparing these results with experimental data. Six recreationally active females performed five anticipated side step cuts both before and after an isolated hamstrings fatigue protocol using the right lower extremity. Root mean square (RMS) differences were calculated between both fatigue models and the experimental hamstrings muscle force 1.91 $N \cdot kg^{-1}$ and 1.88 $N \cdot kg^{-1}$, for RMS_{Tang} and RMS_{Xia}, respectively. Despite similar RMS differences,

the Xia *et al* (2008) model was selected for analysis of fatigue as this model utilized general input parameters. The total quadriceps and hamstrings muscle forces demonstrated significant decreases ($p<0.05$) as an effect of fatigue yet the gastrocnemius muscle forces increased ($p<0.05$). Knee joint extension moment demonstrated significant increases ($p<0.05$) across all fatigue levels. Despite a reduction in hamstrings muscle force producing capabilities, peak ACL loading did not exhibit a significant increase ($p>0.05$) due to fatigue. The limited number of participants in this study suggested an underpowered study and may help explain the lack of significance in various dependent variables including peak ACL loading. Using the model developed in this study can aid researchers in understanding the effects of fatigue on risk of ACL injury in order to develop better training programs in order to reduce the risk of injury.

This dissertation is dedicated to my fiancée Erica Helms and my parents Aida and Samaan Samaan. Thank you all for your support, love and guidance.

ACKNOWLEDGMENTS

I would like to acknowledge my dissertation committee for their support and efforts in my research. A large amount of appreciation is to be given to Dr. Stacie Ringleb, my mentor and advisor, as she has provided me with the guidance, support and knowledge that I needed to complete this work. Dr. Sebastian Bawab is more than just an advisor, he also treated me like a son. He would acknowledge my successes but would also make sure that I knew when I made a mistake, so that I can better myself as a researcher and most importantly as a person. I would like to extend my gratitude for the amount of time, guidance and knowledge that Dr. Joshua Weinhandl provided me while completing my dissertation work. I would also like to thank Dr. Gene Hou for his input and vast knowledge, while I completed my research. Another vital resource to this work is Dr. Steven Hans. I would like to thank Dr. Hans for the time, effort and knowledge he provided to this work.

A large amount of gratitude has to go to my parents, Aida and Samaan Samaan. I truly do appreciate the support, love and guidance that you both have provided me throughout my entire educational career. Erica Helms, my fiancée, I am truly blessed to have found you as you have given me the strength and motivation to complete this dissertation.

TABLE OF CONTENTS

Page

Page

LIST OF TABLES

Page

LIST OF FIGURES

Page

Page

Page

CHAPTER 1

INTRODUCTION

Injury to the anterior cruciate ligament (ACL), one of the 4 main ligaments of the human knee joint, can prevent participation in sporting activities [1] and increase risk of developing osteoarthritis [1, 2]. Neuromuscular fatigue, a reduction in muscle force producing capabilities [3-6], is one of many factors that contribute to an increased risk of non-contact ACL injury [7-10] particularly in females [7, 10, 11]. Neuromuscular fatigue alters lower extremity mechanics and increases ACL loading through an increase in anterior tibial translation [7, 8], anterior shear [7, 8] and rotational forces [12]. Computational modeling allows for the measurement of muscle forces, which are difficult to measure *in-vivo*, thereby aiding researchers to understand the effects of neuromuscular fatigue on muscle force production. Analytical models were developed to improve understanding of the effect of fatigue [6, 13-17] yet these models were not used to study dynamic, athletic maneuvers such as a side step cut. Implementation of an analytical fatigue model into a dynamic simulation would aid researchers to better understand the effects of fatigue on risk of ACL injury.

1.1 Anterior Cruciate Ligament Injury

The human knee joint (Figure 1-1) is the largest joint in the human body consisting of the femur, tibia, fibula and patella [18, 19]. The ACL is one of the 4 main ligaments of the human knee joint. The ACL provides joint stability by limiting tibial translation, rotational translation and mediolateral movement [2, 12, 20]. ACL injuries can cause extended disability and place athletes at a higher risk of developing knee

osteoarthritis as well as an increase in knee pain and instability [21, 22]. Females are 2-5 times more likely to rupture their ACL compared to males [21, 23] with 80% of these injuries occurring in a non-contact manner [24]. The cost of treatment and rehabilitation associated with female ACL injury totals to an approximate $646 million annually [25]. ACL injury causes a change in kinematic and loading patterns in the knee leading to an initial degeneration of cartilage and eventually the onset of osteoarthritis [2].

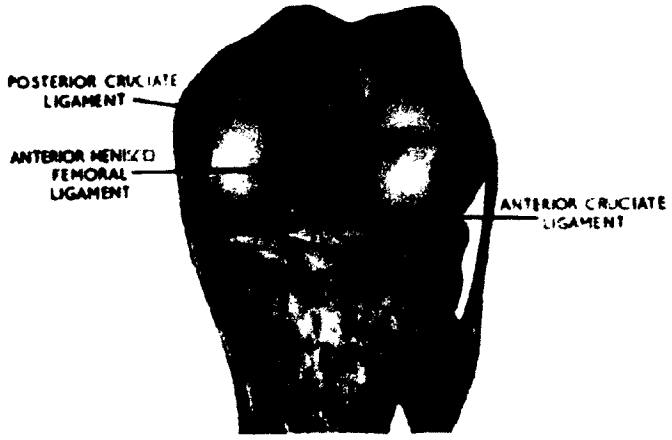

Figure 1-1: Anterior view of human knee [26]

There are anatomical, hormonal parameters and biomechanical factors that may result in an increase in the ACL injury rate in women [27]. Anatomical parameters such as the Q angle [21] and the tibial plateau slope [28, 29] as well as hormonal parameters [25] may affect injury rates. However, the contribution of these parameters on risk of injury is unclear [25]. Females, compared to males, tended to land with a more extended and internally rotated lower extremity during an unanticipated side step cut [30]. It is unclear whether or not anatomical and hormonal parameters are modifiable [25]. However, biomechanical factors (i.e. lower extremity mechanics) are modifiable and have been studied considering the effects of anticipation and other types of neuromuscular perturbations [31-33]. Determining the effects of various perturbations

(i.e. anticipation, fatigue, etc.) on the lower extremity may be a better method of understanding risk of ACL injury in female athletes.

Females tend towards different muscle activation patterns in comparison to males while performing a side step cut but the results are not similar between studies [30, 34, 35]. There are discrepancies between studies when it comes to quadriceps activity during a side step cut yet the results seem to be similar between studies when hamstrings activity is considered. Females exhibited a greater amount of quadriceps activation throughout early deceleration and stance compared to males [30, 35] yet another study [34] found no differences in quadriceps activity between genders during a pre-activity phase (50ms prior to initial contact). Males demonstrated greater activity in the lateral hamstrings compared to the medial hamstrings while females do not exhibit this medial hamstrings imbalance [30, 34, 35].

One common shortcoming of current biomechanical studies is that these studies are unable to account for the multi-factorial nature of the ACL injury mechanism [36]. This may be due to the limitations and differences in the methods used to study ACL injury(i.e. equipment, software, etc.) but also due to the difficulty associated with measuring particular physiological (i.e. muscle forces, ACL loading, etc.) and anatomical parameters *in-vivo* [36]. Musculoskeletal modeling methods can overcome the difficulties in studying knee joint injury risk. Musculoskeletal modeling has been used to study injury risk factors and estimate ACL forces in side step cutting [32, 37], drop landings [38] and stop jumps [39-41].

1.2 Neuromuscular Fatigue

Neuromuscular fatigue, (referred to as fatigue from this point on), is defined as a decrease or lack in the ability to generate maximal muscle force or power occurring after the onset of sustained physical activity [42-45] and limits maximal voluntary muscle force production [17]. Fatigue is an extrinsic factor that affects the musculoskeletal and neurologic systems [7]. There is no single mechanism that can solely account for fatigue [46, 47] as the underlying physiological mechanisms in the decline of muscle force are complex, multifactorial and task dependent [4, 5, 13, 45, 47, 48] thereby making it difficult to represent fatigue analytically [6]. Fatigue is dependent on multiple factors which include the type and intensity of exercise, the muscle groups involved, neural strategy, subject motivation and the physical environment in which the task is performed [5, 47]. Varying these fatigue dependent factors will stress different components (central and peripheral nervous systems) of the neuromuscular system and therefore will influence the amount of muscle fatigue within the system. The central nervous system (CNS) provides the central drive to maintain muscle activation of the nerve-muscle complex within the peripheral nervous system (PNS) which controls the propagation of action potentials. Prolonged stimulation of isolated muscle, under anaerobic conditions, may result in a total loss of mechanical power despite the normal functioning of the contractile elements of the muscle [3]. In other words, if the CNS continuously provides adequate muscle activation yet the propagation of action potentials within the PNS fails, then the force producing capabilities of the muscle fail [46]. It has been shown that fatigue due to high-intensity isometric exercise is associated with both central and peripheral factors [49]. In order to truly understand the effects of fatigue, it would be

ideal to measure fatigue during activity, as fatigue is a continuous rather than a failure-point phenomenon [48].

Alterations in lower extremity kinematics occur following neuromuscular fatigue [7, 9, 10, 33, 50-52]. Fatigue altered lower extremity kinematics in a side step cut [9, 50], drop landings [10, 33, 51, 52] and stop-jump tasks [7, 53]. An epidemiological study supported the notion that fatigue may be a predisposing factor responsible for the increased number of injuries at the end of games or halves in soccer [54]. The effects of fatigue on side step cutting are conflicting [9, 50] and may be due to the varied methods used to induce fatigue [55]. Specifically, sagittal plane alterations at the hip and knee at initial contact after fatigue were observed in one study [50], while fatigue caused an increase in hip, knee and ankle external rotation at initial contact, but had no effect on sagittal or frontal plane kinematics [9] in another. Agility drills, jumps, squats and sprints to induce a short term fatigue protocol [7, 10, 33, 50, 51] while a long term fatigue protocol consisted of sustained periods of activity of high intensity effort [9] in order to replicate a game-play environment and induce a general or functional type of fatigue.

Previous studies [7, 9, 33, 50] have used general fatigue models to determine the effects of fatigue on the lower extremity during dynamic maneuvers. General fatigue models do not allow for the determination of how specific muscle groups may respond to fatigue and the overall contributions of these specific muscles to dynamic lower extremity control [56]. The hamstrings aid in dynamic control of tibial rotation[57] and therefore, isolated hamstrings fatigue may affect an athlete's ability to perform a dynamic maneuver such as a side step cut. Larger variability in tibial rotation was displayed in females compared to males while performing a side step cut, which may increase the risk

of ACL injury [58]. Significant increases in anterior tibial translation were caused by isolated hamstrings fatigue and may be associated with a reduction in muscle force producing capabilities [59]. Despite the numerous amounts of studies performed on the effects of fatigue on lower extremity kinematics, it is still unclear as to how fatigue contributes to noncontact ACL injuries [7].

1.2.1 Motor Unit Activation

Motor units consist of a group of muscle fibers that are innervated by the same motor neuron. The number of muscle fibers controlled by a given motor neuron depends on the function of that specific muscle. If a motor neuron is stimulated, a nerve impulse known as a motor unit action potential (MUAP) is generated. The MUAP is a propagated impulse, meaning that the amplitude of the impulse remains the same as it travels down the axon to the neuromuscular junction. At the neuromuscular junction, the MUAP becomes a muscle action potential (MAP) traveling down through the muscle. Externally, these two actions are indistinguishable. If the MAP exceeds a certain threshold it will result in depolarization of the muscle cell membrane, releasing calcium ions and initiating the development of the cross-bridging and shortening within the muscle sarcomere in an all or nothing type of excitation [60]. This total process is referred to as excitation-contraction coupling. Traditionally, motor units are recruited in a particular order depending on the force that the neuromuscular system is required to produce. Depending on the type of contraction, submaximal or maximal, a particular amount of force to be produced will be determined by the neuromuscular system and will achieved by controlling the amount of motor units that are recruited and the rates at which the motor units discharge action potentials [5, 61]. When fatigue occurs, the

threshold required to trigger an action potential increases and the motor unit's tendency to fire decreases. The motor unit will eventually reach a critical point where it can no longer be activated [17].

Each motor unit consists of a particular fiber type with the same histochemical and biomechanical characteristics and when activated, the fibers contract synchronously and act in the same manner [17, 62]. It was determined that the sequence of recruitment is in the order of threshold for activation and follows the recruitment pattern of: slow twitch fibers (type I), fast fatigue resistant fibers (type IIA) and fast fatigable fibers (type IIB). At the start of a submaximal contraction, type I fibers are recruited first and possibly some type IIA fibers. As physical activity progresses, an additional number of type II fibers are recruited and when the muscle is fatigued, all motor units would have been recruited [63]. Despite the existence of a known motor unit recruitment pattern, it is possible that the recruitment pattern may be modified during a particular movement, in order to match the neural command to the continuously changing mechanical characteristics of muscle [64].

Type I fibers are the most oxidative and contain only slow myosin, whereas the type II fibers are less oxidative and only contain fast myosin [65]. Type I fibers have a long twitch time, slow conduction and are fatigue-resistant. While the type IIB fibers have a short twitch time, high conduction velocity and fatigue rapidly. The type IIA fibers are an intermediate group as far its physiological characteristics are concerned [62].

1.2.2 Hamstrings Muscle Composition

The hamstrings muscle group consists of the semimembranosus, semitendinosus and biceps femoris. The hamstrings are a two joint muscle group, spanning the hip and knee joints. The hamstrings are responsible for the simultaneous flexion of the leg at the knee joint and extension of the thigh at the hip [66]. The biceps femoris is composed of approximately 44.1 – 66.9% type I fibers [67, 68] and 26.8 – 59.2% type II fibers. The semitendinosus contains approximately 54.6 – 60.4% type II fibers while the semimembranosus contains approximately 50.5 – 51% type II fibers [69]. The composition of type II muscle fibers within in the semitendinosus was significantly different between the proximal and distal sites of the muscle [69].

Muscles that require faster action or phasic activity have a higher percent of type II fibers [68]. The amount of force that a muscle can produce is proportional to the fiber type content thereby suggesting the high type II fiber content in the hamstrings is evidence that the hamstrings must be capable of producing large amounts of force [69]. The physiological cross-sectional area (PCSA) of a muscle is directly related to the amount of tension or force a muscle is able to produce [70]. The PCSA of the hamstrings muscle group, consisting of the semitendinosus, semimembranosus and both the long and short heads of the biceps femoris, is approximately 41 cm^2. The PCSA of the hamstrings muscle group is approximately 60% less than that of the quadriceps [70]. The reduced PCSA of the hamstrings, in relation to the quadriceps, means that the hamstrings produce a smaller amount of force than the quadriceps.

1.3 Fatigue Models

Muscle models that incorporate fatigue may help researchers to better understand the effects of fatigue on injury mechanisms and in turn may lead to better injury prevention and training programs [16]. Muscle fatigue models capable of quantifying isometric fatiguing contractions [13, 16] as well as dynamic fatigue [6, 14] were developed, yet an experimentally validated model that can predict force and motion both prior to and during a non-isometric contraction has yet to be developed [15]. The current issue in fatigue modeling involves the difficulty in quantifying the multi-factorial nature of fatigue during a particular exercise or activity [48]. Two of the current fatigue models require numerous physiological inputs (i.e. muscle contraction velocities, metabolite levels, etc.) [13, 71] that need to be determined from other experiments. It is difficult to achieve accuracy in determining these parameters and therefore these models may not provide a satisfactory prediction of force.

An analytical model was developed by Tang *et al* [16] to predict the effect of fatigue on muscle force under arbitrary conditions of activation (α). This model incorporated differential equations into Hill's muscle model [72], a three element model consisting of a contractile element and two non-linear spring elements. The differential equations were used to determine the fatigue, recovery and endurance properties of skeletal muscle. Fatigue, recovery and endurance were all used to determine the fitness function, which quantified the overall effects of fatigue on the muscle over a pre-defined time period. Tang's model was validated numerically using previous experimental data [13]. This fatigue model was also implemented into a finite element model to validate experimental data on a frog gastrocnemius muscle [44]. The proximal end of a frog

gastrocnemius muscle was fixed while a 10g load was applied to the Achilles tendon. A cyclic activation (0.25Hz, 50 duty cycle) was applied to the frog muscle to simulate muscle deformation. Force and strain data were recorded using a force transducer and two digital cameras, respectively in order to quantify the effects of fatigue on muscle stresses and strains. Replicating this experimental setup in a finite element model, the Tang *et al* fatigue model [16, 44] provided a reasonable prediction of the effects of fatigue, when compared to the experimental data, on 3-dimensional stresses and strains in the frog gastrocnemius muscle.

Both the endurance and fatigue parameters are functions of activation. The fatigue function was determined using the fatigue vs. time curve. Curve fitting methods are used to determine the fatigue function from the fatigue vs. time curve. The model also assumed the fatigue trend with respect to time is similar for both an arbitrary submaximal activation and a maximal activation (Figure 1-2). Therefore, the fatigue rate under arbitrary activation can be also assumed to be equal to the fatigue rate under constant activation. The fatigue rate for skeletal muscle is usually dependent on the current fatigue level and the fatigue history [44]. The endurance function proposed by Tang *et al* [16] (equation 1) was determined by fitting a curve to the number of active motor units vs. time data provided by Liu *et al* [17]. The exponent of 2.4, used in the endurance function, is a ratio between the fatigue velocities of the muscle under submaximal and maximal activations [73].

$$\theta(\alpha) = \alpha^{2.4} \qquad (1)$$

where α is the muscle activation. The endurance function was also referred to as a time stretch ratio and must satisfy the following conditions [16]:

$$0 \leq \theta(\alpha) \leq 1, \theta(\alpha = 1) = 1, \theta(\alpha = 0) = 0 \qquad (2)$$

Recovery was also a function of activation and was determined from the recovery vs. time curve. Tang's model assumed that a muscle recovers when there was no activation. The period of recovery allowed the muscle to rest and to recover its ability to maximally shorten. The recovery curve was determined by measuring maximal output force of a muscle in very short intervals from a state of complete fatigue to no fatigue [16, 44].

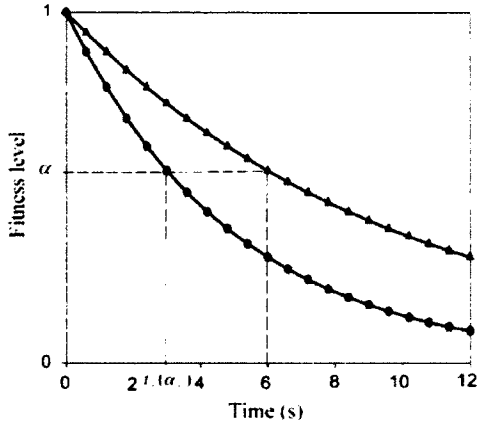

Figure 1-2: Fatigue curves under maximal activation and submaximal activation [16]

Using the values of fatigue and endurance, a fitness function was determined and used to describe the effects of fatigue ($\alpha > 0$) on the muscle over a specified time period. Similarly, the recovery function was used to determine a fitness function that incorporated the effects of muscle recovery ($\alpha = 0$) on overall muscle capabilities. When the fitness level or maximal output force was equal to one the muscle had no fatigue. On the other hand, if the fitness level or maximal output was equal to zero then the muscle was assumed to be completely fatigued. The fitness function was calculated using a finite difference method (equation 3).

$$^{t+\Delta t}fitness = {}^{t}fitness + \theta(^{t+\Delta t}\alpha) \times (^{t+\Delta t}fatigue - {}^{t}fatigue);\ when\ \alpha > 0$$

$$^{t+\Delta t}fitness = {}^{t}fitness + (^{t+\Delta t}recovery - {}^{t}recovery);\ when\ \alpha = 0 \qquad (3)$$

Tang's model was validated *in-vitro* for a frog gastrocnemius muscle [44], where the fatigue and recovery curves were adopted from previously published muscle force vs. time data [45]. Tang's model was versatile in its ability to accurately predict the effects of fatigue on skeletal muscle [44] under an isometric activation pattern. However, both the fitness and recovery functions were pre-determined from experimental data in order to accurately predict the effects of fatigue.

Another analytical model developed by Liu *et al* [17] is capable of predicting the effects of fatigue for both simple and complex tasks at various intensities using a minimal number of pre-determined inputs. The model developed by Liu *et al* [17] used a dynamic framework to understand muscle activation, fatigue and recovery. The model required the determination of fatigue (F) and recovery (R) factors that are used to solve a set of equations in order to describe the behavior of muscles as a group of motor units under voluntary activation [17]. Both F and R are constant values across time for activities that last seconds to several minutes. The values of F and R are combinations of the various fatigue and recovery factors for each of the different muscle fiber types found within a particular muscle [17].

The model developed by Xia *et al* [6], a modified version of the Liu *et al* [17] fatigue model, uses a three-compartment fatigue model which includes activated (M_A), fatigued (M_F) and resting (M_R) motor units (Figure 1-3). The muscle force generated by

the motor unit pool is proportional to the size of the activated motor unit pool. The initial conditions (t = 0) of this model are M_A, M_F and M_R are equal to 0, 0 and 100% respectively [6]. In other words, at time equals 0, there are 0 motor units activated or fatigued and all motor units are at rest. This system assumes a unit-less measure of muscle force in percent of maximum voluntary contraction (%MVC). The activated, fatigued and resting motor units are calculated at finite time intervals (equation 4).

Figure 1-3: Compartmental model representing the dynamic behavior of muscle motor units [6]

$$\frac{dM_A}{dt} = C(t) - F\ x\ M_A$$

$$\frac{dM_F}{dt} = F\ x\ M_A - R\ x\ M_F$$

$$\frac{dM_R}{dt} = -C(t) + R\ x\ M_F \qquad (4)$$

The compartment model used fatigue and recovery factors similar to that of Liu *et al* [17] but also incorporated a bidirectional, time-varying proportional controller, C(t). C(t) was modeled as a bounded proportional controller (Eq. 5) that is dependent on

whether or not the M_A is able to achieve the required muscle force or target load (TL) and the availability of M_R [6]. The functions used to determine controller, C(t), also include muscle force development (L_D) and force relaxation (L_R) factors. The fatigue model is relatively insensitive to the values of muscle force development and force relaxation and therefore the values of L_D and L_R were set to be the same arbitrary values [6].

$$If\ M_A > TL\ and\ M_R > TL - M_A, C(t) = L_D \times (TL - M_A)$$

$$If\ M_A < TL\ and\ M_R < TL - M_A, C(t) = L_D \times M_R$$

$$If\ M_A \geq TL, C(t) = L_R \times (TL - M_A) \quad (5)$$

Residual capacity (RC) was used to describe the remaining muscle strength capability due to fatigue (equation 6). A value of 0% indicates no strength reserve (not physiologically possible) and a value of 100% indicates a state of full strength. The RC parameter can be used as a multiplier to determine the decayed maximum strength capabilities. Similar to Liu *et al* [17], brain effort (BE) was incorporated into this fatigue model (equation 7) and is understood to be the central drive that is necessary to perform a task or a simple estimate of perceived exertion [6].

$$RC(t) = M_A + M_R = 100\% - M_F \quad (6)$$

$$If\ TL \leq RC, BE = \frac{TL}{RC} x\ 100\%$$

$$If\ TL > RC, BE = 100\% \quad (7)$$

The fatigue (F) and recovery (R) parameters for individual joint regions (i.e. ankle, knee, trunk, shoulder and elbow) as well as a general set of F and R parameters were determined via a global optimization search strategy [74] and validated against existing task-intensity endurance-time (ET) relationships [75] for task intensities from 10% to 90% in increments of 10% using the Xia *et al* fatigue model [6]. Once a set of optimal F and R parameters were determined and validated, the fatigue model developed by Xia *et al* [6] using these validated F and R parameters, was tested for 9 different task intensities ranging from 15% to 95% in increments of 10%. Minor differences were observed between the ET between the different joint regions and task intensities as compared to previously published joint region ETs by Frey Law and Avin [75]. A sensitivity analysis was performed on the F and R values in order to determine the effects of changes in these two parameters on the fatigue model [6] outputs. It was determined that the F parameter had the largest influence on the task intensity-ET relationship as the changes in F altered the inflection points of the intensity-ET curves, particularly at the lower intensity levels. The R parameter had minimal influence on the task intensity-ET relationship as the changes in R influenced the spread of ETs at the lower intensity levels [74]. The overall effects of the sensitivity analysis on the Xia *et al* model [6] were displayed in figure 1-4.

Using various isometric loading conditions and observing the ET and %MVC relationships the model developed by Xia *et al* [6] was able to produce results similar to previously published ET curves [76] for static endurance tasks. Despite being validated for sustained isometric contractions [6, 74] this model may not directly translate to other tasks conditions (i.e. isometric tasks with intermittent rest intervals or dynamic

contractions) and further work is needed to understand whether or not this model can predict the effects of fatigue during non-isometric activations [74].

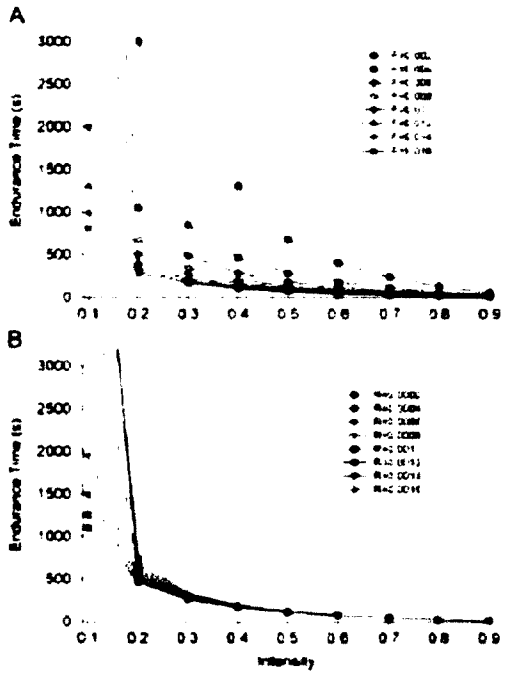

Figure 1-4: The effects of varying the: A) fatigue parameter and B) recovery parameter values on the task intensity-endurance time relationship [74]

The model developed by Xia *et al* [6] has the capability of predicting the effects of fatigue at the joint level [6, 74]. An advantage of using the model developed by Xia *et al* [6] is that the F and R coefficients have already been determined for various joints [74]. The RC in this model was similar to the fitness equation in Tang *et al* [16, 44] in that they both describe the effect of fatigue on the muscle's ability to contract. Another advantage of the model developed by Xia *et al* [6] is that a simplified estimate of perceived exertion, BE, can be obtained in real-time. Both the models developed by Tang *et al* [16] and Xia *et al* [6] incorporate the Hill-type muscle model [72], which

accounts for the dynamic force producing capabilities of a muscle and are therefore able to predict physiologically relevant muscle forces. Despite their positive attributes, both the Tang *et al* [16] and Xia *et al* [6] models have not been validated for dynamic types of activation which are evident in most athletic maneuvers such as a side step cut [6, 16, 74]. However, these two models provide a simplistic approach to understanding and analytically modeling the effects of fatigue on the force production capabilities of a muscle. Therefore, the application of these models into a dynamic model of fatigue should be investigated.

1.4 Musculoskeletal Modeling

Musculoskeletal models are developed to predict specific phenomena that may be too costly or difficult to investigate *in-situ* and may also be used as tools where it is impossible to perform certain experiments due to ethical or safety reasons [77]. The use of musculoskeletal models usually includes some sort of validation, indirect or direct. Indirect validation consists of comparing one's results to those of another study whereas direct validation consists of comparing one's results to a previously collected data set. It is difficult to directly validate a model as many of the parameters that are studied using a model are difficult to measure *in-vivo* and therefore, researchers use more of an indirect validation and focus on other variables in the model that are easier to measure experimentally [77].

Advances in technology have increased the types of modeling techniques available for use in research of lower extremity kinematics and risk of injury. One method of biomechanical analyses used to study joint forces and moments is inverse dynamics. Despite the vast amounts of information that can be obtained through inverse

dynamics analyses, it is difficult to determine the function or dysfunction of individual muscles and establish a cause-effect relationship from kinematic or kinetic data alone [78-80]. Dynamic simulations using forward dynamics provide a means of understanding the mechanics of locomotion that is not possible with motion analysis and inverse dynamics alone in understanding novel and hypothetical movements [78, 81]. Through the use of forward dynamics simulations, the effects of various neuromuscular conditions, pathologies, athletic performance, etc. on muscle, joint forces and kinematics can be estimated.

1.4.1 Uses of Musculoskeletal Modeling in the Knee

The knee is a complex joint and was studied using various methods of musculoskeletal modeling ranging from finite element modeling [82, 83] to multi-body modeling [40, 84, 85]. OpenSim (SimTK, Stanford, CA) is an open-source musculoskeletal modeling software that allows for simulation of various dynamic tasks and calculations of various parameters through the use of inverse dynamics, inverse kinematics and forward dynamics [80]. OpenSim was used to understand the effects of various dynamic maneuvers on the ACL strains and loads [37, 40, 86, 87] as well as the effects of these maneuvers on joint mechanics and the risk of ACL injury [88, 89].

It is important for fatigue to be considered in the formulation of musculoskeletal models that analyze dynamic motions while requiring large amounts of muscular activity because fatigue was shown to alter lower extremity mechanics during athletic maneuvers and may increase risk of injury [7, 9, 33, 50]. However, many multi-body models do not consider the effects of fatigue in their determination of muscle forces [90]. Multi-body models that incorporate fatigue were developed [90, 91], yet they did not directly validate

the effects of fatigue on muscle force production through experimental trials [91]. The muscle fatigue model developed by Xia *et al* [6] was incorporated into an inverse dynamic analysis of the elbow joint in which a prescribed motion was applied to the joint. An increase in the number of activated motor units was required as muscular force production had decreased over time in order to maintain the desired joint motion over a prolonged period of time (~80 seconds) [90]. Although the fatigue model was successfully applied to a multi-body model, knowing whether or not the fatigue model is able to accurately predict the effects of muscular fatigue for a non-isometric or dynamic activation pattern is still unknown.

1.5 Specific Aims

Two analytical models, Xia *et al* [6] and Tang *et al* [16], can predict the effects of fatigue using a minimal number of non-physiologic inputs. Incorporating an analytical model, to predict the effects of fatigue, during a dynamic task such as a side step cut would aid researchers in understanding the effects of fatigue on risk of injury. Therefore, this study had three specific aims to address the gaps within the literature surrounding the effects of muscle fatigue on risk of ACL injury.

Aim 1: Develop and validate a 29 degree of freedom musculoskeletal model which incorporates analytical models that can be used to estimate the effects of neuromuscular fatigue.

The first aim of this study will be to investigate the effects of fatigue on the lower extremity during a side step cut through development and validation of a dynamic simulation using OpenSim [80]. Recreationally active females will be asked to perform the side step cut both before and after fatigue while kinematic, kinetic and

electromyography (EMG) data are collected. Isolated fatigue of the hamstrings will be induced through a modification of an established isometric fatigue protocol [92]. The pre-fatigue *in-vivo* data will be used as the inputs to the dynamic simulation. Analytical fatigue models [6, 16] will be implemented into the dynamic simulations in order to assess the ability of these models to predict the effects of fatigue on the lower extremity. The results of the analytical fatigue models will be compared to the post-fatigue experimental data. In addition, one analytical model will be determined as the model that best estimates the effects of fatigue for this application.

Hypothesis 1: The Tang *et al* [16] analytical model will be able to best predict the effects of fatigue as it includes more subject specific parameters.

Aim 2: Determine the effects of various levels of fatigue on lower extremity muscle forces.

The second aim of this study will be to determine the effects of various levels of fatigue on lower extremity muscle force production. Forward dynamic simulations will be used to determine the effects of various levels of fatigue (i.e. 10%, 25%, 50%, 75% and 90%) and compare these muscle forces to the pre-fatigue muscle force data.

Hypothesis 2: Hamstrings muscle force producing capabilities will decrease as fatigue levels increase.

Aim 3: Determine the effects of various levels of fatigue on ACL load.

The third aim of this project is to determine the ACL loading at various levels of fatigue (i.e. 10%, 25%, 50%, 75% and 90%).

Hypothesis 3: Peak ACL load will increase as fatigue levels increase.

1.6 Assumptions of the Study

1. The participant's starting approach to the side step cut is similar for both the pre- and post-fatigue trials.
2. The residual effects of hamstrings fatigue in other muscle groups (quadriceps, gastrocnemius, etc.) are minimal.
3. The musculoskeletal models used to calculate muscle forces and ACL loads will provide accurate estimations of the participant's anatomical and physiological systems.
4. The planar knee model used in the musculoskeletal models with a posterior tibial slope of 0° will provide an accurate estimate of knee joint contact forces and ACL loads.

CHAPTER 2

METHODS

The effects of an isolated hamstrings fatigue protocol was analyzed using a musculoskeletal modeling approach. Kinematic, kinetic and electromyography (EMG) data were collected on six healthy, recreationally active females while performing an anticipated side step cut using the right lower extremity both pre- and post-fatigue. The processed kinematic, kinetic and EMG data were used as inputs into a dynamic musculoskeletal simulation using OpenSim [80]. Both the Tang *et al* [16] and Xia *et al* [6] analytical fatigue models were implemented into OpenSim [80] via custom external MATLAB (The Mathworks, Natick, MA) routines.

Various tools within the OpenSim [80] software were used to determine muscle and joint contact forces for each individual participant while performing the side step cut. A 29 degree of freedom (DOF) model was created for each participant and the right lower extremity muscle forces as well as the knee joint contact forces were determined at various levels of neuromuscular fatigue. The muscle and joint contact force data were used to calculate ACL loading for that particular participant.

2.1 Participants

This study recruited six healthy, recreationally active females with an age, height and mass of 22.1±2.9 years, 1.67±0.04m and 62.8±7.3kg, respectively. Recreationally active was defined as participating in activities involving running and cutting (i.e. soccer, basketball, tennis, etc.) for a minimum of 30 minutes at least 3 times a week. A background questionnaire was administered to each participant to assess previous injuries

and health status. This study was approved by the Old Dominion University Institutional Review Board. Written informed consent was obtained from each participant prior to data collection. Volunteers were accepted for this study if they did not have any type of lower extremity injury within 6 months prior to participation and have not had any lower extremity surgical reconstruction. A total of 14 participants were recruited for the study yet two participants were unable to complete the study due to physical complications and data from six participants were not used to due experimental protocol issues.

The data collection process of this study consisted of 2 separate sessions with a minimum and maximum of 7 days and 21 days, respectively, between each testing session. There were no restrictions placed on subject activity between testing sessions. All testing sessions took place in the Neuromechanics Laboratory at Old Dominion University. The first testing session determined the fatigue and recovery coefficients needed for the Tang *et al* [16] fatigue model. The second testing session included collection of *in-vivo* kinematics, kinetics and electromyography while performing the side step cutting task for both the pre-fatigue and post-fatigue conditions. Each of the above testing sessions were conducted for the right lower extremity of each participant in the study. Upon completion of data collection, the data were processed and implemented into a dynamic simulation of an anticipated side step cut using OpenSim [80]. Each simulation included the fatigue models of Tang *et al* [16] and Xia *et al* [6].

2.2 Experimental Protocol

2.2.1 Test Session 1: Determination of Fatigue and Recovery Protocol

Each participant underwent an isolated hamstrings fatigue protocol in order to determine the fatigue and recovery parameters for the hamstrings muscles. There are

many types of protocols that have been used to induce isolated muscle fatigue [92-98]. Some fatigue protocols require the participant to perform submaximal contractions for a prescribed amount of time [93], while others require the participant to perform a set number of maximal contractions for a particular time period [95]. Other fatigue protocols require the participant to produce a required load and consider the participant fatigued when they are either not able to hold that pre-determined load for a certain time [94], while others consider the participant fatigued when he/she are not able to perform a certain number of consecutive contractions at the particular load [92, 96-98]. Studies have tracked recovery of muscle groups for several minutes [99-101], hours [3] and even days [102] after inducing fatigue.

Participants were provided a 10-minute warm-up period on a stationary bicycle followed by self-directed stretching. The participant was seated with their hips and knees flexed to 90°. Velcro straps across the torso, waist and both thighs (just proximal to the femoral epicondyles) in order to prevent any compensating motion. The fatigue protocol was induced using a modified portable fixed dynamometer system (Figure 2-1) [103]. The modified portable fixed dynamometer system included a load cell, in which one end was attached to the proximal end of the malleoli via an ankle strap and the other end was attached to a wall mount. The electrical signal produced by the load cell was processed and displayed in real-time using the Evaluator Software System (BTE Technologies, Hanover, MD). Participants completed a set of three – 5 second maximum voluntary isometric contractions (MVIC), where each repetition was separated by a 30 second rest period. The maximum of the three MVICs was selected as the baseline MVIC. After completing the 3 MVICs, each participant was given a 2 minute rest period. Following

the rest period, each participant underwent continuous 5 second MVICs, followed by a 2 second rest period, until 3 consecutive contractions fell below 25% of the subject's baseline MVIC. Verbal encouragement was provided during the fatigue protocol in order to motivate the participant to continuously produce maximal hamstrings muscle force. The protocol that was used is a modification of a previously developed isometric fatigue protocol by Bizid *et al* [92]. Originally, the fatigue protocol [92] was used to induce quadriceps muscle fatigue, through maximal isometric contraction, where the force output of the three consecutive repetitions fell below 50% of the measured peak force [96, 98].

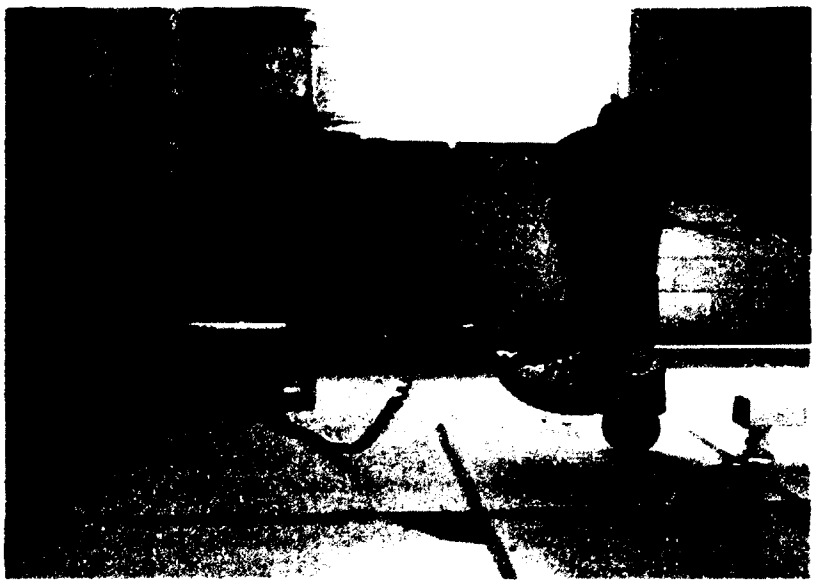

Figure 2-1: The portable fixed dynamometer system [103] that was modified in order to induce fatigue and track recovery

A pilot study, consisting of 5 male recreationally active males with an age, height and mass of 27.4±5.07years, 1.753±0.09meters and 81.1±41.5kg, respectively, was performed in order to determine the fatigue and recovery protocol criterion. The observations from the pilot study suggested that each participant be fatigued to 25% of

the baseline MVIC. In addition, recovery was tracked for at least 30 minutes and until the participant's maximal effort contraction was at least 80% of the baseline MVIC. A cut-off value of 350 maximal effort contractions during the fatigue protocol was used in order to standardize the number of contractions for each participant. Recovery of the hamstrings muscle was tracked for no more than 60 minutes. In addition, verbal encouragement was provided during the recovery protocol.

The recovery curve was generally determined by measuring maximal effort contractions from a state of total fatigue to no fatigue [16] after fatigue has been induced. Therefore, in order to track recovery of the hamstrings muscle group, the participant was asked to produce maximum effort contractions at the following time periods: 30 seconds, 60 seconds, 90 seconds, 2 minutes, 3 minutes, 4 minutes and in 2 minute periods for at least 30 minutes immediately after the fatigue criteria have been met and until the participant's maximal effort contraction was equal to 80% of the MVIC measured prior to the onset of the fatigue protocol. Recovery of the hamstrings muscle was tracked for no more than 60 minutes. Once the fatigue and recovery portions of the data collection were completed, the participants were given an opportunity to practice the side step cut.

2.2.3 Test Session 2: In-vivo data collection

The second testing session occurred at least 7 days but no more than 21 days after the second testing session to allow for adequate recovery time from the effects of testing session 1. Following a 10 minute warm-up on a stationary bicycle and self-directed stretching, EMG electrodes were applied to the vastus medialis oblique (VMO), vastus lateralis (VL), rectus femoris (RF), medial hamstrings(MH), lateral hamstrings(LH), the medial head of the gastrocnemius (MG), the lateral head of the gastrocnemius (LG) and

the tibialis anterior (TA) of the right leg. All electrodes were placed according to the Surface Electromyography for the Non-Invasive Assessment of Muscles (SENIAM) recommendations [104] by locating specified landmarks for the aforementioned muscles. All electrode sites were abraded and cleaned with alcohol wipes prior to electrode placement. EMG data were collected at 2000Hz using a Delsys Trigno Wireless system (Delsys Inc., Boston, MA) with electrodes that were single differential, pre-amplified, composed of 99.9% silver and had a contact area of $5mm^2$. All electrodes were attached using an adhesive skin interface specifically designed for these electrodes.

Seventy four light-reflecting skin markers with a diameter of 12.7mm were placed bilaterally on each participant. The markers that were used for the calibration trials (calibration markers) included the acromion processes, medial and lateral humeral epicondyles, ulnar and radial styloid processes, iliac crests, greater trochanters, medial and lateral femoral epicondyles, medial and lateral malleoli, the head of the first distal phalanges, and the fifth metatarsal heads. Custom made rigid plates with four markers (Appendix J) were attached to the thoracic spine, pelvis, bilateral upper arms, forearms, thighs, shanks and heels of the shoes. Marker trajectories were collected at 200 Hz with an 8 camera Vicon motion capture system (Vicon Motion Systems Ltd., Oxford, England) and ground reaction force (GRF) were collected synchronously at 2000 Hz with Bertec force plates (Bertec Corporation, Columbus, OH, USA).

After all EMG electrodes and markers were attached, a standing calibration trial was collected. After performing the calibration trial, the participants were allowed to practice the side step cut until they felt comfortable with the task. After the practice period, the participants were asked to complete 5 anticipated side step cutting tasks [58].

The approach speed of the participants were controlled to be 3.8 – 4.2 $m \cdot s^{-1}$. This speed range was selected as it was determined that a speed of 4 $m \cdot s^{-1}$ is ideal for investigating knee loading mechanisms during side step cuts in females [105]. A Brower timing system (Brower Timing Systems, Draper, UT) was used to control the approach speed. Participants were instructed to strike the force plate with their right foot and cut to the contralateral side at a 45° angle. Participants completed 5 successful trials of the anticipated cutting task (pre-fatigue cuts). A trial was deemed successful if the participant maintained the approach speed, if the participant's entire right foot made contact with the force plate and the maneuver was performed correctly by maintaining a 45° angle upon propulsion from the force plate (Figure 2-2). If a trial was deemed unsuccessful, the participants performed that particular trial again. After completion of the first five side step cuts, the participants underwent the same fatigue protocol as described above, where the hamstrings MVIC were reduced by 75%. Once the fatigue protocol was completed, the participants performed another set of five side step cuts (post-fatigue cuts).

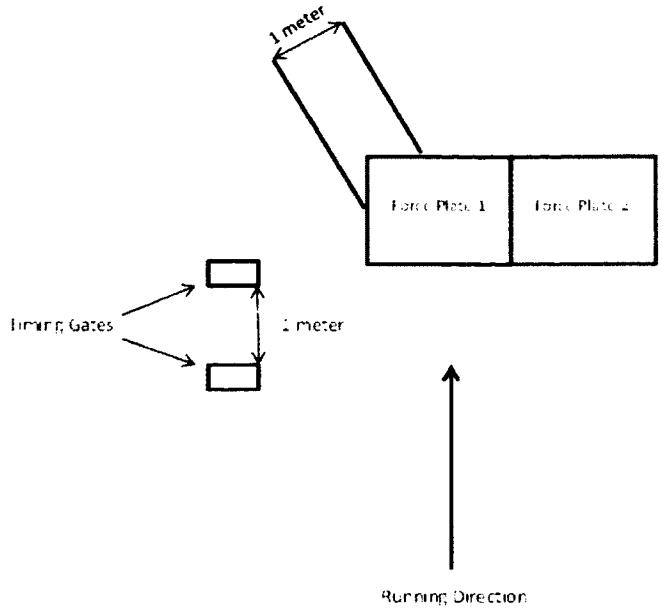

Figure 2-2: Schematic of the experimental setup used to perform the side step cuts

2.3 Data Reduction

All raw three dimensional data and GRF data for the side step cutting trials were filtered using a fourth order, zero lag, Butterworth filter with cutoff frequencies of 6 Hz and 50 Hz, respectively. A kinematic model composed of twelve skeletal segments (trunk, pelvis, bilateral upper-arms, forearms, thighs, shanks and feet) was created using Visual 3D software (5.00.31, C-Motion Inc., Rockville, MD). Hip joint centers were placed at one-quarter of the distance from the ipsolateral to the contralateral greater trochanter [106]. Knee joint centers were defined as the midpoint between the medial and lateral knee femoral epicondyles and ankle joint centers were defined as the midpoint between the medial and lateral malleoli markers. The elbow joint centers were defined as the midpoint between the medial and lateral humeral epicondyle markers. The wrist joint centers were defined as the midpoint between the ulnar and radial styloid processes. The shoulder joint centers were defined as a 2cm vertical shift from the acromion processes.

The segment coordinate systems were defined to describe position and orientation of each segment using an unweighted least squares procedure [107]. Joint angles were determined using an inverse kinematics algorithm that minimizes the effect of the soft tissue and measurement error in the experimentally measured marker positions [108].

All raw EMG data were high pass filtered using a 30 Hz zero-lag, 4^{th} order, recursive Butterworth filter, then full-wave rectified and low-pass filtered using a 6 Hz zero-lag 4^{th} order, recursive Butterworth filter [109]. All EMG data for the side step cut trials were normalized by the maximum recorded signal for that particular muscle over the entire trial so that muscle activity was normalized from zero to one.

Equations for the fatigue and recovery of the hamstrings muscle group were determined for the Tang *et al* [16] model using the fatigue and recovery data obtained in session 1 and the fatigue data obtained in session 2. The fatigue and recovery equations for each participant were determined by curve fitting the normalized force data using the Levenberg-Marquardt method [110]. The fatigue and recovery equations were approximated using exponential equations of the form $y = ae^{(bt)}$, where a and b were the coefficients determined by the Levenberg-Marquardt method and t was time.

2.4 Musculoskeletal Model

OpenSim v3.1 was used to simulate all side step cutting trials [80]. A twelve segment, 29 degree of freedom (DOF) musculoskeletal model, modified from a previous musculoskeletal model [111], was created for each participant and used to create computer simulations of the side step cutting tasks. A full body musculoskeletal model [111] was modified in order to simulate the side step cutting task. The pelvis includes 6 DOFs (i.e. 3 translations and 3 rotations). Both hip joints were modeled using as a ball

and socket joints (3 DOF), the right knee was modeled using 3 DOFs (i.e. flexion/extension, adduction/abduction, internal/external rotation) while the left knee was modeled as a 1 DOF revolute joint. Tibiofemoral translations were defined according to the knee extensor mechanism proposed by Yamaguchi *et al* [112]. Both the right and left ankles were modeled as a 1 DOF of freedom revolute joints [113]. Lumbar motion was modeled as a 3 DOF ball and socket joint [114]. Each arm consisted of 4 DOFs; the shoulder was modeled as a ball and socket joint (3 DOFs) [115] and the elbow was modeled as a revolute joint (1 DOF). Each model was scaled using experimentally measured markers that were placed on anatomical landmarks. The anatomical landmarks used for model scaling were the acromioclavicular, elbow, wrist, hip, knee and ankle joints.

The right leg of the model was actuated by 43 muscles [113, 116, 117] while the left leg and upper body (torso and arms) were driven by torque actuators. Each of the muscles used were modeled as a three-element muscle in series [118]. Previously reported optimal muscle fiber lengths (l_o^m) and pennation angles (α) of the muscles in the model were used [116]. Each individual muscle was composed of a variety of both slow and fast twitch fibers. Therefore, maximum shortening velocity (v_{max}^m) of all muscles in the model was assumed to be 10 $l_o^m \cdot s^{-1}$ to model the presence of mixed fiber types within the muscles of the body [118]. The delay between muscle excitation and activation was modeled as a first-order process using values of 10 and 40 milliseconds for activation and deactivation, respectively [118]. The equilibrium musculoskeletal model incorporated the damped equilibrium musculotendon model [119]. Musculotendon actuators consisted of an active contractile element connected in series to a passive elastic

element and an elastic tendon yet singularities in the normalized muscle velocity were encountered [119]. The damped equilibrium musculotendon model eliminated singularities in normalized muscle velocity by limiting the maximum pennation angle of the muscle and adding a damper in parallel to the contractile element of the equilibrium musculoskeletal model. Since the damped equilibrium musculotendon model was free of singularities, it generated similar force profiles as previously implemented musculotendon models and performed these computations in a fraction of the time [119].

In order to accurately track the participant's motion, joint moments were needed and these joint moments were calculated using a residual reduction algorithm (RRA) [80]. The RRA algorithm reduced the amount of error or difference between the experimental and model marker trajectories by applying a set of non-physical external forces and moments (i.e., residuals) to a body (e.g., pelvis) [120]. These residuals were averaged over the entire duration of the movement and the algorithm recommended changes in the model mass properties and slightly adjusted the joint kinematics so that the average value of the residuals throughout the movement was reduced. An external optimization routine using the particle swarm optimization (PSO) [121] was used to determine the optimal input parameters that would produce a simulation that closely tracks the experimental data with minimal residuals.

The particle swarm optimization (PSO) methodology was used to solve non-linear functions by implementing a defined swarm size of 35 in which the optimal solution of this initial swarm was used to determine the next set of given inputs that were used to solve the nonlinear function until an optimal solution was determined [121]. The PSO optimization routine was used to determine the weighting factors (w_q) of each of the 29

degrees of freedom of the musculoskeletal model through a minimization of the difference in error between the experimental and model kinematic trajectories. More specifically, the objective function (equation 8) was used to determine a set of weighting factors that minimized the cube root-mean-square (rms) error between the experimental and simulated kinematics (q^{err}) of the pelvis, with rms error values for the kinematic (W_K) and residuals (W_L), cubed rms of the q^{err} over the remaining DOFs (nq) and cubed rms magnitude of the residuals (R) [8, 37].

$$\min_{w_q}\left[\sum_{i=1}^{6}\left(\text{rms}\left(q_i^{err}\right)\right)^3+\sum_{i=7}^{nq-3}\left(\frac{\text{rms}\left(q_i^{err}\right)}{W_K}\right)^3+\sum_{i=nq-2}^{nq}\left(\frac{\text{rms}\left(q_i^{err}\right)}{W_L}\right)^3+\sum_{j=1}^{6}\left(\text{rms}\left(R_j\right)\right)^3\right] \quad (8)$$

Computed muscle control (CMC) was used to compute muscle forces that were required to track the kinematics produced by RRA of the side step cutting tasks [122, 123] using a closed loop system. The experimental EMG data were used to constrain the CMC excitation profiles. EMG data for the vastus lateralis, rectus femoris, vastus medialis, tibialis anterior, lateral hamstrings, medial hamstrings, lateral and medial gastrocnemii muscles were used to limit the excitation profiles of these same muscles within the musculoskeletal model. CMC used a static optimization problem [124] to resolve muscle activation redundancies by minimizing the sum of the squares of the muscle activations. Both muscle activation and contraction dynamics were accounted for in the static optimization [118]. In addition to computing muscle forces, CMC computed joint kinematics that closely resembled those produced by RRA. CMC was performed for all of the experimental pre- and post-fatigue trials. The default isometric strengths of the hamstrings muscles in the OpenSim model were reduced by 75% in order to replicate the experimental protocol for the post-fatigue trials.

Upon completion of CMC, the pre-fatigue CMC excitation profiles were used as inputs into both fatigue models in order to predict excitation profiles in which a level of 10%, 25%, 50%, 75% and 90% fatigue were induced by the analytical models. The analytical fatigue models were used in order to determine the effects of fatigue while performing the side step cut. While performing a side step cut, the hamstrings muscles do not experience any significant amount of recovery (i.e. activation > 0) as the side step cut is a dynamic maneuver. Therefore, the participant specific fatigue equations, determined from the experimental force vs. time data, from session 2 were used as inputs into the Tang *et al* [16] model. The participant specific fatigue equations from session 2 were used as this was the muscle force profile during the day of *in-vivo* data collection. Unlike the Tang *et al* [16] model, the Xia *et al* [6] model did not require any subject specific parameters.

Forward dynamics (FD) simulations were performed using both fatigue models. In contrast to CMC, forward dynamics (FD) used an open-loop system to determine joint kinematics, kinetics and muscle forces. The outputs of CMC (i.e. joint kinematics and muscle excitations) were used as inputs into the forward dynamics simulations, in which the simulations apply the respective fatigued muscle excitation profiles to the model without any type of feedback or correction mechanism. A total of 10 FD simulations were produced for each fatigue condition consisting of five trials for each of the two fatigue models. Each fatigue model was run from 20ms prior to initial contact and up to 50ms after initial contact as this is the time period in which non-contact ACL injuries were observed to occur [125]. The default isometric strengths of the hamstrings muscles were reduced in order to replicate the various levels of fatigue. Muscle forces were

determined using FD and used to determine joint contact forces and moments. The workflow used in the musculoskeletal modeling portion of this study is displayed in figure J-1.

2.4.1 Determination of Anterior Cruciate Ligament Loading

ACL loading was estimated using methods similar to previous studies [37-39, 86], in which total ACL load (ACL_{Total}) was calculated as the summation of the sagittal plane (ACL_S), transverse plane (ACL_T) and frontal plane (ACL_F) loading (equation 9):

$$ACL_{Total} = ACL_S + ACL_T + ACL_F \tag{9}$$

The sagittal plane loading of the ACL was calculated using equation 10 [38, 86] in which the tibiofemoral contact force (F_{TF}) was calculated from the net axial knee joint reaction (F_{Axial}), patellar (F_{Pat}), hamstrings (F_{Hams}) and gastrocnemius (F_{Gas}) forces. The patellar force was the summation of all of the quadriceps muscle force estimates. The tibial slope (φ_{TF}) was assumed to be zero degrees in order to match the OpenSim knee model. The patellar, hamstrings and gastrocnemius tendon angles were accounted for within the muscle force calculations from FD and therefore equation 10 was simplified as shown in equation 11. The anteroposterior ligamentous forces (F_{Lig}) were calculated from the net anteroposterior knee joint reaction force (F_{AP}) (equation 12). Similar to the equation used to determine the tibiofemoral contact force, equation 12 was simplified into equation 13.

$$F_{Axial} = F_{TF} \cdot cos\varphi_{TF} - F_{Pat} \cdot cos\varphi_{Pat} - F_{Hams} \cdot cos\varphi_{Hams} - F_{Gas} \cdot cos\varphi_{Gas} \quad (10)$$

$$F_{Axial} = F_{TF} - F_{Pat} - F_{Hams} - F_{Gas} \quad (11)$$

$$F_{AP} = F_{TF} \cdot sin\varphi_{TF} + F_{Pat} \cdot sin\varphi_{Pat} - F_{Hams} \cdot sin\varphi_{Hams} + F_{Lig} \quad (12)$$

$$F_{AP} = F_{Pat} - F_{Hams} + F_{Lig} \quad (13)$$

The sagittal plane ACL force, ACL_S, was estimated, using equation 14, as a proportion of the F_{Lig} using previous cadaveric knee measurements [8, 12, 37, 126]. In equation 14, the ACL load for an applied F_{Lig} of 100N (F_{100N}) [12] and the ACL load without an applied anterior force (F_0) [126] were both functions of knee flexion (θ_{Knee}) and were used to determine the ACL_S.

$$ACL_S = \frac{F_{100N}(\theta_{Knee}) - F_0(\theta_{Knee})}{100N} F_{Lig} + F_0(\theta_{Knee}) \quad (14)$$

ACL_F and ACL_T were estimated as a function of their respective joint moment and the knee flexion angle, as suggested by previous studies [12, 126] and displayed in equations 15 – 18.

For adduction moments (M_{AD}):

$$ACL_F = (-7.5003e^{-0.041M_{AD}}) \cdot \theta_{Knee} \quad (15)$$

For abduction moments (M_{AB}):

$$ACL_F = (3.8054e^{-0.001M_{AB}}) \cdot \theta_{Knee} \quad (16)$$

For internal rotation moments (M_{IR}):

$$ACL_T = (-27.57e^{-0.045M_{IR}}) \cdot \theta_{Knee} \quad (17)$$

For external rotation moments (M_{ER}):

$$ACL_T = (8.6485e^{-0.032M_{ER}}) \cdot \theta_{Knee} \quad (18)$$

2.5 Data Analysis

2.5.1 Validation of the Analytical Fatigue Models

The hamstrings muscle group within the OpenSim model consisted of 4 muscles, the biceps femoris long head (BFLH), biceps femoris short head (BFSH), semimembranosus (SM) and the semitendinosus (ST). The muscle forces for each of the four combined hamstrings muscles were determined for both the post-fatigue experimental data and the fatigue model data using an initial condition of 75% fatigue from 20ms prior to initial contact up to 50ms after initial contact. The post-fatigue experimental hamstrings muscle force data were compared to the hamstrings muscle forces of each of the fatigue models through the determination of the total root mean square (RMS) difference. RMS_{Tang} represented the RMS difference between the experimental data and the Tang model hamstrings forces. RMS_{Xia} represented the RMS difference between the experimental data and the Xia model hamstrings forces. Once the model was validated, one fatigue model was selected as the model that best estimates the effects of hamstrings fatigue. This was done by selecting the model with the lowest total RMS value, assuming that one or more model produced reasonable RMS differences.

In addition, the numbers of contractions to fatigue as well as the baseline MVIC values during the fatigue protocol from sessions one and two were analyzed in order to determine the differences in maximal voluntary isometric contraction force and the number of trials required to achieve 75% hamstrings muscle fatigue. These variables were compared using a paired t-test, where alpha was set *a priori* at the 0.05 level. The statistical analysis was conducted using Microsoft Excel 2010 (Microsoft Inc., Redmond, WA).

2.5.2 Determination of Lower Extremity Kinematics, Kinetics and ACL Loading Across Various Levels of Fatigue

The selected fatigue model was used to test the effects of various levels of hamstrings fatigue on muscle force production, knee joint contact forces, lower extremity kinematics, knee joint moments and ACL loading from 20ms prior to initial contact up to 50ms after initial contact. The effects of fatigue on muscle force production, knee joint contact forces, lower extremity kinematics, knee joint moments and ACL loading were analyzed similar to previous studies [8, 37]. Peak ACL_{Total} was determined for each subject at each level of fatigue and compared across all fatigue levels. In addition, the planar components of the ACL_{Total}, the total quadriceps, hamstrings, gastrocnemius muscle forces, knee joint contact forces and knee joint moments at peak ACL_{Total} were compared across all fatigue levels. All of the dependent variables were compared using repeated measures ANOVA, where alpha was set *a priori* at the 0.05 level. Effect sizes were reported as partial eta squared (η_p^2) where a small, medium and large effect sizes were classified as 0.02, 0.13 and 0.26, respectively. The statistical analyses were conducted using SPSS Statistics (v21, IBM Corporation, Armonk, NY).

CHAPTER 3

RESULTS

Experimental kinematic data were compared to the torque-driven kinematics estimated by RRA, by determining the average RMS differences in the residual forces and torques as well as all 29 degrees of freedom of the musculoskeletal models [8, 37]. The RRA kinematic data were also compared to the muscle-actuated kinematics produced by CMC. The RMS differences between both fatigue models and the experimental hamstrings muscle force were 1.91 $N \cdot kg^{-1}$ and 1.88 $N \cdot kg^{-1}$, for RMS_{Tang} and RMS_{Xia}, respectively. Lower extremity kinematics predicted by the Xia *et al* [6] fatigue model were compared to the experimental post fatigue kinematic data in order to assess this fatigue model's ability to estimate kinematic data. RMS differences between the post-fatigue experimental and Xia fatigue model predicted kinematic data ranged from 0.74° - 11.8°.

Although peak ACL_{Total} increased with fatigue these changes in peak ACL_{Total} were not significantly affected by hamstrings fatigue. Similarly, all three planar components of ACL loading experienced non-significant changes as an effect of fatigue. Total quadriceps, hamstrings and gastrocnemius muscle forces experienced significant differences due to fatigue. Knee joint extension moments were significantly increased due to fatigue. Hip joint sagittal and frontal plane rotations, knee joint sagittal and transverse rotations as well as ankle joint sagittal plane rotation, predicted by the Xia *et al* [6] model, experienced significant changes due to fatigue.

3.1 Experimental and Computed Data

The experimental kinematic data were compared to the RRA computed kinematic data for the lumbar, pelvis and right lower extremity (Figures 3-1 and 3-2). The mean RMS differences over a time frame of 20ms prior to and 50ms after initial contact for both the pre- and post-fatigue kinematic tracking had an average RMS difference of 1.51°, 0.77° and 0.16°, respectively (Table A-1). Average RMS differences between the RRA and CMC kinematic data at the lumbar, pelvis and right lower extremity were tracked with an average RMS difference of 0.16°, 0.13° and 1.41°, respectively (Table A-2). Experimental pre-fatigue EMG data (Figure 3-3) for the VL, RF, VMO, TA, MH, LH and MG are compared to EMG data of a previous study [127].

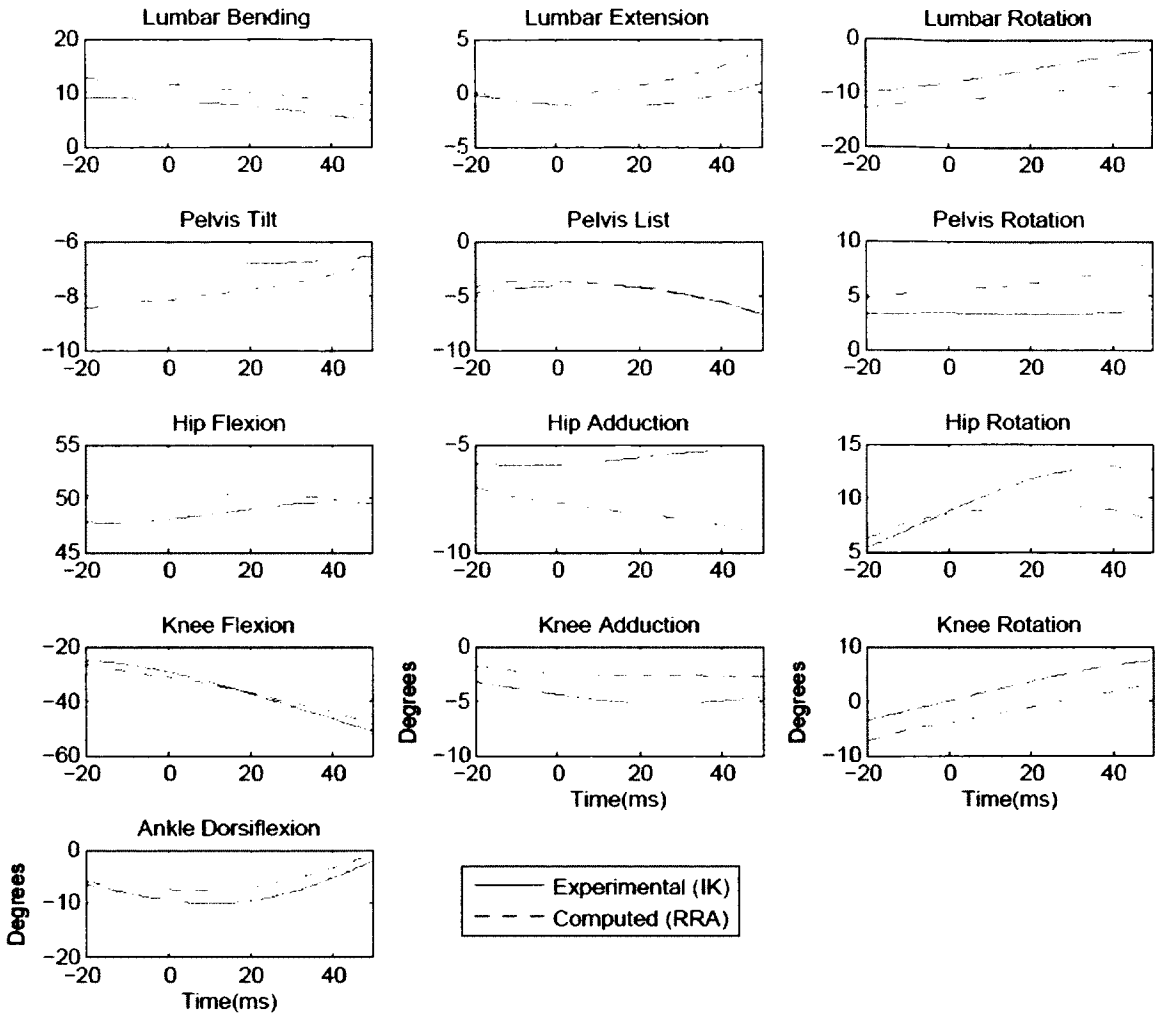

Figure 3-1: Mean pre-fatigue experimental (solid line) and RRA computed (dashed line) kinematics for the anticipated cutting task

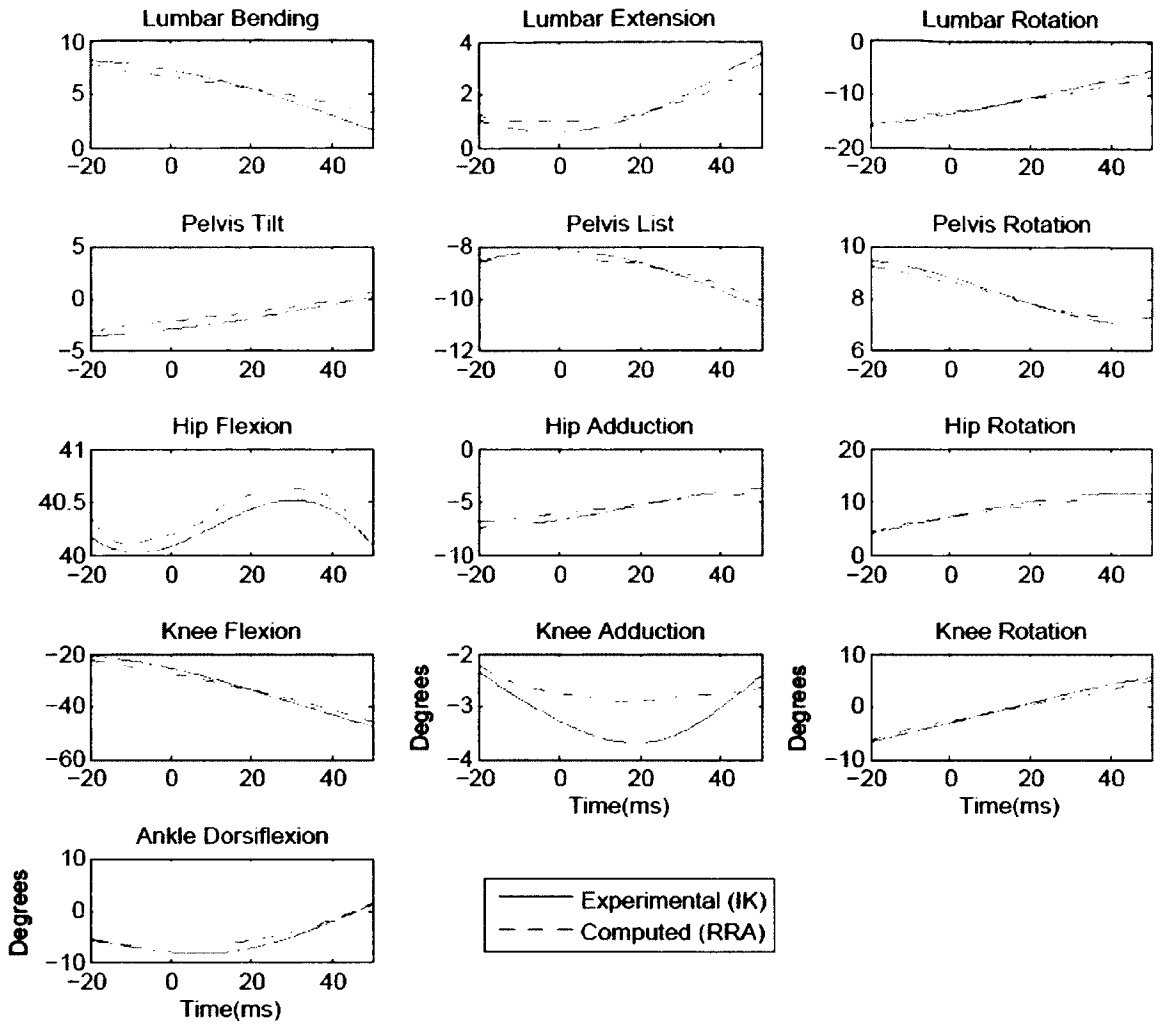

Figure 3-2: Mean post-fatigue experimental (solid line) and RRA computed (dashed line) kinematics for the anticipated cutting task

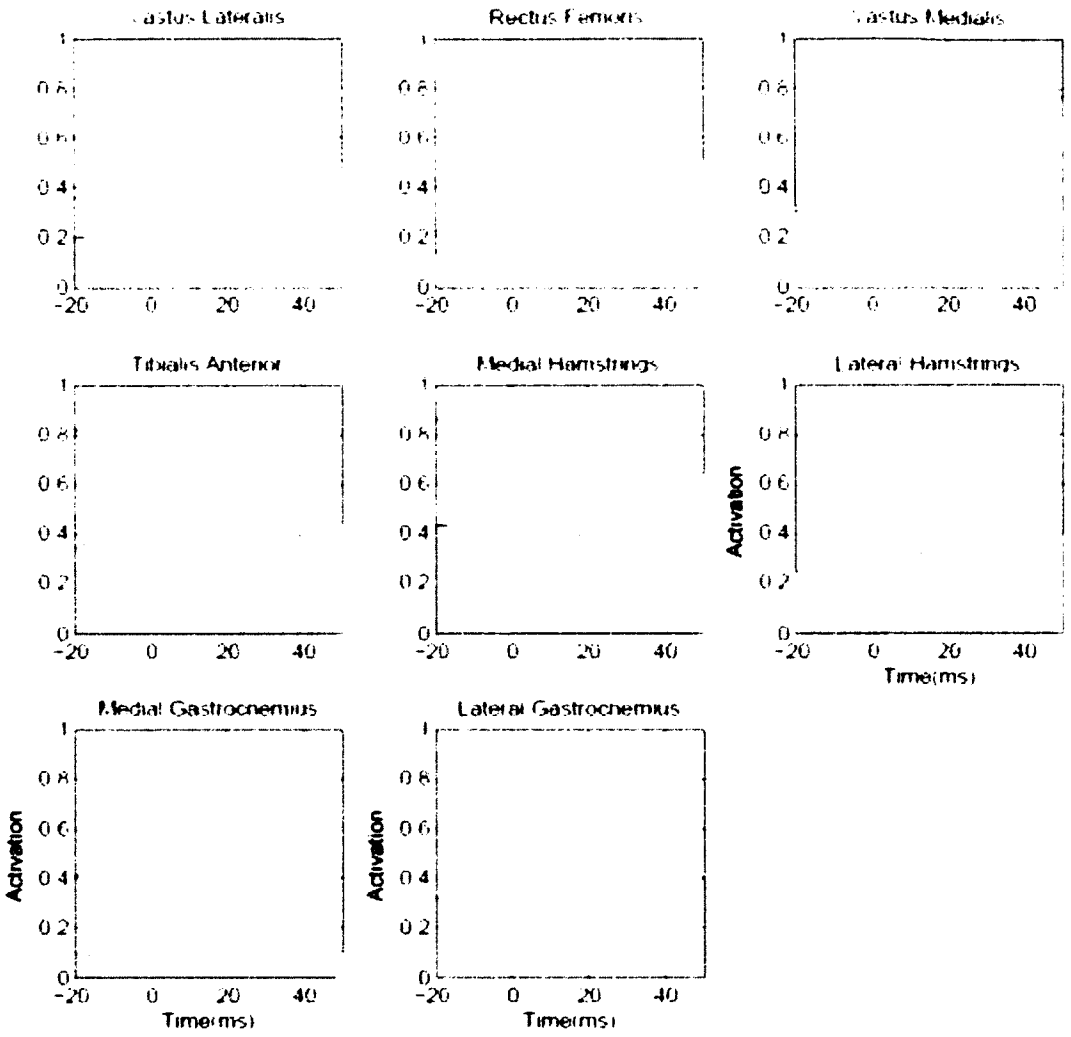

Figure 3-3: Experimental EMG data (dashed line) compared to EMG data collected by Neptune *et al.* [127] (shaded area) for an anticipated cutting task

3.2 Analytical Fatigue Model Validation

The number of repetitions needed to achieve hamstrings fatigue as well as the maximal contraction force in testing sessions 1 and 2 were analyzed using t-tests, where alpha was set *a priori* at the 0.05 level. In the first testing session, the group achieved an average of 251±127 repetitions while in the second testing session the group achieved an average of 70±51 repetitions. The overall number of repetitions needed to achieve hamstrings fatigue were found to be significantly different ($p<0.01$). The overall

maximal contraction force between testing session one (49.7±11.1 lbs.) and testing session two (39.9±9.96 lbs.) were similar ($p>0.05$). Fatigue and recovery curves from sessions one and two are presented in Appendix B.

The hamstrings muscle forces produced by the Tang *et al* [16] and Xia *et al* [6] fatigue models at an initial level of 75% fatigue were compared to the experimental post-fatigue hamstrings muscle force data. The total RMS differences between both the Tang (RMS_{Tang}) and Xia (RMS_{Xia}) fatigue models and the post-fatigue experimental data were calculated and used to determine the fatigue model that more closely predicts fatigued behavior. The total RMS_{Tang} and RMS_{Xia} values were 1.91 $N \cdot kg^{-1}$ and 1.88 $N \cdot kg^{-1}$, respectively (Table 3-1). The Xia fatigue model produced the most similar hamstrings forces when compared to the experimental data. Therefore, for this study, the Xia fatigue model was selected to estimate the effects of fatigue. The force predicted by both fatigue models as well as the experimental data of each of the muscles within the hamstrings group were plotted (Figures C-1 – C-4). The semitendinosus and semimembranosus demonstrated the smallest (0.14 $N \cdot kg^{-1}$) and largest (0.86 $N \cdot kg^{-1}$) RMS differences, respectively, when compared to the experimental data. Post-fatigue experimental kinematic data were compared to the kinematic data produced by the Xia fatigue model (Table 3-2). RMS differences ranged from 0.74° - 11.8° with knee adduction/abduction and hip flexion extension demonstrating the smallest and largest RMS differences, respectively.

Table 3-1: The muscle forces ($N \cdot kg^{-1}$) of each of the hamstrings muscle (mean±st.dev.) of the experimental data were compared to those forces predicted by the Tang and Xia fatigue models at the 75% fatigue level. The RMS difference was calculated between the post-fatigue experimental and fatigue model muscle forces.

	Pre-Fatigue	Post-Fatigue	Tang	Xia	RMS_{Tang}	RMS_{Xia}
Biceps Femoris Long Head	13.1±3.86	3.22±0.80	3.51±0.70	3.23±0.97	0.36	0.18
Biceps Femoris Short Head	10.0±1.71	2.49±0.45	0.329±0.20	0.64±0.28	0.38	0.70
Semimembranosus	12.6±7.25	2.63±1.48	3.70±1.53	3.46±1.71	1.07	0.86
Semitendinosus	5.37±1.79	1.27±0.39	1.26±0.45	1.22±0.51	0.10	0.14
Total					1.91	1.88

Table 3-2: Post fatigue lower extremity kinematics (degrees) are compared (mean±st.dev.) to the kinematics produced by the Xia fatigue model. RMS differences were calculated for each degree of freedom.

	Post-Fatigue	Xia Fatigue Model	RMS Difference
Hip			
Flexion/Extension	40.2±0.17	52.0±0.97	11.8
Adduction/Abduction	-5.61±1.25	-8.74±1.02	3.85
Rotation	8.90±2.44	8.26±0.83	1.86
Knee			
Flexion/Extension	-32.2±8.33	-30.9±2.80	5.67
Adduction/Abduction	-3.18±0.41	-2.48±0.24	0.74
Rotation	-0.27±3.69	-0.26±4.46	0.77
Ankle Dorsi/Plantarflexion	-5.71±2.67	-5.36±2.04	0.79

3.3 Analytical Fatigue Model Testing

The Xia *et al* [6] fatigue model was used to test the effects of various levels of hamstrings fatigue on total muscle force production and peak ACL load. The total quadriceps (Figure 3-4), hamstrings (Figure 3-5) and gastrocnemius (Figure 3-6) muscle forces were significantly altered ($p< 0.05$) due to various levels of hamstrings fatigue (Table 3-3). The force output of each individual hamstrings muscle significantly decreased as an effect of fatigue (Table 3-4). The timing of the peak ACL_{Total} loading did not significantly differ as hamstrings fatigue increased (Table 3-5). Although peak ACL_{Total} loading (Figure 3-7) increased, these changes were similar ($p>0.05$) across all fatigue levels despite a moderate effect size ($\eta_p^2 = 0.19$). The changes in all three planar components of ACL loading (Figures D-1 – D-3) were similar across all fatigue levels ($p>0.05$). The peak ACL_{Total} loading across the analyzed time frame increased by 2.2% (0.19 $N \cdot kg^{-1}$) at the 90% fatigue level. Both the ACL_S and ACL_F loading decreased by 1.7% (0.11 $N \cdot kg^{-1}$) and 6.1% (0.08 $N \cdot kg^{-1}$), respectively, at the 90% fatigue level. The ACL_T loading increased by 54.1% (0.39 $N \cdot kg^{-1}$) at the 90% fatigue level

Tibiofemoral contact forces (Figures F-1 – F-2) at peak ACL_{Total} loading did not exhibit any significant effects ($p>0.05$) due to fatigue (Table 3-6). Sagittal plane knee extension moment demonstrated significant increases ($p<0.001$) due to hamstrings fatigue. Hip flexion and abduction as well as knee extension and internal rotation exhibited significant increases due to fatigue (Table 3-7). Ankle sagittal plane rotation demonstrated a main effect due to fatigue ($p=0.04$) yet post-hoc analyses did not reveal significant changes between fatigue levels. The partial eta squared value ($\eta_p^2 = 0.19$) obtained from the repeated measures ANOVA performed on the peak ACL_{Total} data was

used to perform a post-hoc power analysis of this study. The power of this study was determined to be 53% and therefore, it is suggested that this current study is unpowered.

Table 3-3: Descriptive statistics (mean±st.dev.) for the total quadriceps, hamstrings and gastrocnemius muscle forces ($N \cdot kg^{-1}$) for various fatigue levels

	Pre-Fatigue	10% Fatigue	25% Fatigue	50% Fatigue	75% Fatigue	90% Fatigue	p-value	η_p^2
Quadriceps	117.1±11.5	114.6±11.1[a]	115.6±17.1	108.2±16.4[c]	98.9±15.5[a,b,c,d]	93.0±15.3[e]	<0.001	0.70
Hamstrings[f]	26.8±5.63	23.3±3.01	19.4±2.55	13.6±2.33	7.19±1.97	2.91±1.15	<0.001	0.91
Gastrocnemius	12.9±12.3	13.7±12.3[a]	15.7±11.9	18.0±11.8[a,b,c]	20.5±12.0[a,b,c,d]	21.8±12.2[e]	<0.001	0.63

a indicates muscle force is significantly different compared to pre-fatigue level ($p<0.05$)
b indicates muscle force is significantly different compared to 10% fatigue ($p<0.05$)
c indicates muscle force is significantly different compared to 25% fatigue ($p<0.05$)
d indicates muscle force is significantly different compared to 50% fatigue ($p<0.05$)
e indicates muscle force is significantly different compared to pre-fatigue and all other fatigue levels ($p<0.05$)
f indicates all muscle forces are significantly different compared to each other ($p<0.05$)

Table 3-4: Average (mean±st.dev.) hamstrings muscle forces ($N \cdot kg^{-1}$) for various fatigue levels

	Pre-Fatigue	10% Fatigue	25% Fatigue	50% Fatigue	75% Fatigue	90% Fatigue	p-value	η_p^2
Biceps Femoris Long Head	8.78±3.80	8.14±3.38[a]	6.38±2.35	4.41±1.42[a,b,c]	2.13±0.58[a,b,c,d]	0.77±0.19[e]	<0.001	0.82
Biceps Femoris Short Head	8.25±1.98	7.12±1.50[a]	5.54±0.88[a,b]	3.16±0.36[a,b,c]	1.19±0.21[a,b,c,d]	0.37±0.09[e]	<0.001	0.94
Semimembranosus	4.47±2.74	4.36±2.79	3.44±2.40	2.69±1.89[c]	1.46±0.93[a,b,c,d]	0.58±0.36[e]	<0.001	0.65
Semitendinosus	3.32±1.21	2.96±1.05[a]	2.29±0.78[a,b]	1.48±0.52[a,b,c]	0.70±0.27[a,b,c,d]	0.26±0.11[e]	<0.001	0.88

a indicates muscle force is significantly different compared to pre-fatigue ($p<0.05$)
b indicates muscle force is significantly different compared to 10% fatigue ($p<0.05$)
c indicates muscle force is significantly different compared to 25% fatigue ($p<0.05$)
d indicates muscle force is significantly different compared to 50% fatigue ($p<0.05$)
e indicates muscle force is significantly different compared to pre-fatigue and all other fatigue levels ($p<0.05$)

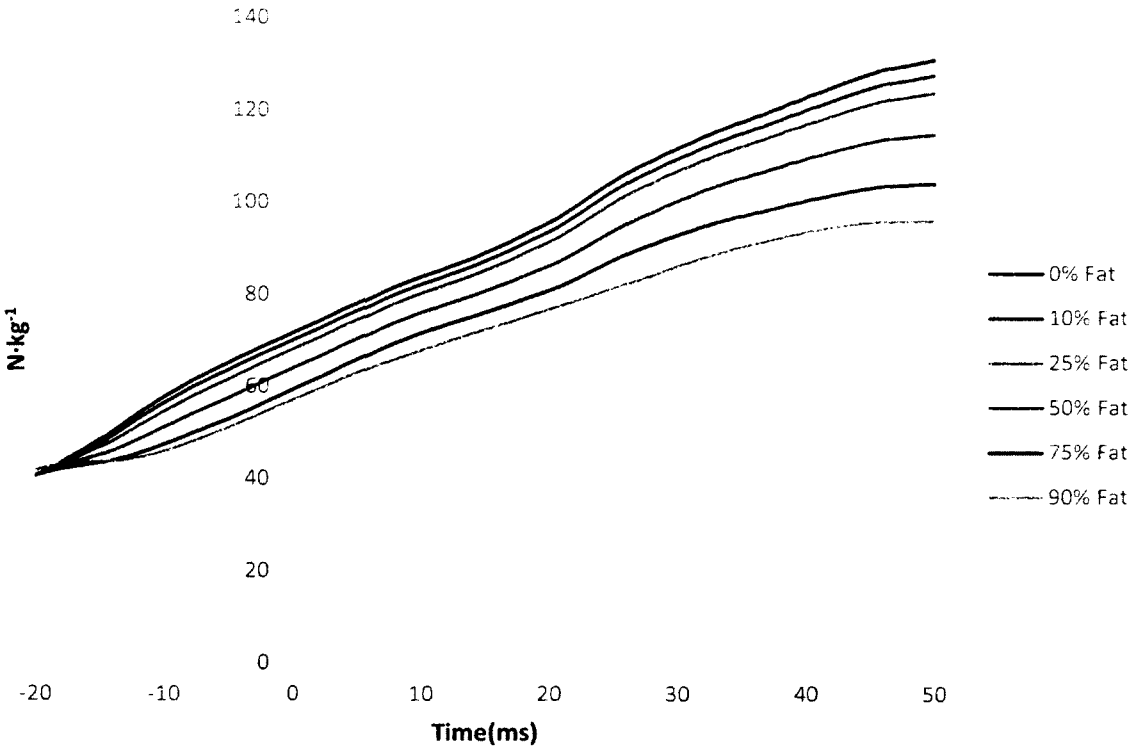

Figure 3-4: Group average total quadriceps muscle force across all fatigue levels

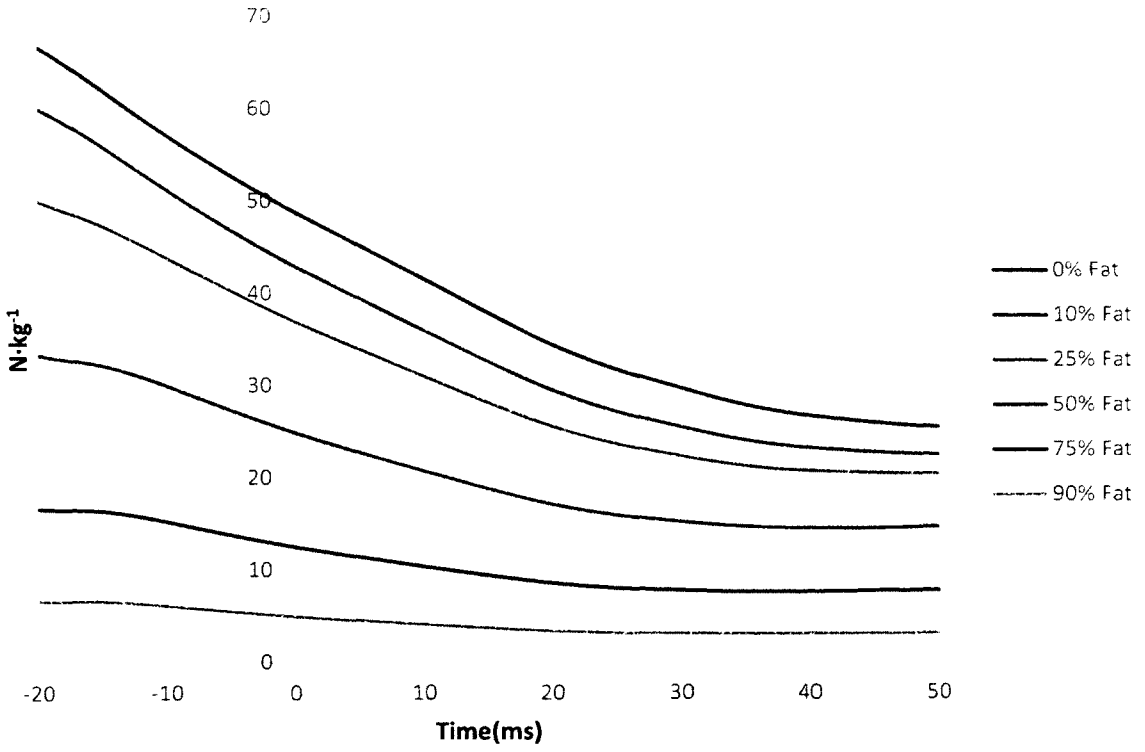

Figure 3-5: Group average total hamstrings muscle force across all fatigue levels

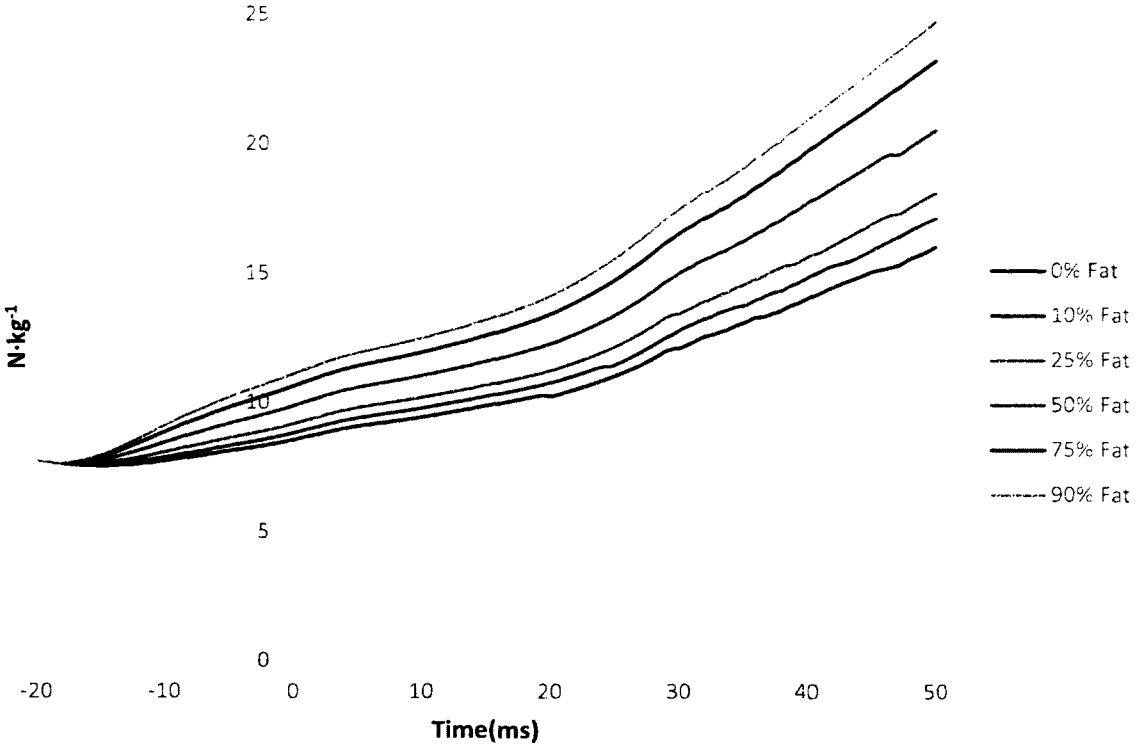

Figure 3-6: Group average total gastrocnemius muscle force across all fatigue levels

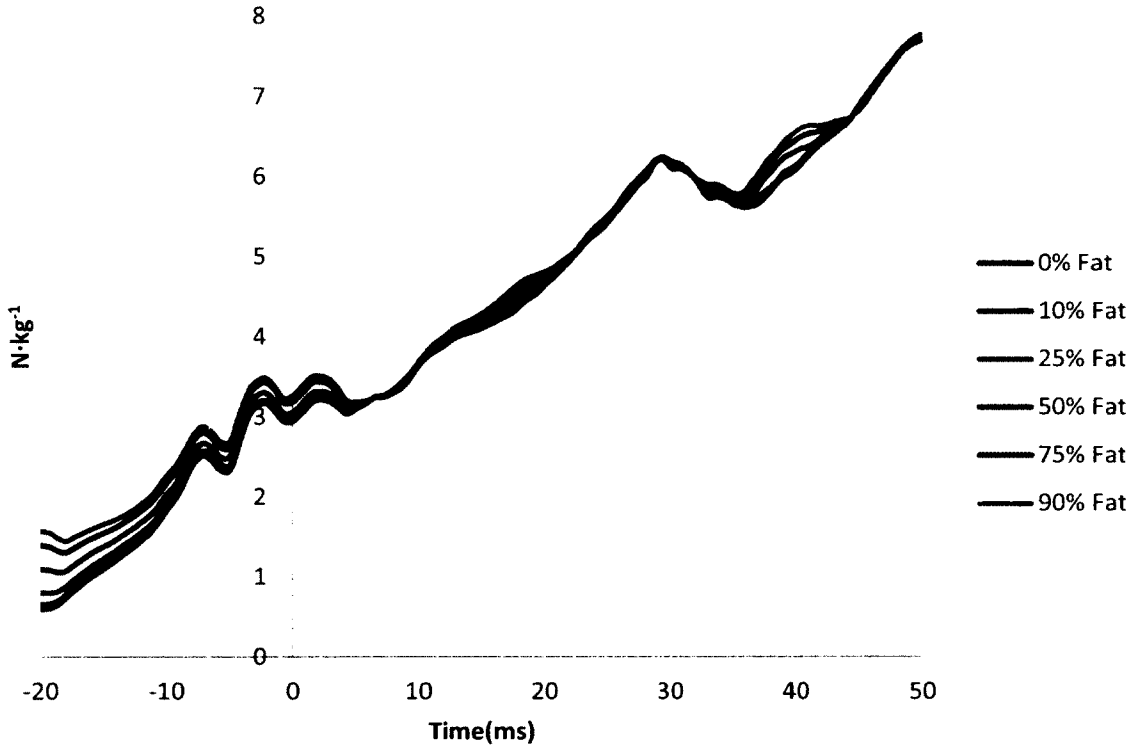

Figure 3-7: Group average ACL_{Total} loading across all fatigue levels

Table 3-5: Group average (mean±st.dev.) time, sagittal (ACL_S), frontal (ACL_F) and transverse (ACL_T) load values at peak ACL_{Total} load

	Pre-Fatigue	10% Fatigue	25% Fatigue	50% Fatigue	75% Fatigue	90% Fatigue	p-value	η_p^2
Peak ACL_{Total} time (ms)	37.8±13.6	37.8±13.6	41.1±13.6	41.4±13.8	41.4±13.8	41.4±13.8	0.41	0.17
Peak ACL_{Total} ($N \cdot kg^{-1}$)	8.38±2.65	8.39±2.66	8.39±2.66	8.47±2.76	8.54±2.87	8.57±2.94	0.33	0.19
Planar ACL Components ($N \cdot kg^{-1}$)								
ACL_S	6.34±2.06	6.31±2.10	6.49±2.30	6.37±2.39	6.28±2.48	6.23±2.53	0.83	0.07
ACL_F	1.31±1.38	1.36±1.38	1.03±0.40	1.14±0.32	1.19±0.13	1.23±0.15	0.96	0.03
ACL_T	0.72±0.47	0.72±0.47	0.86±0.42	0.96±0.53	1.06 ±0.78	1.11±0.96	0.54	0.14

Table 3-6: Effects of fatigue on average (mean±st.dev.) tibiofemoral contact forces and knee joint moments at peak ACL_{Total} load

	Pre-Fatigue	10% Fatigue	25% Fatigue	50% Fatigue	75% Fatigue	90% Fatigue	p-value	η_p^2
Tibiofemoral Contact Forces ($N \cdot kg^{-1}$)								
Shear	-7.25±1.97	-7.11±1.99	-7.70±2.66	-7.33±2.69	-6.98 ±2.69	-6.79±2.69	0.69	0.10
Compressive	2.06±4.0	2.07±3.94	3.37±4.79	3.59±4.87	3.82±4.97	3.97±5.04	0.29	0.20
Knee Joint Moments ($Nm \cdot kg^{-1}$)								
Sagittal	1.96±1.06	2.06±1.08[a]	2.56±0.88	2.81±0.97[c]	3.03±1.06[a,c,d]	3.15±1.11[e]	0.001	0.56
Frontal	-0.25±0.70	-0.25±0.70	-0.37±0.45	-0.36±0.44	-0.40±0.42	-0.42±0.39	0.29	0.20
Transverse	-0.09±0.18	-0.08±0.17	-0.15±0.14	-0.15±0.16	-0.15±0.18	-0.15±0.19	0.86	0.06

a indicates joint moment is significantly different compared to pre-fatigue ($p<0.05$)
b indicates joint moment is significantly different compared to 10% fatigue ($p<0.05$)
c indicates joint moment is significantly different compared to 25% fatigue ($p<0.05$)
d indicates joint moment is significantly different compared to 50% fatigue ($p<0.05$)
e indicates joint moment is significantly different compared to pre-fatigue and all other fatigue levels ($p<0.05$)

Table 3-7: Xia fatigue model average (mean±st.dev.) predicted kinematics (degrees) for the hip, knee and ankle joints at peak ACL load. Positive joint angles represent hip flexion, adduction and internal rotation; knee flexion, adduction and internal rotation; and ankle dorsiflexion

	Pre-Fatigue	10% Fatigue	25% Fatigue	50% Fatigue	75% Fatigue	90% Fatigue	p-value	η_p^2
Hip								
Sagittal[f]	49.3±17.0	49.7±17.1	50.6±17.5	51.9±17.9	53.3±18.4	54.2±18.7	<0.001	0.74
Frontal	-9.44±5.32	-9.57±5.30[a]	-10.0 ±5.50	-10.4±5.41[a,b,c]	-10.7±5.25[a,b,c,d]	-10.9±5.19[e]	<0.001	0.67
Transverse	8.62±16.5	8.65±16.5	8.30±15.7	8.40±15.7	8.54±15.7	8.62±15.7	0.76	0.09
Knee								
Sagittal	-44.1±7.36	-42.6±6.86[a]	-41.6±7.17	-37.8±5.93[a,b,c]	-34.3±4.85[a,b,c,d]	-32.4±4.43[e]	<0.001	0.79
Frontal	-3.28±6.14	-3.16±6.01	-3.11±5.93	-2.95±5.62	-2.93±5.30	-2.96±5.12	0.88	0.064
Transverse	4.09±3.91	4.28±3.86[a]	4.79±3.76[a]	5.26±3.58[a,b,c]	5.62±3.48[a,b,c,d]	5.81±3.46[e]	<0.001	0.78
Ankle								
Sagittal	-4.82±10.3	-4.77±10.3	-4.27±10.6	-4.13±10.6	-4.08±10.7	-4.06±10.7	0.04	0.35

a indicates rotation is significantly different compared to pre-fatigue ($p<0.05$)
b indicates rotation is significantly different compared to 10% fatigue ($p<0.05$)
c indicates rotation is significantly different compared to 25% fatigue ($p<0.05$)
d indicates rotation is significantly different compared to 50% fatigue ($p<0.05$)
e indicates rotation is significantly different compared to pre-fatigue and all other fatigue levels ($p<0.05$)
f indicates all rotations are significantly different when compared to pre-fatigue and all other fatigue levels($p<0.05$)

CHAPTER 4

DISCUSSION

Two analytical fatigue models were implemented into a 29 DOF musculoskeletal model and validated using experimental data. It was hypothesized that the Tang *et al* [16] model would better estimate the effects of fatigue due to the subject specific nature of the analytical model. The second purpose of this study was to determine the effects of various levels of hamstrings fatigue on lower extremity muscle forces. The second hypothesis stated hamstrings force producing capabilities would decrease as hamstrings fatigue increased. The third purpose of this study was to determine the effects of various levels of hamstrings fatigue on ACL load. It was hypothesized that peak ACL load would increase as hamstrings fatigue increased.

4.1 Comparison of Analytical Fatigue Models

The analytical fatigue models by Tang *et al* [16] and Xia *et al* [6] were compared to the experimental muscle force data in order to determine which analytical fatigue model was the most accurate. The Xia *et al* [6] and Tang *et al* [16] models produced similar RMS differences compared to the experimental kinematics at 1.88 $N \cdot kg^{-1}$ and 1.91 $N \cdot kg^{-1}$, respectively. Therefore, the Xia *et al* [6] model was chosen to test the effects of fatigue due to its ease of use (i.e. general fatigue and recovery paramters). While the Xia *et al* [6] model was chosen, the similar RMS difference observed with the Tang *et al* [16] model suggests that both models have similar abilities in estimating the effects of fatigue and further analysis of both models with a larger sample size is recommended.

Lower extremity kinematic data produced by the Xia *et al* [6] model were compared to the post-fatigue experimental kinematic data by determining the RMS differences between the experimental and fatigue model estimated kinematic data. Knee sagittal plane rotation demonstrated an RMS difference of 5.67° when compared to the post-fatigue experimental data. Both the knee frontal and transverse plane rotations demonstrated RMS differences of less than 1°. Both heads of the gastrocnemius, sartorius and gracilis muscles are considered the most important muscles in knee flexion while performing long-range, fast types of movements [128]. In this study, the sartorius and gracilis muscle activations were not constrained using experimental EMG data, as was done with the hamstrings and gastrocnemius muscles and may therefore account for the large differences in knee sagittal plane rotation.

The muscle forces and kinematics predicted, in this study, by the Xia *et al* [6] model provided an estimation of the effects of fatigue for a complex task, such as the side step cut, at a known level of fatigue. The Xia *et al* [6] fatigue model was previously validated for isometric tasks at various loading conditions and was used to estimate the effects of peripheral fatigue. Athletic activities, which involve landing, running, etc., may induce central fatigue in addition to peripheral fatigue [129]. The isolated hamstrings fatigue protocol used in this study may have induced central fatigue within the participants as voluntary force generation can be limited due to inhibitory effects within the central nervous system [130-132] despite strong verbal encouragement [43]. Central fatigue may affect knee dynamics by increasing the chance of errors in placement of the lower extremity upon landing, as knee valgus loading was found to be dependent on lower extremity position at initial contact [133]. Estimation of central fatigue was not

included in the Xia *et al* [6] fatigue model when estimating muscle forces and the results in this study may be limited by the lack of estimation of central fatigue.

4.2 Muscle Force Estimations

Estimations of *in-vivo* muscle forces are difficult to perform yet the use of musculoskeletal modeling software provides an ability to estimate muscle forces under various conditions. Quadriceps, hamstrings and gastrocnemius muscle forces were estimated under various levels of hamstrings fatigue while performing the side step cut. Hamstrings muscle force production exhibited significant decreases as an effect of fatigue and confirmed the hypothesis of aim two. Hamstrings muscle force decreased by 89% (23.8 $N \cdot kg^{-1}$) at the 90% fatigue level. The role of the knee stabilizers (i.e. quadriceps, hamstrings and gastrocnemius) and the torque generating abilities of these muscle play an important role in injury prevention [134]. Large decreases in hamstrings muscle forces, predicted by the Xia *et al* [6] model, may suggest that hamstrings fatigue decreases knee joint stability [59, 134] as one function of the hamstrings muscle is to prevent tibial rotation [57] and translation [59]. The decreased hamstrings muscle activation during this time period may suggest a reduction in force producing capabilities and may place the hamstrings muscle at a mechanical disadvantage (i.e. decrease in knee stability) during a side step cut. Decreased hamstrings muscle force may increase anterior tibial translation [59, 137] and shear loading of the ACL [59], which may increase the risk of ACL injury as fatigue levels increase [135, 136].

The quadriceps muscle group experienced significant decreases in force producing capabilities. Quadriceps muscle force decreased by 20.5% (24.1 $N \cdot kg^{-1}$) at the 90% fatigue level. An overall decrease in hamstrings muscle force, as demonstrated by

the participants in this study, may reduce the force needed by the quadriceps muscle to extend the knee joint, in order to perform the side step cut as the knee extensors are used to eccentrically decelerate the body's center of mass upon landing [127]. The quadriceps muscle activation, prior to initial contact and throughout the braking phase of the side step cut, was found to be higher than that of the hamstrings muscle activation [135, 136]. Despite a decrease in the hamstrings to quadriceps ratio, the quadriceps may still produce a large enough force to cause an increase in the anterior shear force as the fatigued hamstrings muscle is unable to produce a posterior shear force on the tibia [7] and therefore, the hamstrings muscle is unable to counteract the quadriceps muscle force and prevent excess tibial translation.

The gastrocnemius muscle demonstrated a significant increase in force production across multiple levels of fatigue. Gastrocnemius muscle force increased by 69% (8.9 $N \cdot kg^{-1}$) at the 90% fatigue level. The gastrocnemius acts as a secondary knee flexor and contributes to knee joint stability [138]. Therefore, an increase in gastrocnemius muscle force may suggest a compensatory mechanism for knee joint stability, thereby attempting to reduce the effects of hamstrings fatigue on knee joint stability and ACL load.

4.3 ACL Load Estimations

The time point at which peak ACL_{Total} loading occurs was similar across the various fatigue levels. Peak ACL_{Total} loading did not demonstrate significant increases as an effect of hamstrings fatigue, thereby nullifying the hypothesis of aim 3 with the current sample size. The sagittal, frontal and transverse ACL loading contributed 73%, 14% and 13%, respectively, to the peak ACL_{Total} loading at the 90% fatigue level.

Significant increases in peak ACL load, sagittal and frontal plane ACL load were exhibited by recreationally active female athletes while performing an anticipated side step cut after submaximal hamstrings fatigue [8]. Peak, sagittal and transverse plane ACL loads [8] were similar to the present study, yet the frontal plane ACL loads were different (Table 4-1).

Table 4-1: Peak and planar ACL loads ($N \cdot kg^{-1}$) obtained in this study compared to those by Weinhandl *et al* [8] at 75% hamstrings muscle fatigue. The planar components of the ACL load were determined at the time point when peak ACL load occurred.

	Current Study	Weinhandl *et al* [8]
Peak ACL Load	8.54±2.87	13.3±3.5
Sagittal Plane ACL Load	6.28±2.48	8.82±3.03
Frontal Plane ACL Load	1.19±0.13	3.39±0.88
Transverse Plane ACL Load	1.06±0.78	1.10±0.48

Similarities and differences existed between both the experimental and computational modeling aspects of the present study and the study by Weinhandl *et al* [8]. The participants in this study shared similar athletic profiles, performed the anticipated side step cut at a similar speed and were subjected to a similar level of submaximal hamstrings fatigue (75% fatigue) as the athletes in the Weinhandl *et al* [8] study. The present study used an isometric hamstrings fatigue protocol while the Weinhandl *et al* [8] study used an isokinetic hamstrings fatigue protocol and may elicit different effects on the hamstrings muscle force producing capabilities. Differences in neural signals exist between concentric and isometric endurance protocols [139].

Specifically, integrated EMG (IEMG) during the isometric protocol decreased yet the IEMG signal was maintained or increased during the concentric protocol when compared to the pre-fatigue state [139]. Thereby, suggesting a decrease [47] and increase [140], in the isometric and concentric neural drive to peripheral muscle, respectively. The musculoskeletal models developed in this study used generic maximum isometric strengths whereas the models used in the Weinhandl *et al* [8] study used subject specific strength parameters. Six participants were used in this study, 17 participants were used in the Weinhandl *et al* [8] study. In this study, experimental EMG data were used as inputs to the analytical fatigue model in order to estimate "fatigued" activations which were used to constrain activations of the hamstrings muscles in the musculoskeletal models. Excitations of the hamstrings muscles were not constrained in the previous study [8] when developing their musculoskeletal models. Using EMG data to constrain the excitation profiles of the hamstrings muscles may help provide a more accurate estimate of the timing and intensity of hamstrings muscle activations while performing the side step cut. In addition, the study by Weinhandl *et al* [8] reduced the hamstrings muscle maximum isometric strengths of their musculoskeletal models in order to represent a fatigued state. Finally, the posterior tibial slope used in this study to calculate ACL load was 0° and was different than the posterior tibial slope of 8.5° used in previous studies [8, 37, 38, 86]. A sensitivity analysis where the posterior tibial slope was varied incrementally was found to have a large influence on ACL loading [130]. Specifically, increases in posterior tibial slope increased the ACL loading while decreases in posterior tibial slope decreased ACL loading [130]. This difference in posterior tibial slope may

cause a difference in ACL loading estimations between this study and the Weinhandl *et al* [8] study.

4.4 Knee Joint Kinematics and Kinetics

Tibiofemoral shear contact force was not significantly affected by hamstrings fatigue. If an increase in the shear contact force at peak ACL_{Total} occurred in this study, it could be suggested that more of an anterior force on the tibia was applied, thereby placing a larger amount of stress on the ACL. The hamstrings muscle acts on the tibia by providing a posterior shear force in order to prevent anterior translation [7]. Shear tibiofemoral contact force decreased as an effect of hamstrings fatigue and led to an increase in sagittal plane ACL loading [8]. These differences in tibiofemoral contact forces may be due to the use of different posterior tibial slopes (0° vs. 8.5°) between this study and the Weinhandl *et al* [8] study. Chappell *et al* [7] suggested that fatigue of the hamstrings muscle reduces the angle between the hamstrings and tibia, thereby increasing anterior shear force. Despite a decrease in quadriceps muscle force, the quadriceps muscle may have produced an increase in the anterior shear force as the quadriceps muscle is producing a large enough force to cause anterior tibial translation. The athletes in this study exhibited a decrease in knee flexion, due to fatigue, which may suggest an increase in ACL loading [141, 142]. An increase in the gastrocnemius muscle force, as fatigue levels increased, may suggest a compensatory mechanism for the fatigued hamstrings muscle. The increased gastrocnemius muscle force provided additional joint stability, limited anterior shear force and tibial translation despite fatigue and thereby decreased the sagittal plane ACL load.

Frontal plane ACL loading did not demonstrate significant effects due to hamstrings fatigue. Conversely, frontal plane ACL loading significantly increased as an effect of hamstrings fatigue and was due to an increase in the knee abduction moment at peak total ACL loading in a previous study [8]. In the present study, the knee abduction moment did not increase due to fatigue, unlike previous studies which suggest an increase in knee abduction moment may increase frontal plane ACL loading [7, 8, 143]. Additionally, the participants in this study, similar to previous studies [33, 50, 55], demonstrated increased knee extension and internal rotation [33, 50, 55] as an effect of fatigue. An increase in knee extension and internal rotation lead to a more erect and internally rotated lower extremity and have been suggested to increase ACL loading [7, 12]. Despite the similarities, it is difficult to compare the results of this study to previous studies as previous studies that analyzed the effects of fatigue on side step cutting [33, 50, 55] used a general fatigue model compared to the isolated fatigue model used in this study. General fatigue of the knee joint was found to significantly alter joint proprioception without a reduction in torque producing capabilities of the knee extensors and flexors yet local fatigue demonstrated the opposite effect on the knee joint [144]. The torque producing capabilities of the hamstrings muscle, in this study, were reduced as the hamstrings muscle force was decreased as an effect of fatigue. Also, ankle joint sagittal plane rotations demonstrated a significant main effect of fatigue yet the post-hoc analyses did not exhibit any significant differences due to the current study being unpowered. Peak ACL loading data from Weinhandl *et al* [8] was used to perform a power analysis which revealed that a minimum of 11 participants were needed in order to obtain a power of 80% in this study.

4.5 Limitations

The experimental limitations of this study involved the protocol used to induce fatigue, the use of an anticipated cutting task, recreational athletes and a minimal number of subjects. An isokinetic hamstrings fatigue protocol, as used in a previous study [8], may better represent the type of fatigue and muscle activations that are present in an athletic event (i.e. soccer, basketball, etc.). An isometric protocol was chosen as to limit the effects of residual fatigue on the surrounding musculature of the lower extremity. Additionally, this study required a precise measurement of hamstrings force producing capabilities in order to predict the effects of fatigue and therefore, an isometric protocol provided the best approach to obtaining these precise force measurements. An anticipated side step cut was used in this study as to limit the number of variables involved in the effects of hamstrings muscle fatigue yet the anticipated task may not closely simulate an athletic competition and cause differences in results between studies. Task anticipation had different effects on lower extremity mechanics [31, 33] and when combined with fatigue, unanticipated tasks had a more pronounced effect on lower extremity mechanics [33]. Therefore, additional studies should be performed to understand the effects of fatigue on task anticipation. The athletes used in this study were recreational athletes and may exhibit differences in lower extremity loading patterns compared to more experienced (i.e. collegiate, etc.) athletes. Experience level was found to directly correspond to a lower degree of knee joint variability and may have a large impact on ACL injury risk during side step cutting [58]. Six participants were used in this study and did not provide an adequate subject pool to determine accurate effects of fatigue on ACL loading, as a post-hoc power analysis revealed a power of approximately

50% in the current study. In the future, similar studies should be performed using a larger number of participants, a more experienced athletic population and an isokinetic fatigue protocol in order to estimate the effects of fatigue on ACL loading. In addition, the fatigue models could be tested for use in estimating the effects of a generalized fatigue protocol. Current research [7, 9, 10, 33, 50, 51, 55] use general fatigue protocols, in order to replicate the types of fatigue that an athlete may be exposed to during an athletic event and it may be beneficial to determine whether or not the Xia *et al* [6] and Tang *et al* [16] are capable of estimating the effects of a more generalized fatigue protocol.

Physiological inputs used in determining muscle forces and ACL loading within the musculoskeletal models may have affected the results of this study. This study used a posterior tibial slope of 0° compared to other studies that used a slope of 8.5° [8, 38, 86, 145]. In the future, subject-specific geometry obtained from medical imaging techniques should be incorporated into a similar musculoskeletal model to determine the effects of fatigue on ACL loading. Subject-specific geometry will allow for a better representation of the posterior tibial slope and a more accurate estimation of ACL loading. Additionally, subject-specific isokinetic strength values should be used to scale the default maximum isometric muscle forces of the musculoskeletal models similar to Weinhandl *et al* [8, 145] as these strength values may affect the estimation of muscle forces and ACL loading. The maximum isometric forces of the muscles within the musculoskeletal model are based off of a cadaveric data set [70] and therefore, may have affected the accuracy of the analytical fatigue models in estimating the forces of fatigue.

Both the Xia *et al* [6] and Tang *et al* [16] fatigue models were validated for isometric tasks yet were used in this study to estimate the effects of fatigue during a dynamic task. Further studies should be conducted in order understand and possibly validate the use of these analytical models to estimate the effects of fatigue during dynamic tasks. The Xia *et al* [6] model incorporated generic parameters, based upon previous work [74], in order to estimate the effects of fatigue while the Tang *et al* [16] model required subject specific parameters (i.e. fatigue and recovery curves) and therefore, due to its subject specific nature, the Tang *et al* [16] model may be prone to variability in estimation of the effects of fatigue. In this study, the fatigue curve from the second testing session was used rather than the fatigue curve determined in the first testing session as the overall maximal voluntary isometric contraction force of the hamstrings muscle of the group were similar between both testing sessions. Future studies should be performed to determine the inter-day variability in determination of fatigue and recovery parameters of the hamstrings muscle. The variability between the use of fatigue and recovery curves from different testing sessions should be studied as it will help determine the sensitivity of the analytical fatigue models. In addition, future studies should compare the estimations of ACL loading between both fatigue models.

4.6 Future Work

The use of an analytical fatigue model, similar to this study, to study various athletic maneuvers (i.e. drop-landings, stop-jumps, crossover cuts, etc.) may aid researchers in better understanding the effects of fatigue on risk of ACL injury in both healthy and previously injured populations. Repeat ACL rupture after reconstruction occurred in 12% of patients over a five year follow-up period [146]. ACL reconstructed

individuals, when compared to a healthy population, demonstrated significant decreases in the peak external flexion moment (net quadriceps moment) during jogging and cutting yet there were no differences in the peak external extension moment (net hamstrings moment) [147]. With a risk of rupturing the ACL graft, it is important to understand the mechanisms that may increase the risk of a repeat injury in the reconstructed knee, particularly in athletes that perform dynamic tasks such as a side step cut. People with patellofemoral pain (PFP) exhibit differences in the recruitment of the quadriceps muscles [148, 149] and exhibit different lower extremity mechanics when fatigued compared to a healthy population [150]. Using the model developed in this study, may help researchers understand the effects of fatigue on PFP and develop better methods of training and rehabilitation for athletes that experience PFP and wish to perform at high levels of activity.

CHAPTER 5

CONCLUSION

The Xia *et al* [6] analytical fatigue model provided an estimation of the effects of hamstrings fatigue on lower extremity muscle forces and ACL loading in a group of recreationally active females. The results of this study, similar to previous studies [8, 10], suggest that hamstrings fatigue reduces the force producing capabilities of the hamstrings muscle group, alters loading patterns within the knee joint and may lead to an increased risk of injury. Participants appeared to compensate for the reduced hamstrings force producing capabilities by reducing quadriceps and increasing gastrocnemius muscle force production. The results in this study can be improved upon by using subject-specific parameters for maximal isometric muscle forces and recruiting a larger number of participants in order to obtain a better estimation of fatigued muscle forces and ACL loading. Using the model developed in this study can aid researchers in understanding the effects of fatigue on risk of ACL injury in order to develop better training programs in order to reduce the risk of injury.

REFERENCES

[1] D. M. Daniel, M. L. Stone, B. E. Dobson, D. C. Fithian, D. J. Rossman, and K. R. Kaufman, "Fate of the ACL-injured Patient: A Prospective Outcome Study," *The American Journal of Sports Medicine,* vol. 22, pp. 632-644, 1994.

[2] A. M. W. Chaudhari, P. L. Briant, S. L. Bevill, S. Koo, and T. P. Andriacchi, "Knee Kinematics, Cartilage Morphology, and Osteoarthritis after ACL Injury," *Medicine & Science in Sports & Excercise,* vol. 40, pp. 215-222, 2008.

[3] R. H. T. Edwards, D. K. Hill, D. A. Jones, and P. A. Merton, "Fatigue of Long Duration in Human Skeletal Muscle After Exercise," *Journal of Physiology,* vol. 272, pp. 769-778, 1977.

[4] S. K. Hunter, "Sex Differences and Mechanisms of Task-Specific Muscle Fatigue," *Exercise and Sport Sciences Review,* vol. 37, pp. 113-122, 2009.

[5] S. K. Hunter, J. Duchateau, and R. M. Enoka, "Muscle Fatigue and the Mechanisms of Task Failure," *Exercise and Sport Sciences Review,* vol. 32, pp. 44-49, 2004.

[6] T. Xia and L. A. Frey Law, "A theoretical approach for modeling peripheral muscle fatigue and recovery," *Journal of Biomechanics,* vol. 41, pp. 3046-3052, 2008.

[7] J. D. Chappell, D. C. Herman, B. S. Knight, D. T. Kirkendall, W. E. Garrett, and B. Yu, "Effect of Fatigue on Knee Kinetics and Kinematics in Stop-Jump Tasks," *The American Journal of Sports Medicine,* vol. 33, pp. 1022-1029, 2005.

[8] J. T. Weinhandl, J. E. Earl-Boehm, K. T. Ebersole, W. E. Huddleston, B. S. R. Armstrong, and K. M. O'Connor, "Reduced hamstrings strength increases anterior cruciate ligament loading during anticipated sidestep cutting," *Clinical Biomechanics, In Press*, 2014.

[9] G. Sanna and K. M. O'Connor, "Fatigue-related changes in stance leg mechanics during sidestep cutting maneuvers," *Clinical Biomechanics,* vol. 23, pp. 946-954, 2008.

[10] S. G. McLean, R. E. Felin, N. Suedekum, G. Calabrese, A. Passerallo, and S. Joy, "Impact of fatigue on Gender-Based High-Risk Landing Strategies," *Medicine & Science in Sports & Excercise,* vol. 39, pp. 502-514, 2007.

[11] J. Iguchi, H. Tateuchi, M. Taniguchi, and N. Ichihashi, "The effect of sex and fatigue on lower limb kinematics, kinetics, and muscle activity during unanticipated side-step cutting," *Knee Surgery, Sports Traumatology, Arthroscopy,* vol. 22, pp. 41-48, 2014.

[12] K. L. Markolf, D. M. Burchfield, M. M. Shapiro, M. F. Shepard, G. A. M. Finerman, and J. L. Slauterbeck, "Combined knee loading states that generate high anterior cruciate ligament forces," *Journal of Orthopaedic Research,* vol. 13, pp. 930-935, 1995.

[13] D. Hawkins and M. L. Hull, "Muscle force as affected by fatigue: Mathematical model and experimental verification," *Journal of Biomechanics,* vol. 26, pp. 1117-1128, 1993.

[14] L. Ma, D. Chablat, F. Bennis, and W. Zhang, "A new simple dynamic muscle fatigue model and its validation," *International Journal of Industrial Ergonomics,* vol. 39, pp. 211-220, 2009.

[15] M. S. Marion, A. S. Wexler, and M. L. Hull, "Predicting fatigue during electrically stimulated non-isometric contractions," *Muscle & Nerve,* vol. 41, pp. 857-867, 2010.

[16] C. Y. Tang, B. Stojanovic, C. P. Tsui, and M. Kojic, "Modeling of muscle fatigue using Hill's model," *Bio-Medical Materials & Engineering,* vol. 15, pp. 341-348, 2005.
[17] J. Z. Liu, R. W. Brown, and G. H. Yue, "A Dynamical Model of Muscle Activation, Fatigue and Recovery," *Biophysical Journal,* vol. 82, pp. 2344-2359, 2002.
[18] T. A. Blackburn and E. Craig, "Knee Anatomy: A Brief Review," *Physical Therapy,* vol. 60, pp. 1556-1560, 1980.
[19] H. Gray, *Gray's Anatomy.* New York: Churchill Livingstone Inc., 1995.
[20] H. N. Andersen and P. Dyhre-Poulsen, "The anterior cruciate ligament does play a role in controlling axial rotation in the knee," *Knee Surgery, Sports Traumatology, Arthroscopy,* vol. 5, pp. 145-149, 1997.
[21] E. Arendt and R. Dick, "Knee Injury Patterns Among Men and Women in Collegiate Basketball and Soccer: NCAA Data and Review of Literature," *The American Journal of Sports Medicine,* vol. 23, pp. 694-701, 1995.
[22] K. C. Miyasaka, D. M. Daniel, M. L. Stone, and P. Hirshman, "The incidence of knee ligament injuries in the general population," *American Journal of Knee Surgery,* vol. 4, pp. 3-8, 1991.
[23] J. Agel, E. A. Arendt, and B. Bershadsky, "Anterior Cruciate Ligament Injury in National Collegiate Athletic Association Basketball and Soccer," *The American Journal of Sports Medicine,* vol. 33, pp. 524-531, 2005.
[24] F. R. Noyes, P. A. Mooar, D. S. Matthews, and D. L. Butler, "The symptomatic anterior cruciate-deficient knee. Part I: the long-term functional disability in athletically active individuals," *The Journal of Bone and Joint Surgery,* vol. 65, pp. 154-162, 1983.
[25] T. E. Hewett, G. D. Myer, K. R. Ford, R. S. Heidt, A. J. Colosimo, S. G. McLean, A. J. van den Bogert, M. V. Paterno, and P. Succop, "Biomechanical Measures of Neuromuscular Control and Valgus Loading of the Knee Predict Anterior Cruciate Ligament Injury Risk in Female Athletes: A Prospective Study," *The American Journal of Sports Medicine,* vol. 33, pp. 492-501, 2005.
[26] L. Heller and J. Langman, "The Menisco-Femoral Ligaments of the Human Knee," *The Journal of Bone and Joint Surgery [Br],* vol. 46B, pp. 307-313, 1964.
[27] T. E. Hewett, "Neuromuscular and hormonal factors associated with knee injuries in female athletes: strategies for intervention," *Sports Medicine,* vol. 29, pp. 313-327, 2000.
[28] J. Hashemi, R. Breighner, N. Chandrashekar, D. M. Hardy, A. M. W. Chaudhari, S. J. Schultz, J. R. Slauterbeck, and B. D. Beynnon, "Hip extension, knee flexion paradox: A new mechanism for non-contact ACL injury," *Journal of Biomechanics,* vol. 44, pp. 577-585, 2011.
[29] S. G. McLean, S. Lucey, M., S. Rohrer, and C. Brandon, "Knee joint anatomy predicts high-risk *in vivo* dynamic landing knee biomechanics," *Clinical Biomechanics,* vol. 25, pp. 781-788, 2010.
[30] S. C. Landry, K. A. McKean, C. L. Hubley-Kozey, W. D. Stanish, and K. J. Deluzio, "Neuromuscular and Lower Limb Biomechanical Differences Exist Between Male and Female Elite Adolescent Soccer Players During an Unanticipated Side-cut Maneuver," *The American Journal of Sports Medicine,* vol. 35, pp. 1888-1900, 2007.
[31] T. Besier, D. G. Lloyd, T. R. Ackland, and J. L. Cochrane, "Anticipatory effects on knee joint loading during running and cutting maneuvers," *Medicine & Science in Sports & Excercise,* vol. 33, pp. 1176-1181, 2001.

[32] S. G. McLean, X. Huang, A. Su, and A. J. van den Bogert, "Sagittal plane biomechanics cannot injure the ACL during sidestep cutting," *Clinical Biomechanics,* vol. 19, pp. 828-838, 2004.
[33] B. S. Borotikar, R. Newcomer, R. Koppes, and S. G. McLean, "Combined effects of fatigue and decision making on female lower limb landing postures: Central and peripheral contributions to ACL injury risk," *Clin Biomech,* vol. 23, pp. 81-92, 2008.
[34] J. Bencke and M. K. Zebis, "The influence of gender on neuromuscular pre-activity during side-cutting," *Journal of Electromyography and Kinesiology,* vol. 21, pp. 371-375, 2011.
[35] S. M. Sigward and C. M. Powers, "The influence of gender on knee kinematics, kinetics and muscle activation patterns during side-step cutting," *Clinical Biomechanics,* vol. 21, pp. 41-48, 2006.
[36] N. Ali and G. Rouhi, "Barriers to Predicting the Mechanisms and Risk Factors of Non-Contact Anterior Cruciate Ligament Injury," *The Open Biomedical Engineering Journal,* vol. 4, pp. 178-189, 2010.
[37] J. T. Weinhandl, J. E. Earl-Boehm, K. T. Ebersole, H. W.E., B. S. R. Armstrong, and K. M. O'Connor, "Anticipatory effects on anterior cruciate ligament loading during sidestep cutting," *Clinical Biomechanics,* vol. 28, pp. 655-663, 2013.
[38] T. W. Kernozek and R. J. Ragan, "Estimation of anterior cruciate ligament tension from inverse dynamics and electromyography in females during drop landing," *Clinical Biomechanics,* vol. 23, pp. 1279-1286, 2008.
[39] C.-F. Lin, M. Gross, C. Ji, D. Padua, P. Weinhold, W. E. Garrett, and B. Yu, "A stochastic biomechanical model for risk and risk factors of non-contact anterior cruciate ligament injuries," *Journal of Biomechanics,* vol. 42, pp. 418-423, 2009.
[40] J. Kar and P. M. Quesada, "A Musculoskeletal Modeling Approach for Estimating Anterior Cruciate Ligament Strains and Knee Anterior-Posterior Shear Forces in Stop-Jumps Performed by Young Recreational Female Athletes," *Annals of Biomedical Engineering,* vol. 41, pp. 338-348, 2013.
[41] J. Kar and P. M. Quesada, "A Numerical Simulation Approach to Studying Anterior Cruciate Ligament Strains and Internal Froces Among Young Recreational Women Performing Valgus Inducing Stop-Jump Activities," *Annals of Biomedical Engineering,* vol. 40, pp. 1679-1691, 2012.
[42] R. M. Enoka and J. Duchateau, "Muscle fatigue: what, why and how it influences muscle function," *The Journal of Physiology,* vol. 586, pp. 11-23, 2008.
[43] N. K. Vøllestad, "Measurement of human muscle fatigue," *Journal of Neuroscience Methods,* vol. 74, pp. 219-227, 1997.
[44] C. Y. Tang, C. P. Tsui, B. Stojanovic, and M. Kojic, "Finite element modelling of skeletal muscles coupled with fatigue," *International Journal of Mechanical Sciences,* vol. 49, pp. 1179-1191, 2007.
[45] J. H. Williams, "Contractile apparatus and sarcoplasmic reticulum function: effects of fatigue, recovery, and elevated Ca^{2+}," *Journal of Applied Physiology,* vol. 83, pp. 444-450, 1997.
[46] B. Bigland-Ritchie and J. J. Woods, "Changes in Muscle Contractile Properties and Neural Control During Human Muscular Fatigue," *Muscle & Nerve,* vol. 7, pp. 691-699, 1984.

[47] R. M. Enoka and D. G. Stuart, "Neurobiology of muscle fatigue," *Journal of Applied Physiology,* vol. 72, pp. 1631-1648, 1992.
[48] S. P. Cairns, A. J. Knicker, M. W. Thompson, and G. Sjogaard, "Evaluation of Models Used to Study Neuromuscular Fatigue," *Exercise and Sport Sciences Review,* vol. 33, pp. 9-16, 2005.
[49] J. A. Kent-Braun, "Central and peripheral contributions to muscle fatigue in humans during sustained maximal effort," *European Journal of Applied Physiology,* vol. 80, pp. 57-63, 1999.
[50] S. Lucci, N. Cortes, B. Van Lunen, S. Ringleb, and J. Onate, "Knee and hip sagittal and transverse plane changes after two fatigue protocols," *Journal of Science and Medicince in Sport,* vol. 14, pp. 453-459, 2011.
[51] D. M. Brazen, M. K. Todd, J. P. Ambegaonkar, R. Wunderlich, and C. Peterson, "The Effect of Fatigue on Landing Biomechanics in Single-Leg Drop Landings," *Clinical Journal of Sports Medicine,* vol. 20, pp. 286-292, 2010.
[52] J. T. Weinhandl, J. D. Smith, and E. L. Dugan, "The effects of repetitive drop jumps on impact phase joint kinematics and kinetics," *Journal of Applied Biomechanics,* vol. 27, pp. 108-115, 2011.
[53] A. Benjaminse, A. Habu, T. C. Sell, J. P. Abt, F. H. Fu, J. B. Myers, and S. M. Lephart, "Fatigue alters lower extremity kinematics during a single-leg stop-jump task," *Knee Surgery, Sports Traumatology, Arthroscopy,* vol. 16, pp. 400-407, 2008.
[54] R. D. Hawkins, M. A. Hulse, C. Wilkinson, A. Hodson, and M. Gibson, "The association football medical research programme: an audit of injuries in professional football," *British Journal of Sports Medicine,* vol. 35, pp. 43-47, 2001.
[55] N. Cortes, D. Quammen, S. Lucci, E. Greska, and J. Onate, "A functional agility short-term fatigue protocol changes lower extremity mechanics," *Journal of Sports Science,* vol. 30, pp. 797-805, 2012.
[56] A. C. Thomas, R. M. Palmieri-Smith, and S. G. McLean, "Isolated hip and ankle fatigue are unlikely risk factors for anterior cruciate ligament injury," *Scandinavian Journal of Medicine & Science in Sports,* vol. 21, pp. 359-368, 2010.
[57] J. A. Nyland, D. N. M. Caborn, R. Shapiro, and D. L. Johnson, "Crossover cutting during hamstring fatigue produces transverse plane knee control deficits," *Journal of Athletic Training,* vol. 34, pp. 137-143, 1999.
[58] S. G. McLean, R. J. Neal, P. T. Myers, and M. R. Walters, "Knee Joint Kinematics During the Sidestep Cutting Manuever: Potential for Injury in Women," *Medicine & Science in Sports & Exercise,* vol. 31, pp. 959-968, 1999.
[59] M. Melnyk and A. Gollhofer, "Submaximal fatigue of the hamstrings impairs specific reflex components and knee stability," *Knee Surgery, Sports Traumatology, Arthroscopy,* vol. 15, pp. 525-532, 2007.
[60] D. A. Winter, *Biomechanics and Motor Control of Human Movement*, 3rd ed. Hoboken: Wiley, 2005.
[61] E. Henneman, G. Somjen, and D. O. Carpenter, "Functional significance of cell size in spinal motoneurons," *Journal of Neurophysiology,* vol. 28, pp. 560-580, 1965.
[62] E. Stalberg, S. D. Nandedkar, D. B. Sanders, and B. Falck, "Quantitative Motor Unit Potential Analysis," *Journal of Clinical Neurophysiology,* vol. 13, pp. 401-422, 1996.

[63] H. S. Milner-Brown, R. B. Stein, and R. Yemm, "The Orderly Recruitment of Human Motor Units During Voluntary Isometric Contractions," *Journal of Physiology* vol. 230, pp. 359-370, 1973.
[64] A. Nardone, C. Romano, and M. Schieppati, "Selective Recruitment of High-Threshold Human Motor Units During Voluntary Isotonic Lengthening of Active Muscles," *Journal of Physiology,* vol. 409, pp. 451-471, 1989.
[65] R. S. Staron, "Human skeletal muscle fiber types: delineation, development, and distribution," *Canadian Journal of Applied Physiology,* vol. 22, pp. 307-327, 1997.
[66] J. E. Markee, J. T. Logue, M. Williams, W. B. Stanton, R. N. Wrenn, and L. B. Walker, "Two-Joint Muscles of the Thigh," *Journal of Bone and Joint Surgery,* vol. 37A, pp. 125-142, 1995.
[67] R. Dahmane, S. Djordjevič, B. Šimunič, and V. Valenčič, "Spatial fiber type distribution in normal human muscle: Histochemical and tensiomyographical evaluation," *Journal of Biomechanics,* vol. 38, pp. 2451-2459, 2005.
[68] M. A. Johnson, J. Polgar, D. Weightman, and D. Appleton, "Data on the distribution of fibre types in thirty-six human muscles: An autopsy study," *Journal of the Neurological Sciences,* vol. 18, pp. 111-129, 1973.
[69] W. E. Garrett, J. C. Califf, and F. H. Bassett, "Histochemical correlates of hamstring injuries," *The American Journal of Sports Medicine,* vol. 12, pp. 98-103, March 1984 1984.
[70] T. L. Wickiewicz, R. R. Roy, P. L. Powell, and V. R. Edgerton, "Muscle Architecture of the Human Lower Limb," *Clinical Orthopaedics & Related Research,* vol. 179, pp. 275-283, 1983.
[71] Y. Giat, J. Mizrahi, and M. Levy, "A Musculotendon Model of the Fatigue Profiles of Paralyzed Quadriceps Muscle Under FES," *IEEE Transactions on Biomedical Engineering,* vol. 40, pp. 664-674, 1993.
[72] A. V. Hill, "The Heat of Shortening and the Dynamic Constants of Muscle," *Proceedings of the Royal Society of London. Series B, Biological Sciences,* vol. 126, pp. 136-195, 1938.
[73] S. A. Hans and S. Y. Bawab, "Predictive computer modeling of muscle fatigue," presented at the 2012 International Forum on Systems and Mechatronics, Virginia Beach, VA, 2012.
[74] L. A. Frey-Law, J. M. Looft, and J. Heitsman, "A three-compartment muscle fatigue model accurately predicts joint-specific maximum endurance times for sustained isometric tasks," *Journal of Biomechanics,* vol. 45, pp. 1803-1808, 2012.
[75] L. A. Frey Law and K. G. Avin, "Endurance time is joint specific: a modelling and meta-analysis investigation," *Ergonomics,* vol. 53, pp. 109-129, 2010.
[76] W. Rohmert, "Determination of the recovery pause for static work of man," *Internationale Zeitschrift fur Angewandte Physiologie,* vol. 18, pp. 123-164, 1960.
[77] M. E. Lund, M. de Zee, M. S. Andersen, and J. Rasmussen, "On validation of multibody musculoskeletal models," *Proceedings of the Institution of Mechanical Engineers, Part H: Journal of Engineering in Medicine,* vol. 226, pp. 82-94, 2012.
[78] S. J. Piazza, "Muscle-driven forward dynamic simulations for the study of normal and pathological gait," *Journal of NeuroEngineering and Rehabilitation,* vol. 3, 2006.

[79] S. G. McLean, A. Su, and A. J. van den Bogert, "Development and Validation of a 3-D Model to Predict Knee Joint Loading During Dynamic Movement," *Journal of Biomechanical Engineering,* vol. 125, pp. 864-874, 2003.
[80] S. L. Delp, F. C. Anderson, A. S. Arnold, P. Loan, A. Habib, C. T. John, E. Guendelman, and D. G. Thelen, "OpenSim: Open-Source Software to Create and Analyze Dynamic Simulations of Movement," *IEEE Transactions on Biomedical Engineering,* vol. 54, pp. 1940-1950, 2007.
[81] A. J. van den Bogert, D. Blana, and D. Heinrich, "Implicit methods for efficient musculoskeletal simulation and optimal control," *Procedia IUTAM,* vol. 2, pp. 297-316, 2011.
[82] T. M. Guess, "Forward dynamics simulation using a natural knee with menisci in the multibody framework," *Multibody System Dynamics,* vol. 28, pp. 37-53, 2011.
[83] T. M. Guess and A. Stylianou, "Simulation of Anterior Cruciate Ligament Dficiency in a Musculoskeletal Model with Antomical Knees," *The Open Biomedical Engineering Journal,* vol. 6, pp. 23-32, 2012.
[84] M. J. Koehle and M. L. Hull, "The Effect of Knee Model on Estimates of Muscle and Joint Forces in Recumbent Pedaling," *Journal of Biomechanical Engineering,* vol. 132, p. 011007, 2009.
[85] M. Machado, P. Flores, J. C. P. Clar, J. Ambrosio, M. T. Silva, A. Completo, and H. M. Lankarani, "Development of a planar multibody model of the human knee joint," *Nonlinear Dynamics,* vol. 60, pp. 459-478, 2010.
[86] W. A. Laughlin, J. T. Weinhandl, T. W. Kernozek, S. C. Cobb, K. G. Keenan, and K. M. O'Connor, "The effects of single-leg landing technique on ACL loading," *Journal of Biomechanics,* vol. 44, pp. 1845-1851, 2011.
[87] J. Kar and P. M. Quesada, "A Numerical Simulation Approach to Studying Anterior Cruciate Ligament Strains and Internal Forces Among Young Recreational Women Performing Valgus Inducing Stop-Jump Activities," *Annals of Biomedical Engineering,* vol. 40, pp. 1679-1691, 2012.
[88] C. J. Donnelly, D. G. Lloyd, B. C. Elliott, and J. A. Reinbolt, "Optimizing whole-body kinematics to minimize valgus knee loading during sidestepping: Implications for ACL injury risk," *Journal of Biomechanics,* vol. 45, pp. 1491-1497, 2012.
[89] H. Mokhtarzadeh, C. H. Yeow, P. V. S. Lee, J. C. H. Goh, and D. Oetomo, "Understanding Anterior Cruciate Ligament Injury Due to Drop Landing: Effects of Different Landing Techniques and Muscles' Action at the Knee Joint," in *6th World Congress of Biomechanics (WCB 2010). August 1-6, 2010 Singapore.* vol. 31, C. T. Lim and J. C. H. Goh, Eds., ed: Springer Berlin Heidelberg, 2010, pp. 171-173.
[90] M. T. Silva, A. F. Pereira, and J. M. Martins, "An efficient muscle fatigue model for forward and inverse dynamic analysis of human movements," *Procedia IUTAM,* vol. 2, pp. 262-274, 2011.
[91] A. F. Pereira, M. T. Silva, J. M. Martins, and M. d. Carvalho, "Development of a Hill-Type Muscle Model With Fatigue for the Calculation of the Redundant Muscle Forces using Multibody Dynamics," presented at the The 1st Joint International Conference on Multibody System Dynamics, Lappeenranta, Finland, 2010.
[92] R. Bizid, E. Margnes, Y. Francois, J. L. Jully, G. Gonzalez, P. Dupui, and T. Paillard, "Effects of knee and ankle muscle fatigue on postural control in the unipedal stance," *European Journal of Applied Physiology,* vol. 106, pp. 375-380, 2009.

[93] J. R. Fowles, H. J. Green, R. Tupling, S. O'Brien, and B. D. Roy, "Human neuromuscular fatigue is associated with altered Na+-K+-ATPase activity following isometric exercise," *Journal of Applied Physiology,* vol. 92, pp. 1585-1593, 2002.
[94] L. Mademli and A. Arampatzis, "Behaviour of the human gastrocnemius muscle architecture during submaximal isometric fatigue," *European Journal of Applied Physiology,* vol. 94, pp. 611-617, 2005.
[95] S. K. Stackhouse, J. E. Stevens, S. C. Lee, K. M. Pearce, L. Snyder-Mackler, and S. A. Binder-Macleod, "Maximum Voluntary Activation in Nonfatigued and Fatigued Muscle of Young and Elderly Individuals," *Physical Therapy,* vol. 81, pp. 1102-1109, 2001.
[96] P. A. Gribble and J. Hertel, "Effect of hip and ankle muscle fatigue on unipedal postural control," *Journal of Electromyography and Kinesiology,* vol. 14, pp. 641-646, 2004.
[97] S. L. Rozzi, S. M. Lephart, and F. H. Fu, "Effects of Muscular Fatigue on Knee Joint Laxity and Neuromuscular Characteristics of Male and Female Athletes," *Journal of Athletic Training,* vol. 34, pp. 106-114, 1999.
[98] J. A. Yaggie and S. J. McGregor, "Effects of Isokinetic Ankle Fatigue on the Maintenance of Balance and Postural Limits," *Archives of Physical Medicine and Rehabilitation,* vol. 83, pp. 224-228, 2002.
[99] D. G. Behm and D. M. M. St-Pierre, "Effects of fatigue duration and muscle type on voluntary and evoked contractile properties," *Journal of Applied Physiology,* vol. 82, pp. 1654-1661, 1997.
[100] R. C. Harris, R. H. T. Edwards, E. Hultman, L. O. Nordesjo, B. Nylind, and K. Sahlin, "The time course of phophorylcreatine resynthesis during recovery of the quadriceps muscle in man," *Pflugers Archive,* vol. 367, pp. 137-142, 1976.
[101] Fulco, Rock, Muza, Lammi, Cymerman, Butterfield, Moore, Braun, and Lewis, "Slower fatigue and faster recovery of the adductor pollicis muscle in women matched for strength with men," *Acta Physiologica Scandinavica,* vol. 167, pp. 233-239, 1999.
[102] V. Linnamo, K. Hakkinen, and P. V. Komi, "Neuromuscular fatigue and recovery in maximal compared to explosive strength loading," *European Journal of Applied Physiology,* vol. 77, pp. 176-181, 1998.
[103] R. O. Kollock Jr., J. A. Onate, and B. Van Lunen, "The Reliability of Portable Fixed Dynamometry During Hip and Knee strength Assessments," *Journal of Athletic Training,* vol. 45, pp. 349-356, 2010.
[104] H. J. Hermens, B. Freriks, R. Merletti, D. Stegeman, J. Blok, G. Rau, C. Disselhorst-Klug, and G. Hagg, *European Recommendations for Surface ElectroMyoGraphy.* Enschede, the Netherlands: Roessingh Research and Development, 1999.
[105] J. Vanrenterghem, E. Venables, T. Pataky, and M. A. Robinson, "The effect of running speed on knee mechanical loading in females during side cutting," *Journal of Biomechanics,* vol. 45, pp. 2444-2449, 2012.
[106] J. T. Weinhandl and K. M. O'Connor, "Assessment of a greater trochanter-based method of locating the hip joint center," *Journal of Biomechanics,* vol. 43, pp. 2633-2636, 2010.
[107] C. W. Spoor and F. E. Veldpaus, "Rigid Body Motion Calculated From Spatial Co-ordinates of Markers," *Journal of Biomechanics,* vol. 13, pp. 391-393, 1980.

[108] T. W. Lu and J. J. O'Connor, "Bone position estimation from skin marker co-ordinates using global optimisation with joint constraints," *Journal of Biomechanics,* vol. 32, pp. 129-134, 1999.
[109] T. Besier, D. G. Lloyd, and T. R. Ackland, "Muscle Activation Strategies at the Knee during Running and Cutting Maneuvers," *Medicine & Science in Sports & Excercise,* vol. 35, pp. 119-127, 2003.
[110] K. Levenberg, "A Method for the Solution of Certain Non-Linear Problems in Least Squares," *Quarterly of Applied Mathematics,* vol. 2, pp. 164-168, 1944.
[111] S. R. Hamner, A. Seth, and S. L. Delp, "Muscle contributions to propulsion and support during running," *Journal of Biomechanics,* vol. 43, pp. 2709-2716, 2010.
[112] G. T. Yamaguchi and F. E. Zajac, "A planar model of the knee joint to characterize the knee extensor mechanism," *Journal of Biomechanics,* vol. 22, pp. 1-10, 1989.
[113] S. L. Delp, J. P. Loan, M. G. Hoy, F. E. Zajac, E. L. Topp, and J. M. Rosen, "An interactive graphics-based model fo the lower extremity to study orthopaedic surgical procedures," *IEEE Transactions on Biomedical Engineering,* vol. 37, pp. 757-767, 1990.
[114] F. C. Anderson and M. G. Pandy, "Individual muscle contributions to support in normal walking," *Gait & Posture,* vol. 17, pp. 159-169, 2003.
[115] K. R. Holzbaur, W. M. Murray, and S. L. Delp, "A model of the upper extremity for simulating musculoskeletal surgery and analyzing neuromuscular control," *Annals of Biomedical Engineering,* vol. 33, pp. 829-840, 2005.
[116] F. C. Anderson and M. G. Pandy, "A dynamic optimization solution for vertical jumping in three dimensions," *Computer Methods in Biomechanics and Biomedical Engineering,* vol. 2, pp. 201-231, 1999.
[117] F. C. Anderson and M. G. Pandy, "Dynamic optimization of human walking," *Journal of Biomechanical Engineering,* vol. 123, pp. 381-390, 2001.
[118] F. E. Zajac, "Muscle and tendon: properties, models, scaling, and application to biomechanics and motor control," *Critical Reviews in Biomedical Engineering,* vol. 17, pp. 359-411, 1989.
[119] M. Millard, T. Uchida, A. Seth, and S. L. Delp, "Flexing Computational Muscle: Modeling and Simulation of Musculotendon Dynamics," *Journal of Biomechanical Engineering,* vol. 135, pp. 1-11, 2013.
[120] A. D. Kuo, "A least-squares estimation approach to improving the precision of inverse dynamics computations," *Journal of Biomechanical Engineering,* vol. 120, pp. 148-159, 1998.
[121] J. Kennedy and R. Eberhart, "Particle swarm optimization," in *IEEE International Conference on Neural Networks*, 1995, pp. 1942-1948
[122] D. G. Thelen and F. C. Anderson, "Using computed muscle control to generate forward dynamic simulations of human walking from experimental data," *Journal of Biomechanics,* vol. 39, pp. 1107-1115, 2006.
[123] D. G. Thelen, F. C. Anderson, and S. L. Delp, "Generating dynamic simulations of movement using computed muscle control," *Journal of Biomechanics,* vol. 36, pp. 321-328, 2003.
[124] R. D. Crowninshield and R. A. Brand, "A physiologically based criterion of muscle force prediction in locomotion," *Journal of Biomechanics,* vol. 14, pp. 793-801, 1981.

[125] H. Koga, A. Nakamae, Y. Shima, J. Iwasa, G. Myklebust, L. Engebretsen, R. Bahr, and T. Krosshaug, "Mechanisms for Noncontact Anterior Cruciate Ligament Injuries: Knee Joint Kinematics in 10 Injury Situations From Female team Handball and Basketball," *The American Journal of Sports Medicine,* vol. 20, pp. 1-9, 2010.
[126] K. L. Markolf, J. F. Gorek, J. M. Kabo, and M. S. Shapiro, "Direct measurement of resultant forces in the anterior cruciate ligament. An in vitro study performed with a new experimental technique.," *The Journal of Bone and Joint Surgery,* vol. 72, pp. 557-567, 1990.
[127] R. R. Neptune, I. C. Wright, and A. J. Van den Bogert, "Muscle coordination and function during cutting movements," *Medicine & Science in Sports & Excercise,* vol. 31, pp. 294-302, 1999.
[128] J. M. Winters and L. Stark, "Estimated Mechanical Properties of Synergistic Muscles Involved in Movements of a Variety of Human Joints," *Journal of Biomechanics,* vol. 21, pp. 1027-1041, 1988.
[129] R. S. Welsh, J. M. Davis, J. R. Burke, and H. G. Williams, "Carbohydrates and physical/mental performance during intermittent exercise to fatigue," *Medicine & Science in Sports & Excercise,* vol. 34, pp. 723-731, 2002.
[130] N. K. Vollestad, *Changes in activation, contractile speed and electrolyte balance during fatigue of sustained and repeated contractions.* New York: Marcel Dekker, 1995.
[131] S. C. Gandevia, G. M. Allen, and D. K. McKenzie, *Central fatigue - critical issues, quantification and practical implications.* New York: Plenum Press, 1995.
[132] U. Windhorst and G. Boorman, *Overview: Potential role of segmental motor circuitry in muscle fatigue.* New York: Plenum Press, 1995.
[133] S. G. McLean, X. Huang, and A. J. Van den Bogert, "Association between lower extremity posture at contact and peak knee valgus moment during sidestepping: Implications for ACL injury," *Clinical Biomechanics,* vol. 20, pp. 863-870, 2005.
[134] E. M. Wojtys, B. B. Wylie, and L. J. Huston, "The Effects of Muscle Fatigue on Neuromuscular Function and Anterior Tibial Translation in Healthy Knees," *The American Journal of Sports Medicine,* vol. 24, pp. 615-621, 1996.
[135] S. Colby, A. Francisco, B. Yu, D. Kirkendall, M. Finch, and W. Garrett, "Electromyographic and Kinematic Analysis of Cutting Maneuvers: Implications for Anterior Cruciate Ligament Injury," *The American Journal of Sports Medicine,* vol. 28, pp. 234-240, 2000.
[136] E. B. Simonsen, S. P. Magnusson, J. Bencke, H. Naesborg, M. Havkrog, J. F. Ebstrup, and H. Sorensen, "Can the hamstring muscle protect the anterior cruciate ligament during a side-cutting maneuver?," *Scandinavian Journal of Medicine & Science in Sports,* vol. 10, pp. 78-84, 2000.
[137] K. L. Markolf, A. Graff-Radford, and H. C. Amstutz, "In vivo knee stability. A quantitative assessment using an instrumented clinical testing apparatus," *Journal of Bone and Joint Surgery,* vol. 60A, pp. 664-674, 1978.
[138] L. Li, D. Landin, J. Grodesky, and J. Myers, "The function of gastrocnemius as a knee flexor at selected knee and ankle angles," *Journal of Electromyography and Kinesiology,* vol. 12, pp. 385-390, 2002.
[139] D. Kay, A. St Clair Gibson, M. Mitchell, M. Lambert, and T. Noakes, "Different neuromuscular recruitment patterns during eccentric, concentric and isometric contractions," *Journal of Electromyography and Kinesiology,* vol. 10, pp. 425-431, 2000.

[140] A. Taylor, R. Brooks, P. Smith, and H. B, "Myoelectric evidence of peripheral muscle fatigue during exercise in severe hypoxia: some references to m. vastus lateralis myosin heavy chain composition," *European Journal of Applied Physiology,* vol. 75, pp. 151-159, 1997.
[141] R. M. Nunley, D. W. Wright, J. B. Renner, B. Yu, and W. E. Garrett, "Gender comparison of patella-tendon tibial shaft angle with weight-bearing," *Research in Sports Medicine,* vol. 11, pp. 173-185, 2003.
[142] J. G. Smidt, "Biomechanical analysis of knee flexion and extension," *Journal of Biomechanics,* vol. 6, pp. 79-92, 1973.
[143] M. Bendjaballah, A. Shirazi-Adl, and D. Zukor, "Finite Element analysis of human knee joint in varus-valgus," *Clinical Biomechanics,* vol. 12, pp. 139-148, 1996.
[144] K. Miura, Y. Ishibashi, E. Tsuda, Y. Okamura, H. Otsuka, and S. Toh, "The Effect of Loacl and General Fatigue on Knee Proprioception," *Arthroscopy: The Journal Of Arthroscopic and Related Surgery,* vol. 20, pp. 414-418, 2004.
[145] J. T. Weinhandl, J. E. Earl-Boehm, K. T. Ebersole, W. E. Huddleston, B. S. R. Armstrong, and K. M. O'Connor, "Anticipatory effects on anterior cruciate ligament loading during sidestep cutting," *Clinical Biomechanics,* vol. 28, pp. 655-663, 2013.
[146] L. Salmon, V. Russell, T. Musgrove, L. Pinczewski, and K. Reshauge, "Incidence and Risk Factors for Graft Rupture and Contralateral Rupture After Anterior Cruciate Ligament Reconstruction," *Arthroscopy,* vol. 21, pp. 948-957, 2005.
[147] C. A. Bush-Joseph, D. E. Hurwitz, R. R. Patel, Y. Bahrani, R. Garretson, B. R. Bach Jr., and T. P. Andriacchi, "Dynamic Function After Anterior Cruciate Ligament Reocnstruction with Autologous Patellar Tendon," *American Journal of Sports Medicine,* vol. 29, pp. 36-41, 2001.
[148] S. M. Cowan, P. W. Hodges, K. L. Bennell, and K. M. Crossley, "Altered vastii recruitment when people with patellofemoral pain syndrom complete a postural task," *Archives of Physical Medicine and Rehabilitation,* vol. 83, pp. 989-995, 2002.
[149] P. Lam and G. Ng, "Activation of the Quadriceps Muscle During Semisquatting with Different Hip and Knee Positions in Patients with Anterior Knee Pain," *American Journal of Physical Medicine and Rehabilitation,* vol. 80, pp. 804-808, 2001.
[150] J. D. Willson, S. Binder-Macleod, and I. S. Davis, "Lower Extremity Jumping Mechanics of Female Athletes With and Without Patellofemoral Pain Before and After Exertion," *American Journal of Sports Medicine,* vol. 36, pp. 1587-1596, 2008.

Appendix A: Kinematic and Kinetic Data Root Mean Square Differences

Table A-1: Average root mean square differences (mean±st.dev.) between the experimental and RRA produced kinematics for the pelvis, right lower extremity and lumbar

	Pre-Fatigue	Post-Fatigue
Residual Forces (N)		
F_x	3.63±1.45	4.97±2.74
F_y	4.73±2.74	3.63±3.07
F_z	3.22±2.90	2.34±1.53
Residual Moments (Nm)		
M_x	11.2±5.98	7.08±2.90
M_y	21.1±8.65	14.1±6.52
M_z	15.7±4.60	16.0±5.79
Pelvic Translations (mm)		
T_x	0.39±0.23	0.31±0.06
T_y	0.68±0.28	0.61±0.25
T_z	0.38±0.35	0.34±0.18
Pelvic Rotations (deg.)		
Tilt	0.37±0.26	0.25±0.08
List	0.38±0.17	0.36±0.18
Rotation	0.77±0.68	0.42±0.38
Right Hip (deg.)		
Flexion	0.14±0.05	0.15±0.06
Adduction	0.16±0.10	0.11±0.06
Rotation	0.02±0.01	0.03±0.02
Right Knee (deg.)		
Flexion	0.08±0.05	0.06±0.01
Adduction	0.03±0.02	0.07±0.06
Rotation	0.05±0.04	0.06±0.08
Right Ankle (deg.)		
Dorsiflexion	0.06±0.03	0.05±0.02
Lumbar Rotations (deg.)		
Extension	0.98±0.58	0.87±0.37
Bending	0.73±0.67	1.07±0.55
Rotation	1.51±0.92	0.92±0.39

Table A-2: Average root mean square differences (mean±st.dev.) between the RRA and CMC produced kinematics for the pelvis, right lower extremity and lumbar

	Pre-Fatigue	Post-Fatigue
Pelvic Translations (mm)		
T_x	0.010	0.009
T_y	0.019	0.009
T_z	0.007	0.01
Pelvic Rotations (deg.)		
Tilt	0.13	0.06
List	0.12	0.10
Rotation	0.03	0.05
Right Hip (deg.)		
Flexion	0.12	0.11
Adduction	0.10	0.07
Rotation	0.28	0.36
Right Knee (deg.)		
Flexion	0.29	0.25
Adduction	0.33	0.44
Rotation	1.41	1.37
Right Ankle (deg.)		
Dorsiflexion	0.42	0.34
Lumbar Rotations (deg.)		
Extension	0.15	0.07
Bending	0.16	0.13
Rotation	0.03	0.04

Appendix B: Fatigue and Recovery Data

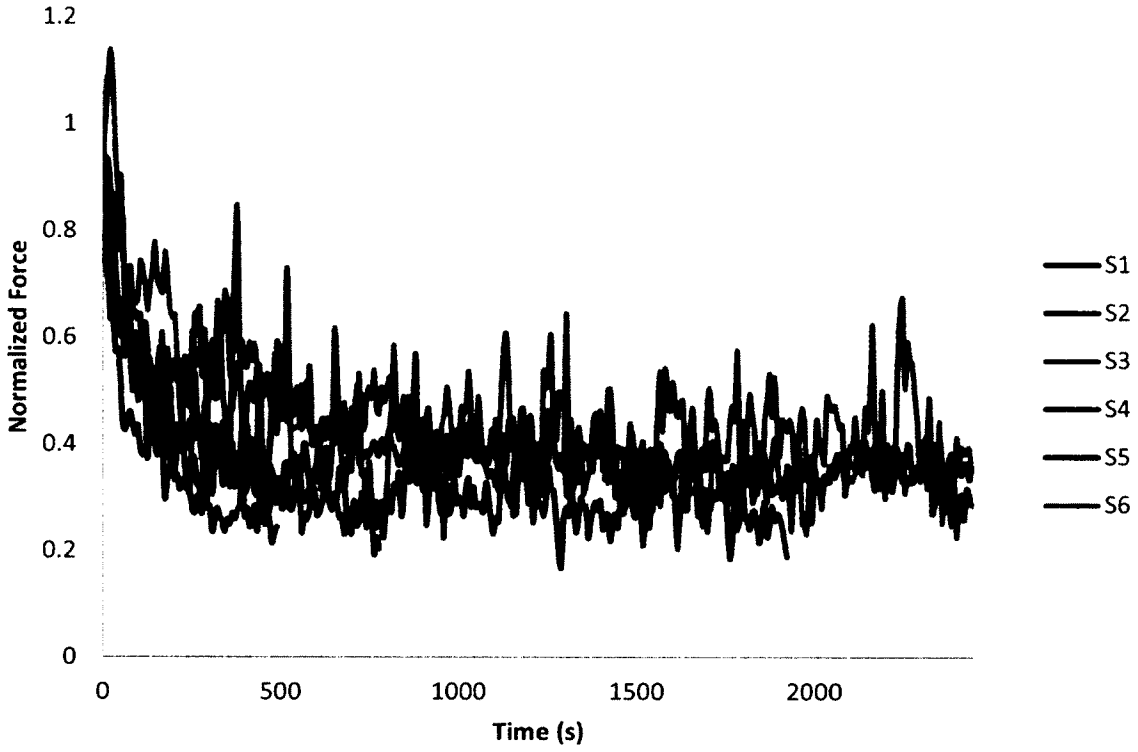

Figure B-1: Normalized force values during the fatigue protocol for testing session 1

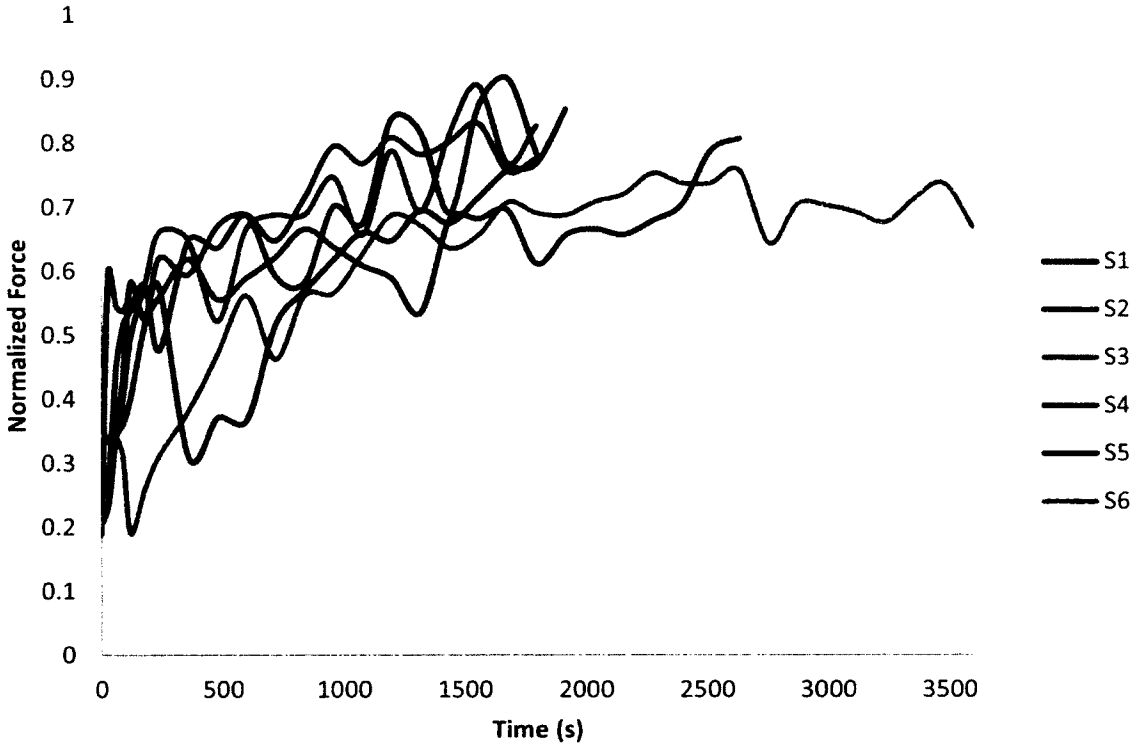

Figure B-2: Normalized force values during recovery protocol for testing session 1

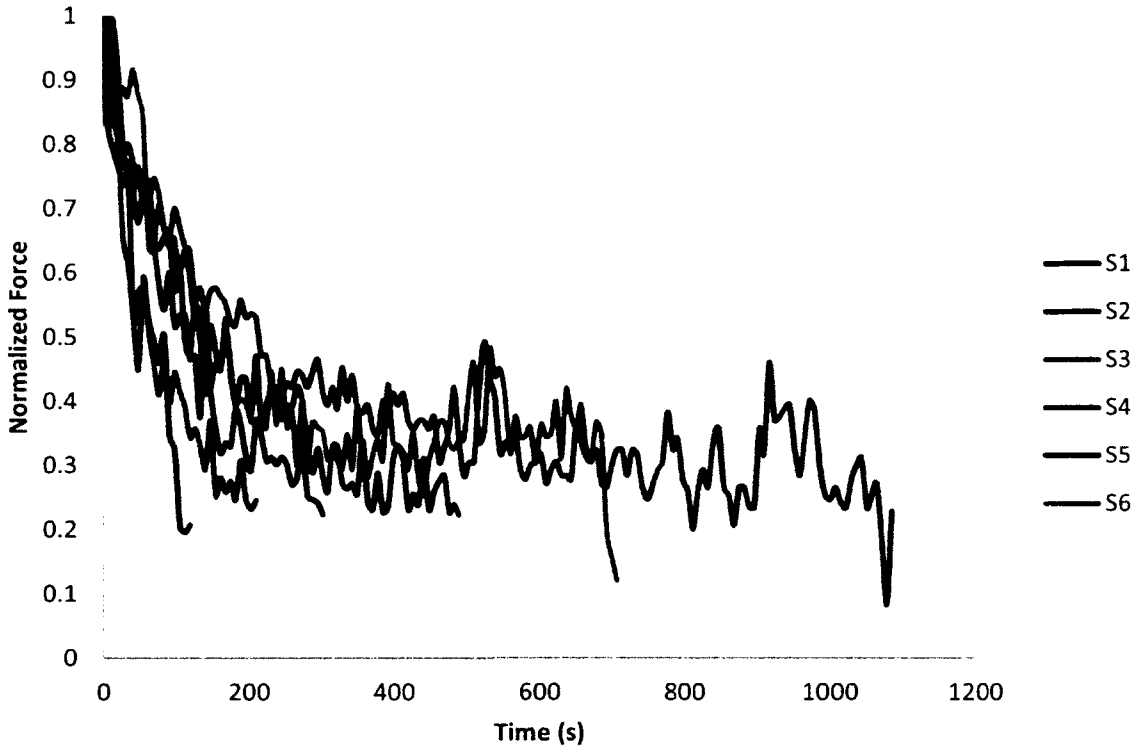

Figure B-3: Normalized force values during fatigue protocol for testing session 2

Table B-1: Fatigue and recovery coefficients, used in the Tang *et al* [16] fatigue model, from testing sessions 1 and 2, with fatigue and recovery equations in the form of $y=ae^{bt}$, where t represents time

	Testing Session 1				Testing Session 2	
	Fatigue Curve		Recovery Curve		Fatigue Curve	
	a	b	a	b	a	b
S1	0.7702	-0.0003147	0.4362	0.000373	1.044	-0.013
S2	0.3949	-0.0002	0.5174	0.000144	0.7825	-0.003
S3	0.5106	-0.000149	0.4624	0.000373	0.7873	-0.006
S4	0.5459	-0.00024	0.4967	0.000327	0.6285	-0.001
S5	0.7704	-0.001749	0.3498	0.000473	0.8835	-0.005
S6	0.6517	-0.000374	04282	0.000182	0.6322	-0.001

Appendix C: Experimental and Fatigue Model Hamstrings Muscle Forces

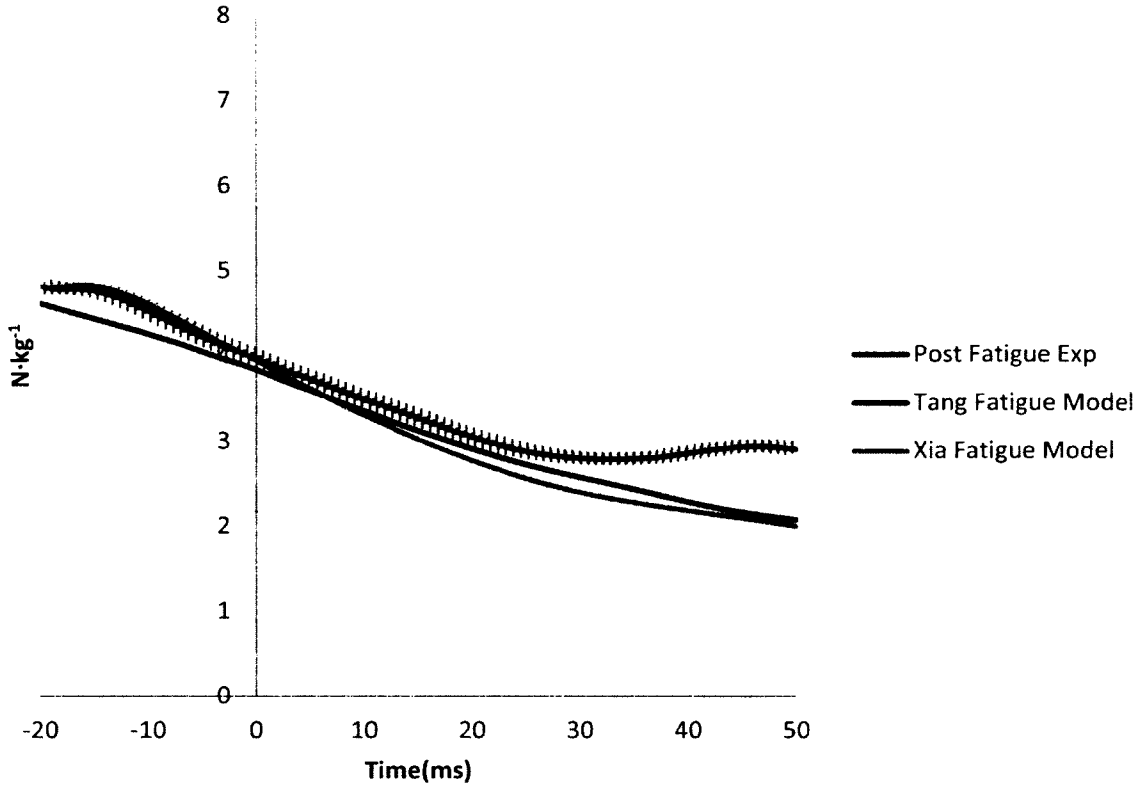

Figure C-1: Experimental post-fatigue Biceps Femoris Long Head muscle force data is compared to the predicted muscle force data by the Tang and Xia fatigue models using the 95% confidence interval of the experimental data.

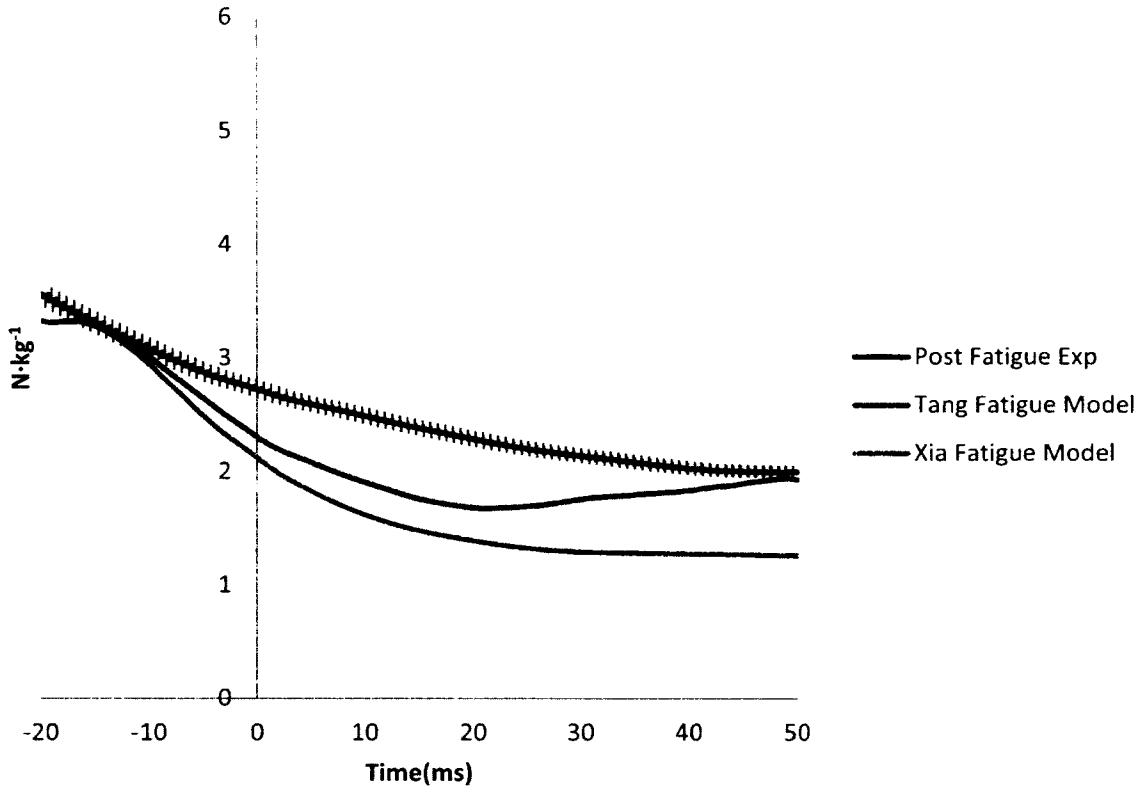

Figure C-2: Experimental post-fatigue Biceps Femoris Short Head muscle force data is compared to the predicted muscle force data by the Tang and Xia fatigue models using the 95% confidence interval of the experimental data.

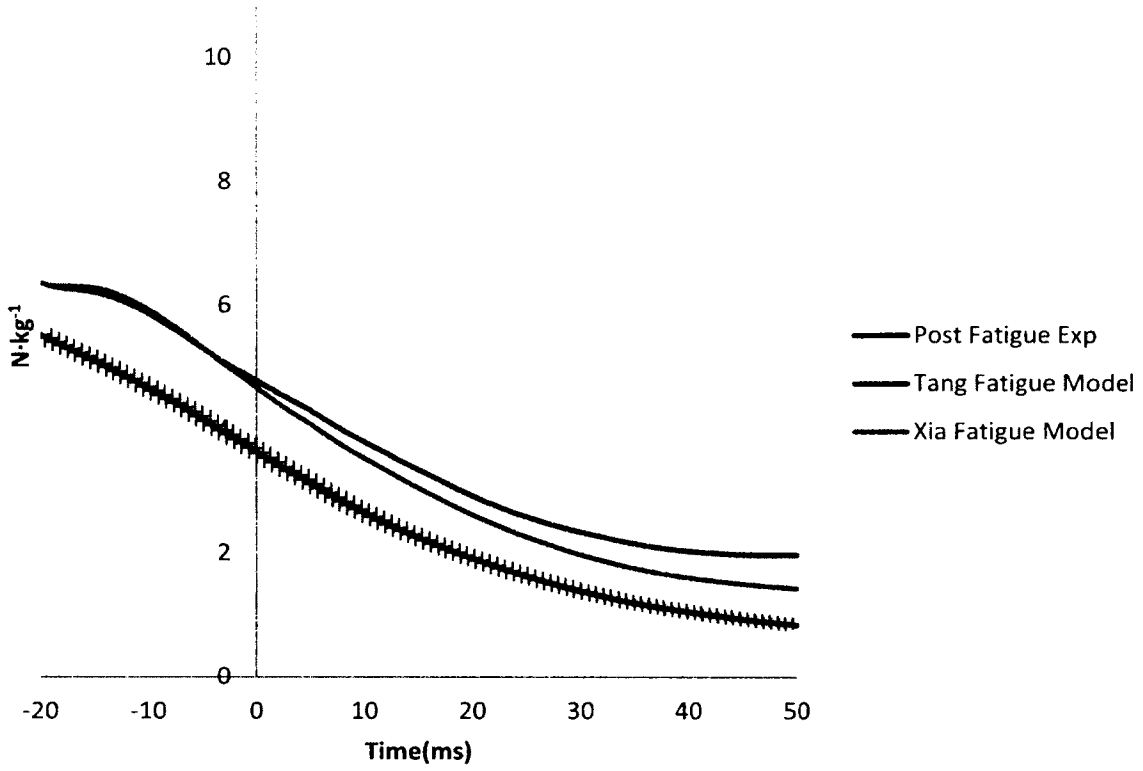

Figure C-3: Experimental post-fatigue Semimembranosus muscle force data is compared to the predicted muscle force data by the Tang and Xia fatigue models using the 95% confidence interval of the experimental data.

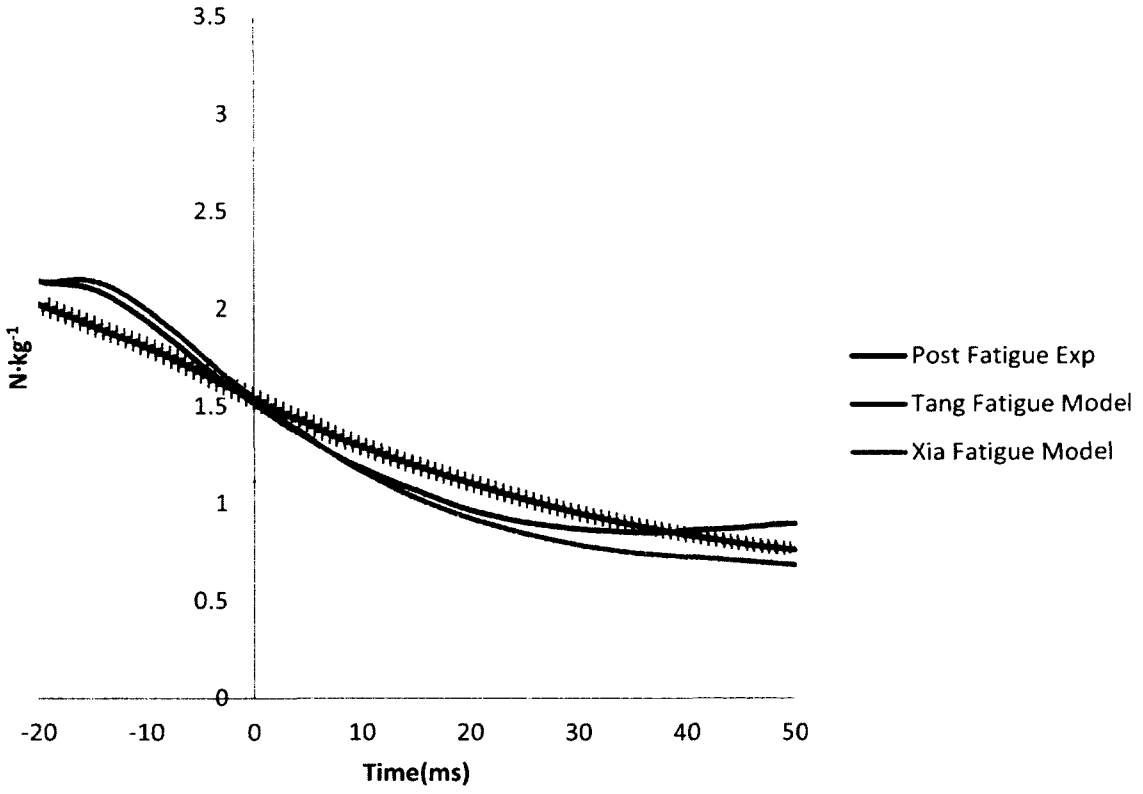

Figure C-4: Experimental post-fatigue Semitendinosus muscle force data is compared to the predicted muscle force data by the Tang and Xia fatigue models using the 95% confidence interval of the experimental data.

Appendix D: Planar ACL Loading at Various Levels of Hamstrings Fatigue

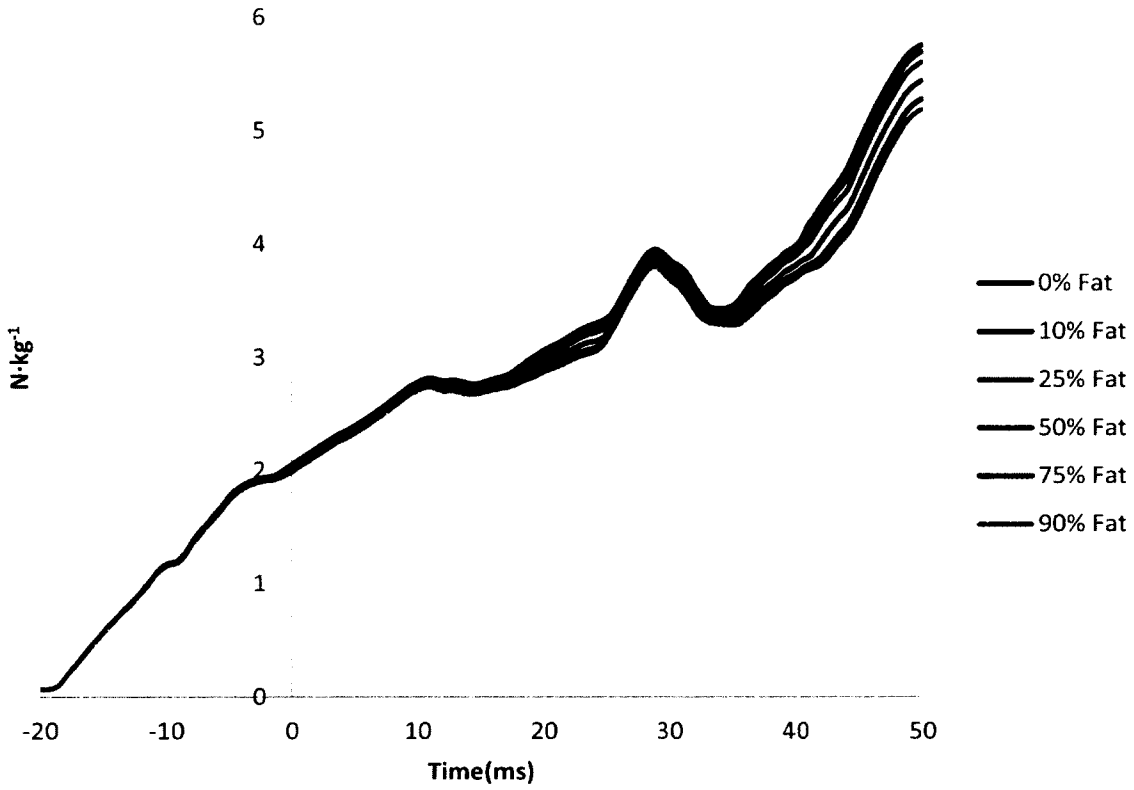

Figure D-1: Group average sagittal plane ACL loading across all fatigue levels

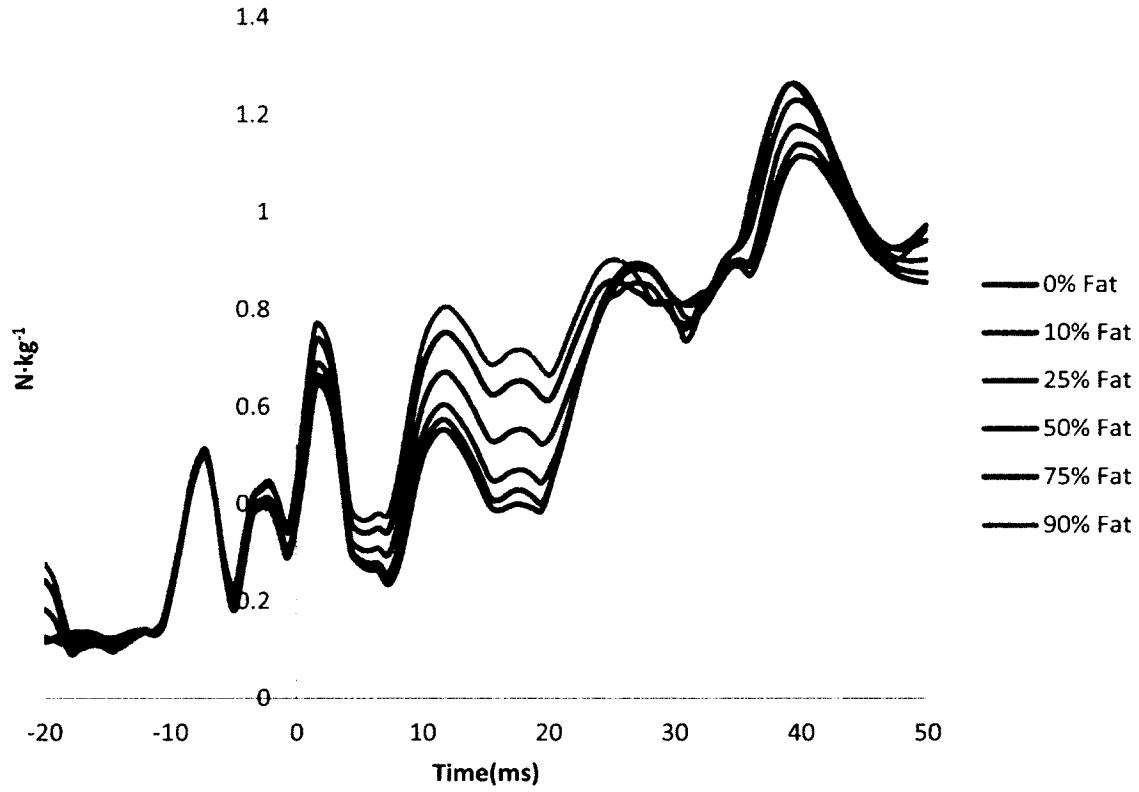

Figure D-2: Group average transverse plane ACL loading across all fatigue levels

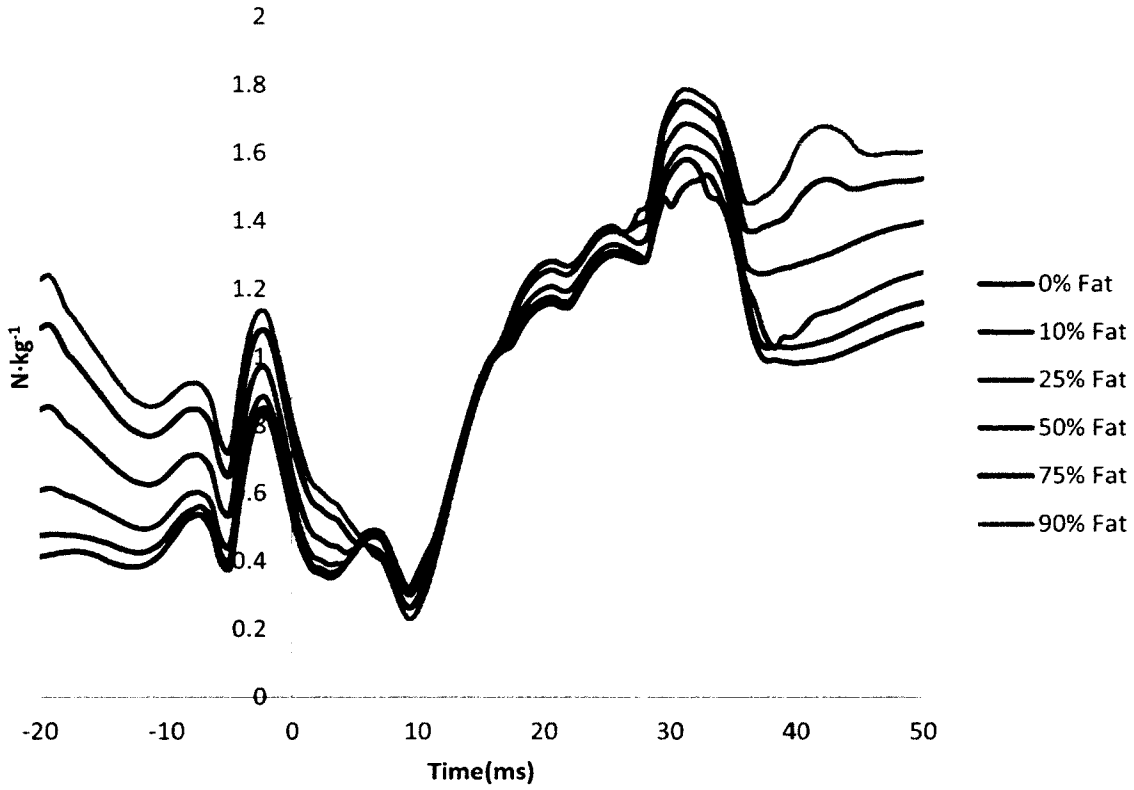

Figure D-3: Group average frontal plane ACL loading across all fatigue levels

Appendix E: ACL Loading Patterns at Various Levels of Hamstrings Fatigue

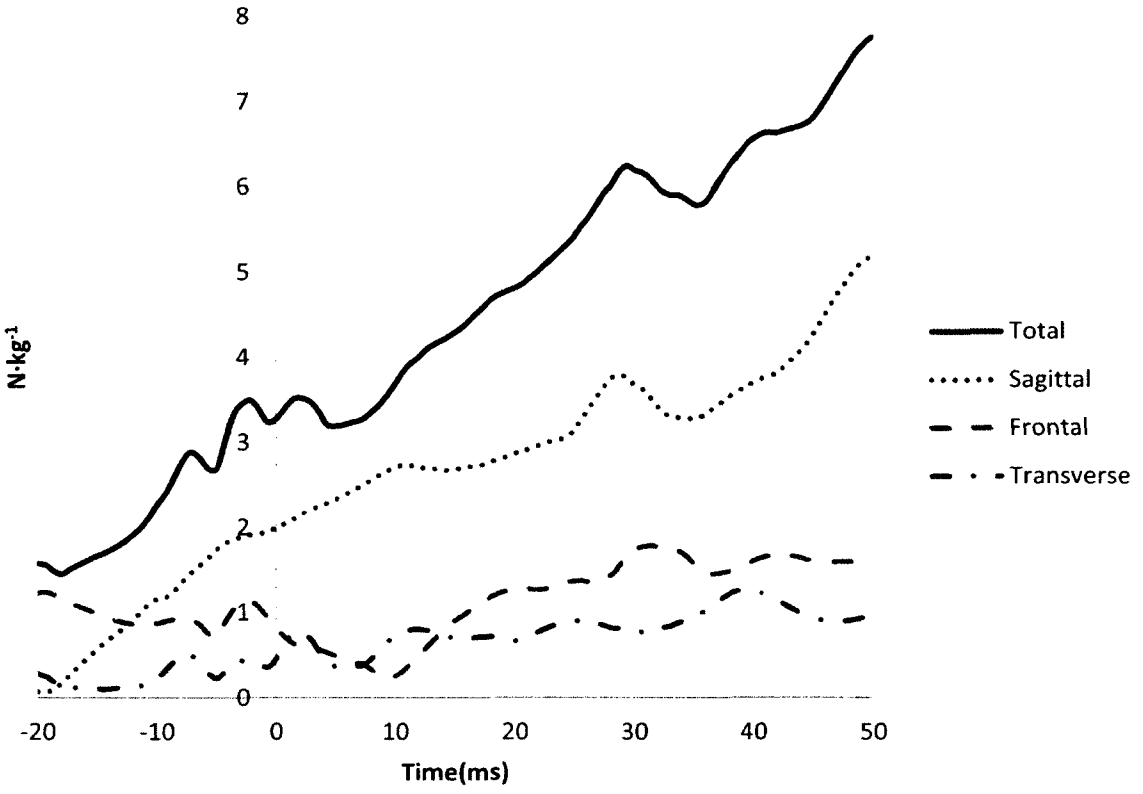

Figure E-1: Group average ACL loading for the pre-fatigue condition

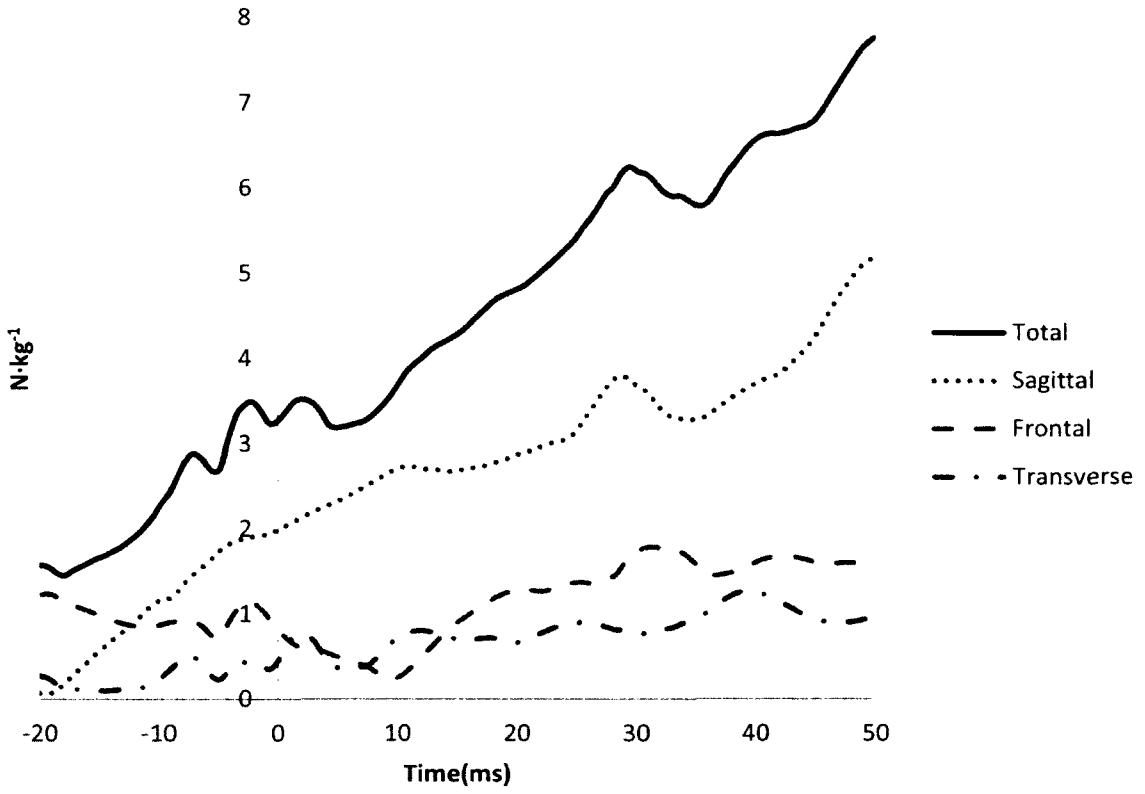

Figure E-2: Group average ACL loading for the 10% hamstrings fatigue level

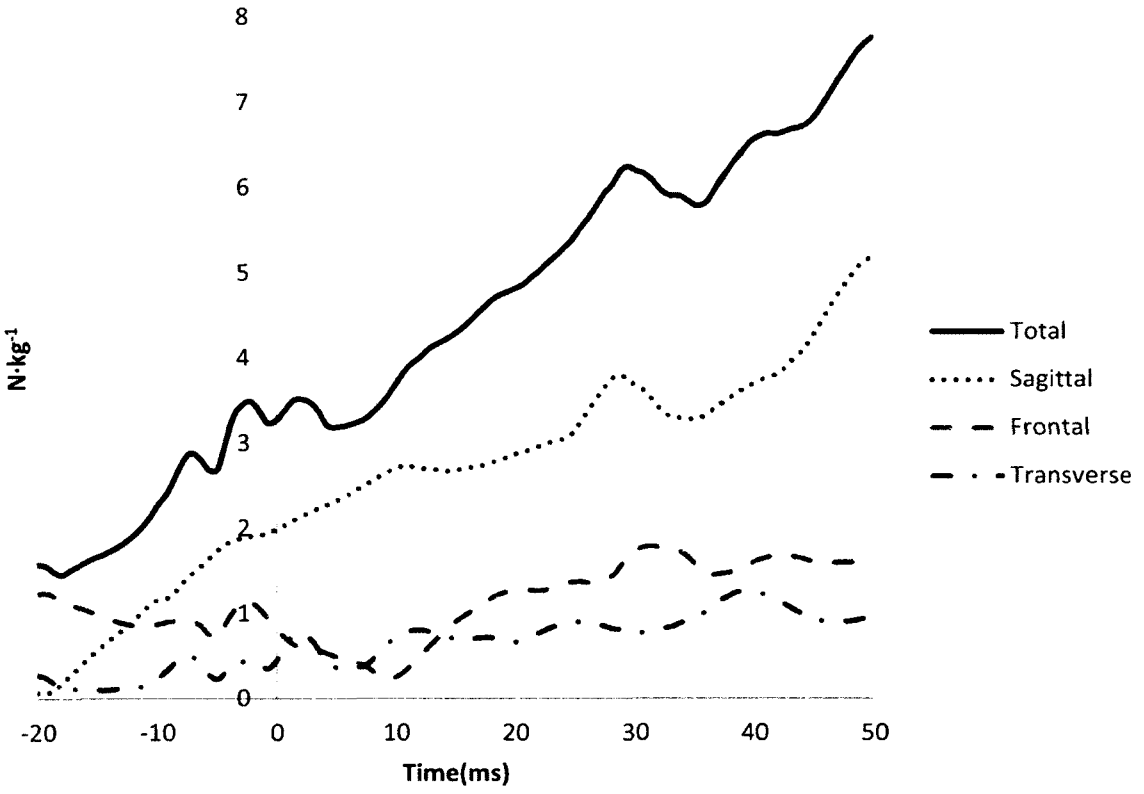

Figure E-3: Group average ACL loading for the 25% hamstrings fatigue level

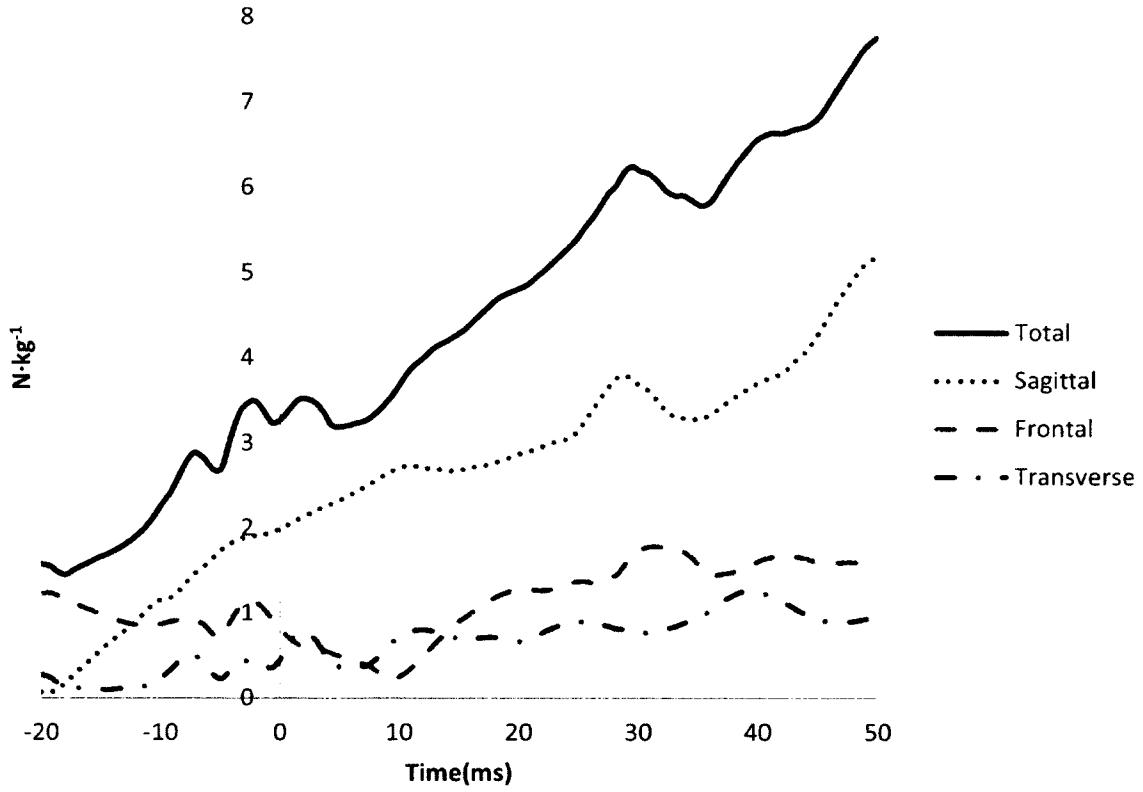

Figure E-4: Group average ACL loading for the 50% hamstrings fatigue level

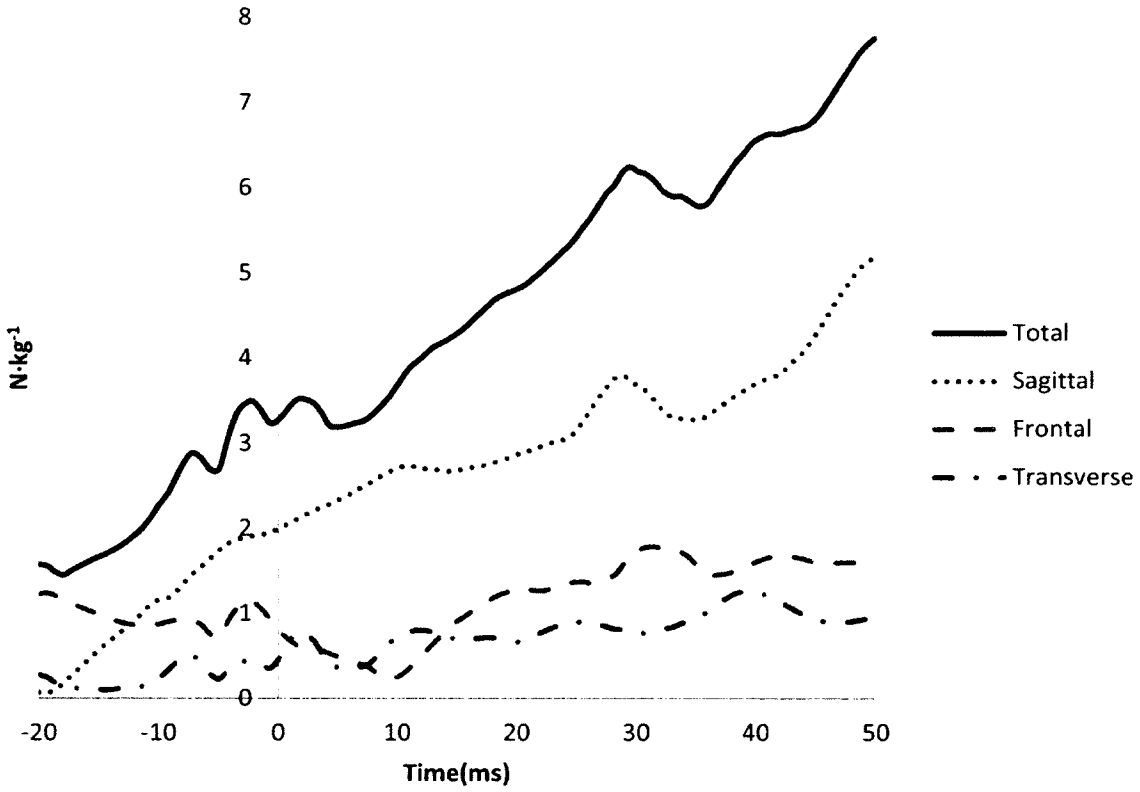

Figure E-5: Group average ACL loading for the 75% hamstrings fatigue level

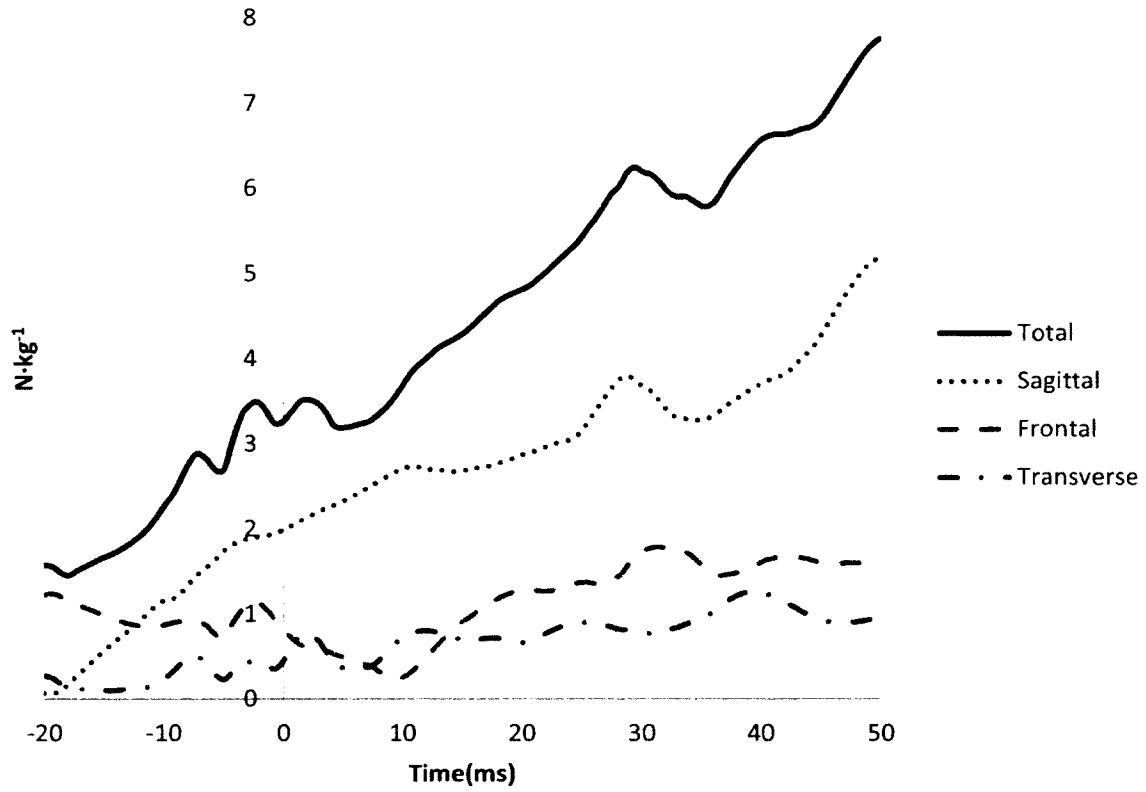

Figure E-6: Group average ACL loading for the 90% hamstrings fatigue level

Appendix F: Xia Fatigue Model Predicted Tibiofemoral Contact Forces at Various Levels of Hamstrings Fatigue

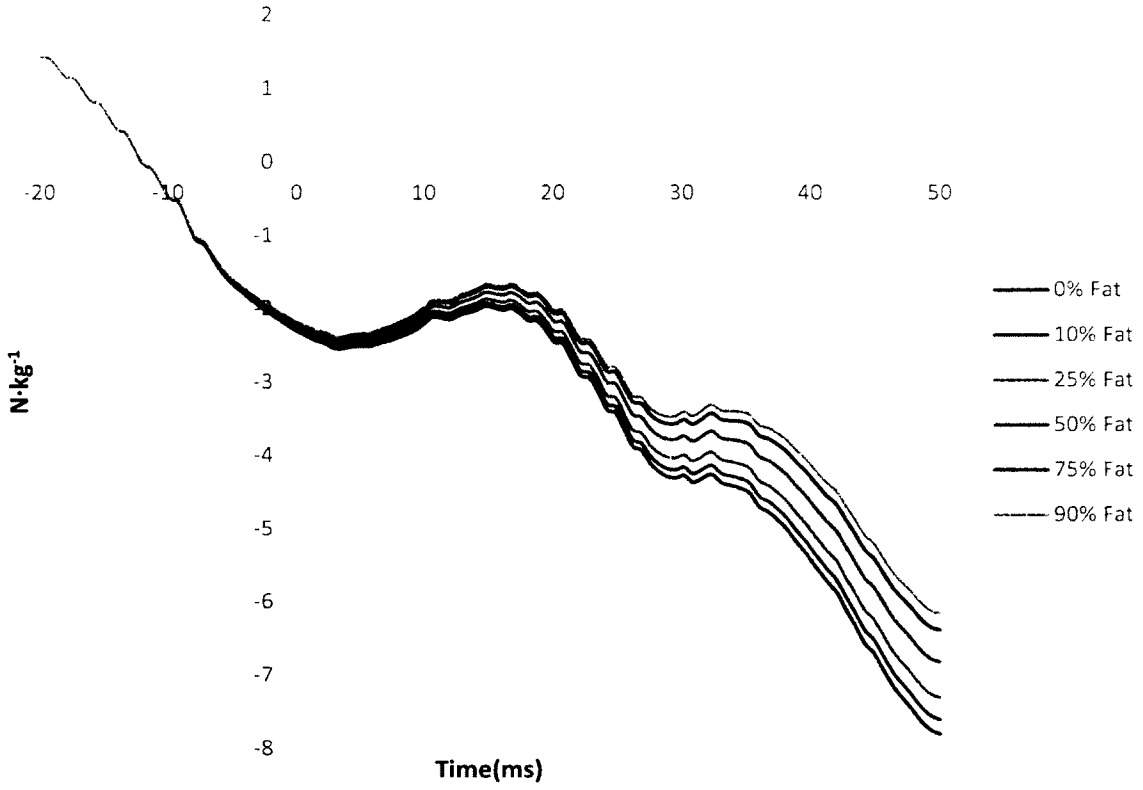

Figure F-1: Shear contact force across various levels of hamstrings fatigue.

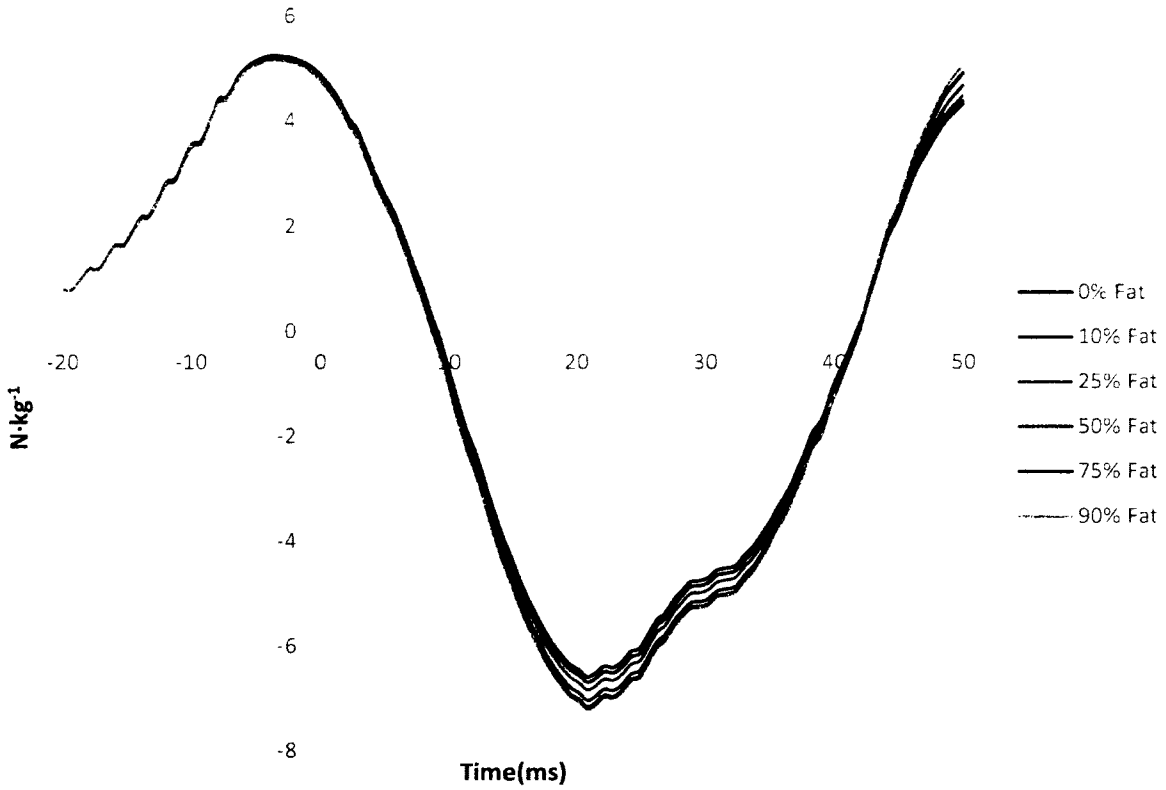

Figure F-2: Compressive force across various levels of hamstrings fatigue

Appendix G: Xia Fatigue Model Predicted Joint Moments at Various Levels of Hamstrings Fatigue

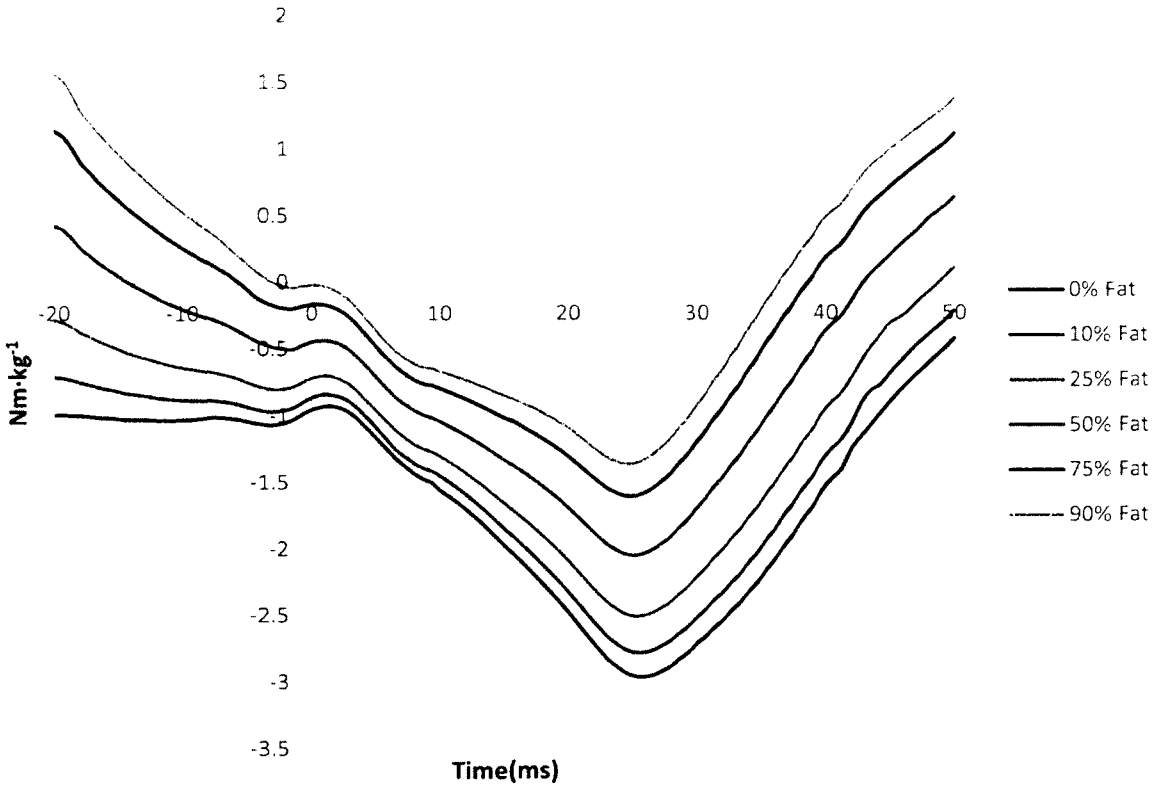

Figure G-1: Hip sagittal plane moment where positive and negative values indicate hip flexion and extension moments, respectively.

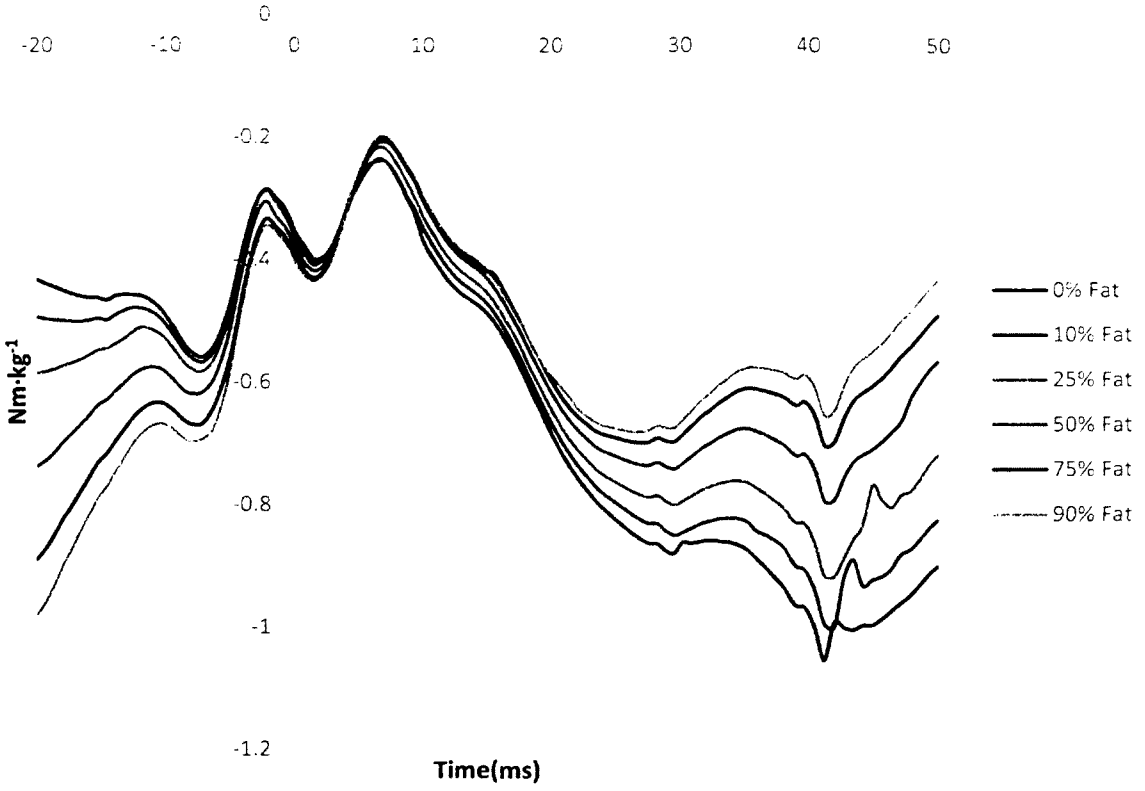

Figure G-2: Hip frontal plane moment, where positive and negative values indicate hip adduction and abduction moments, respectively.

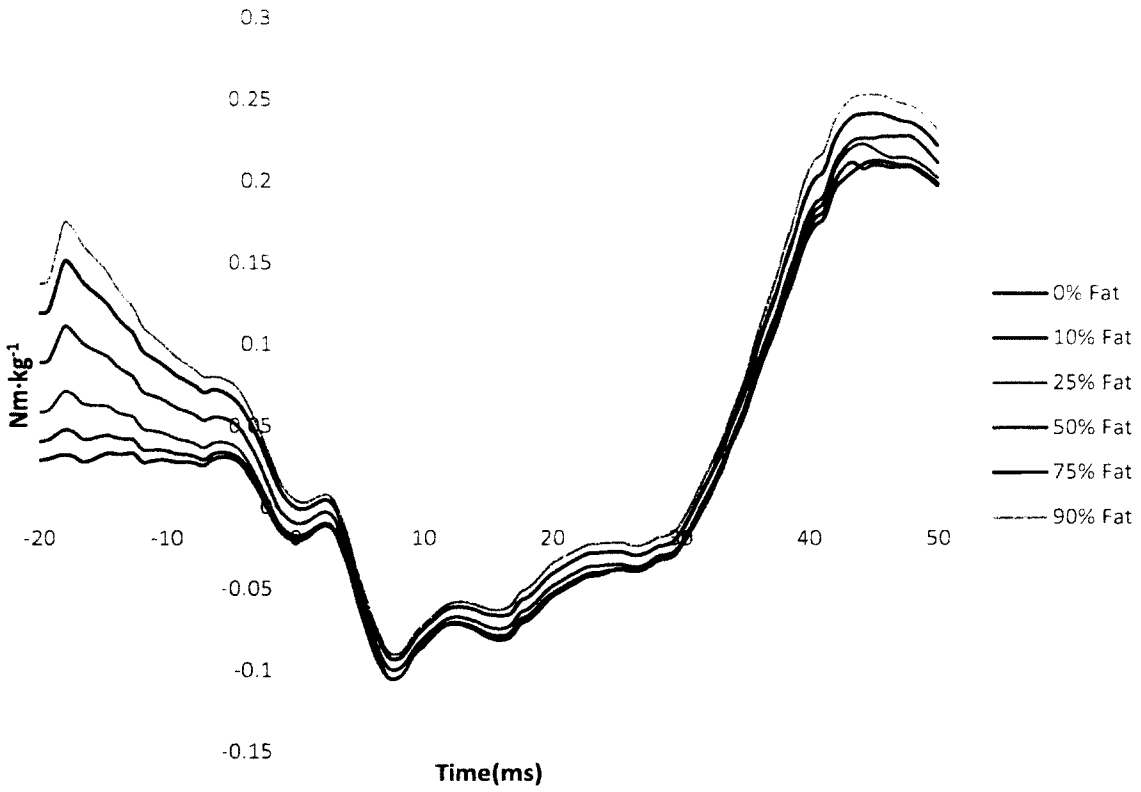

Figure G-3: Hip transverse plane moment, where positive and negative values indicate hip internal and external rotation moments, respectively.

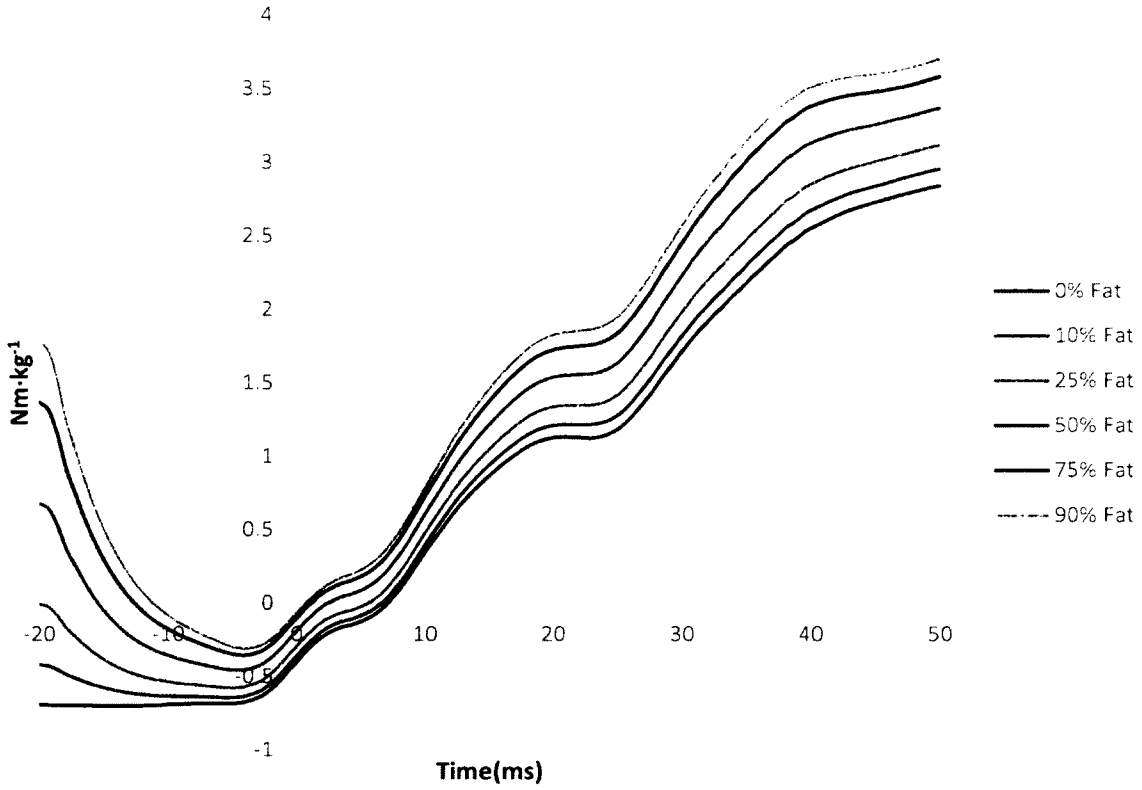

Figure G-4: Knee sagittal plane moment, where positive and negative values indicate knee extension and flexion moments, respectively.

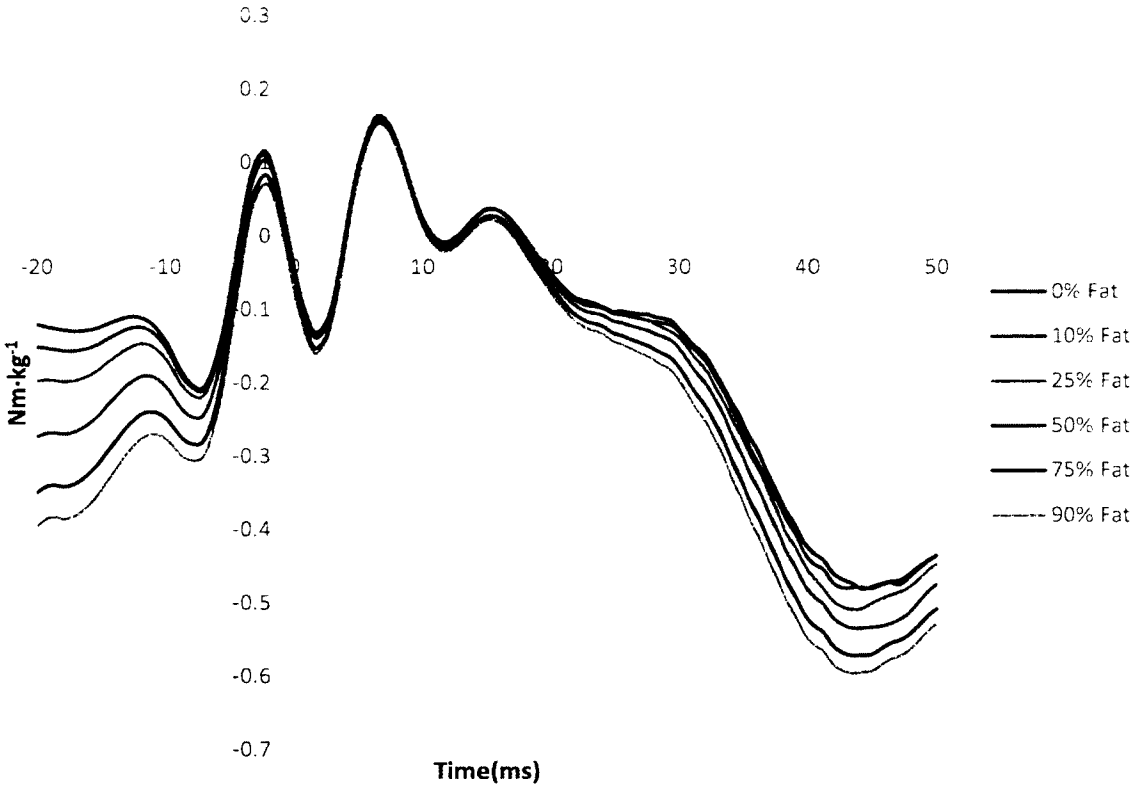

Figure G-5: Knee frontal plane moment, where positive and negative values indicate knee adduction and abduction moments, respectively.

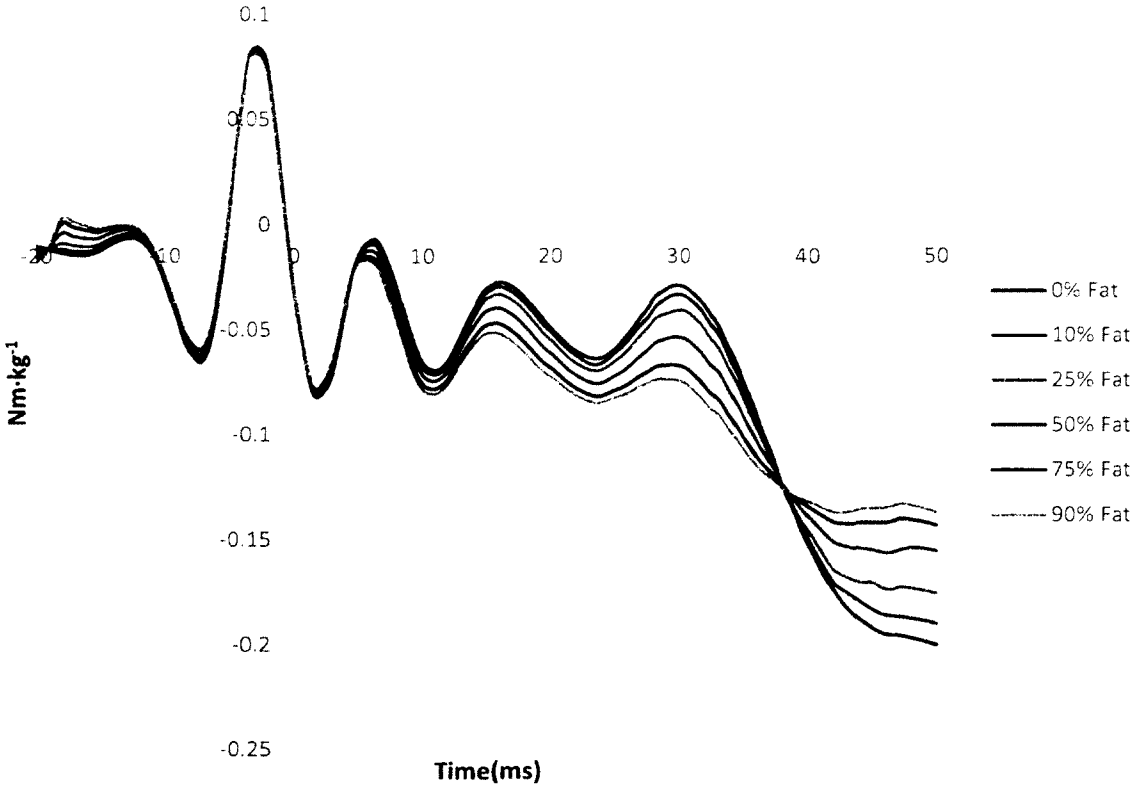

Figure G-6: Knee transverse plane moment, where positive and negative values indicate knee internal and external rotation moments, respectively.

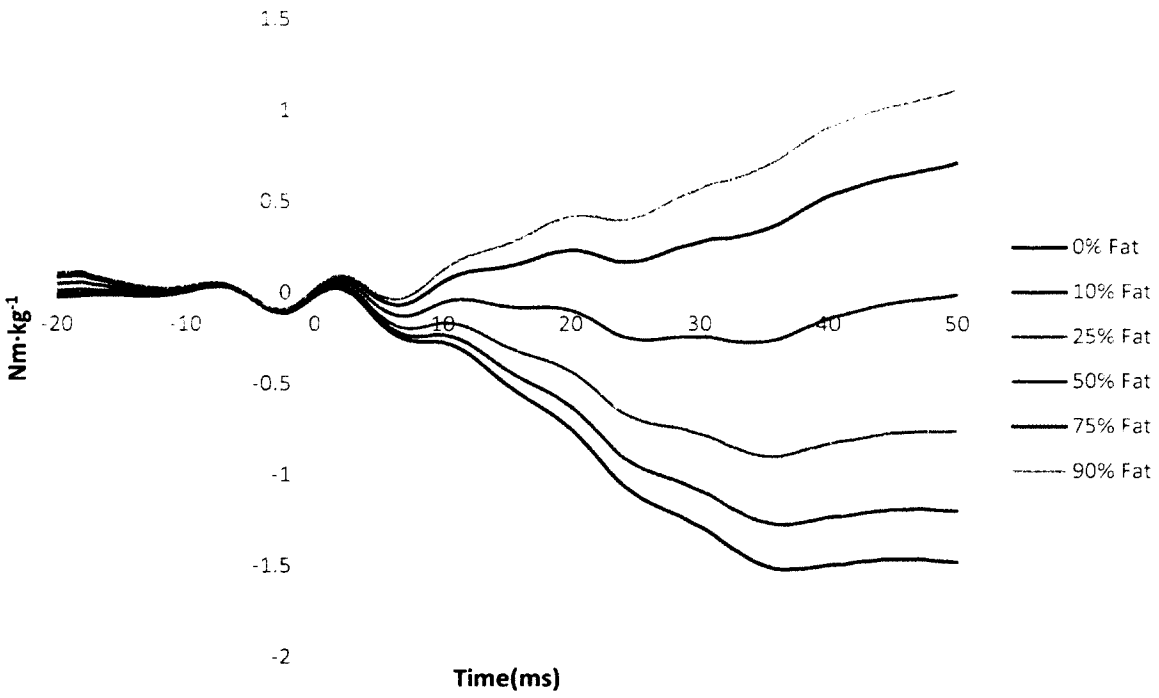

Figure G-7: Ankle sagittal plane moment, where positive and negative values indicate ankle dorsiflexion and plantarflexion moments, respectively.

Appendix H: Xia Fatigue Model Predicted Joint Kinematics at Various Levels of Hamstrings Fatigue

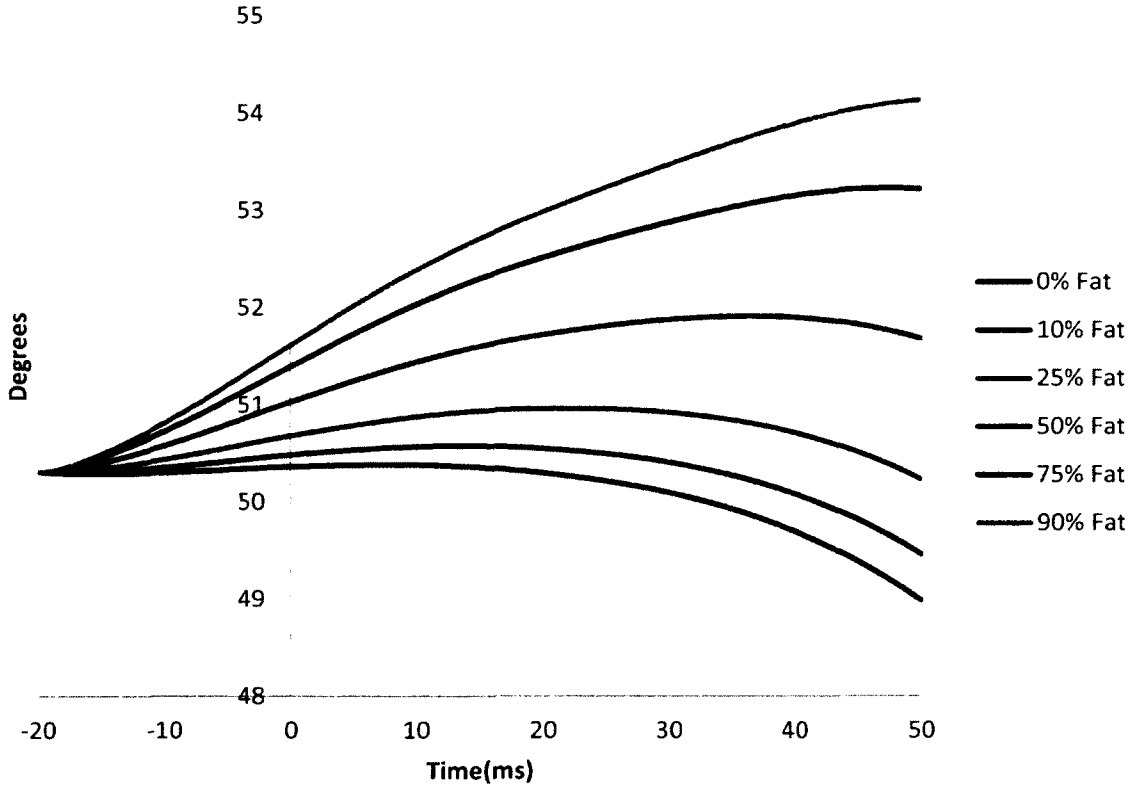

Figure H-1: Hip sagittal plane rotation, where positive and negative values indicate hip flexion and extension, respectively.

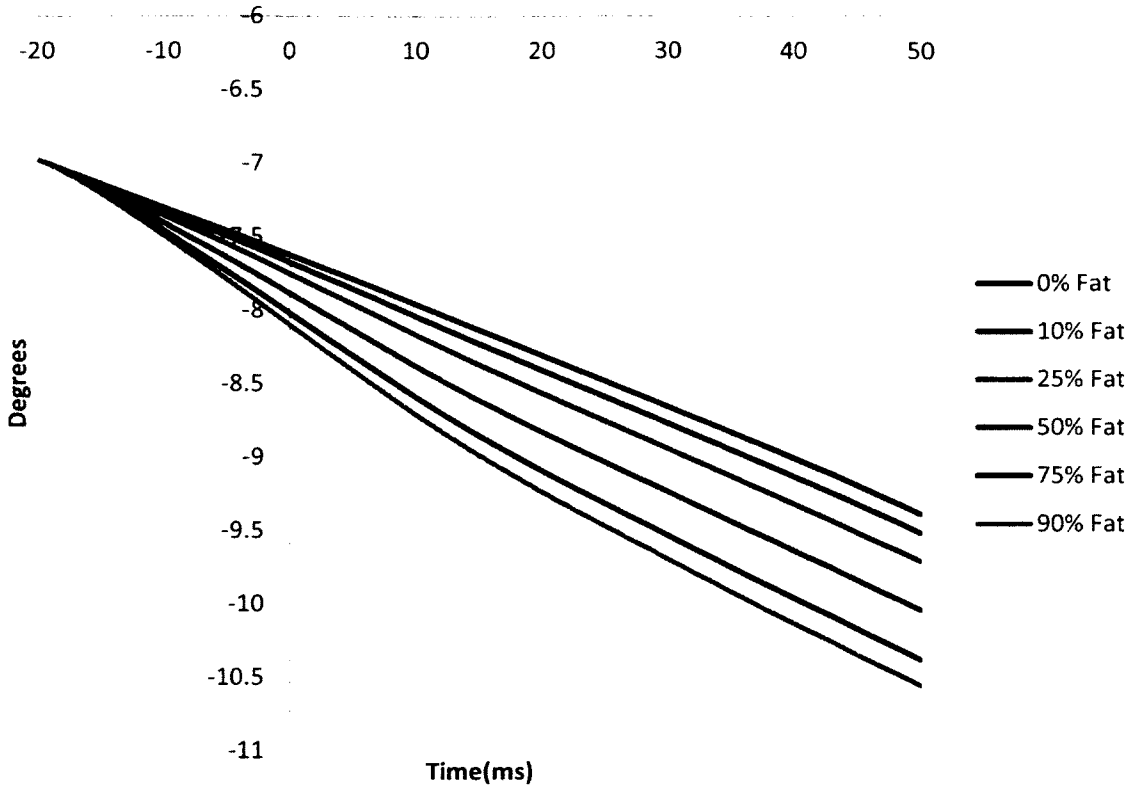

Figure H-2: Hip frontal plane rotation, where positive and negative values indicate hip adduction and abduction, respectively.

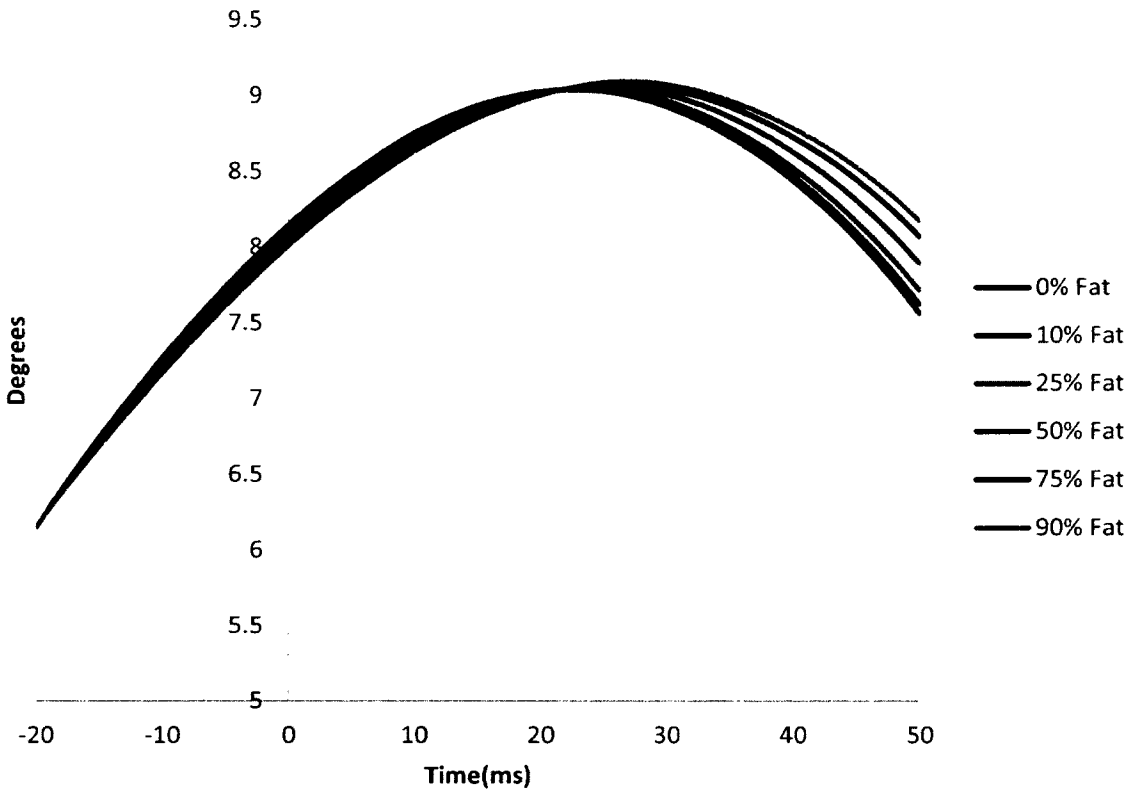

Figure H-3: Hip transverse plane rotation, where positive and negative values indicate hip internal and external rotation, respectively.

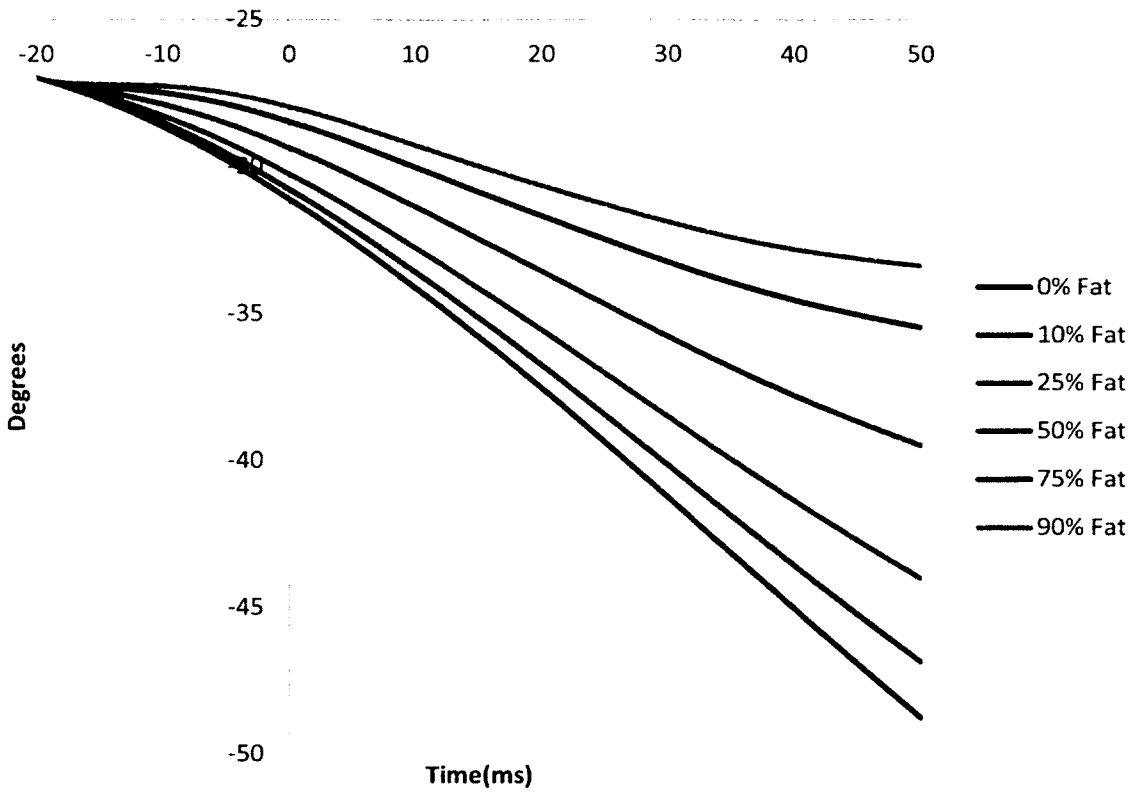

Figure H-4: Knee sagittal plane rotation, where positive and negative values indicate knee extension and flexion, respectively.

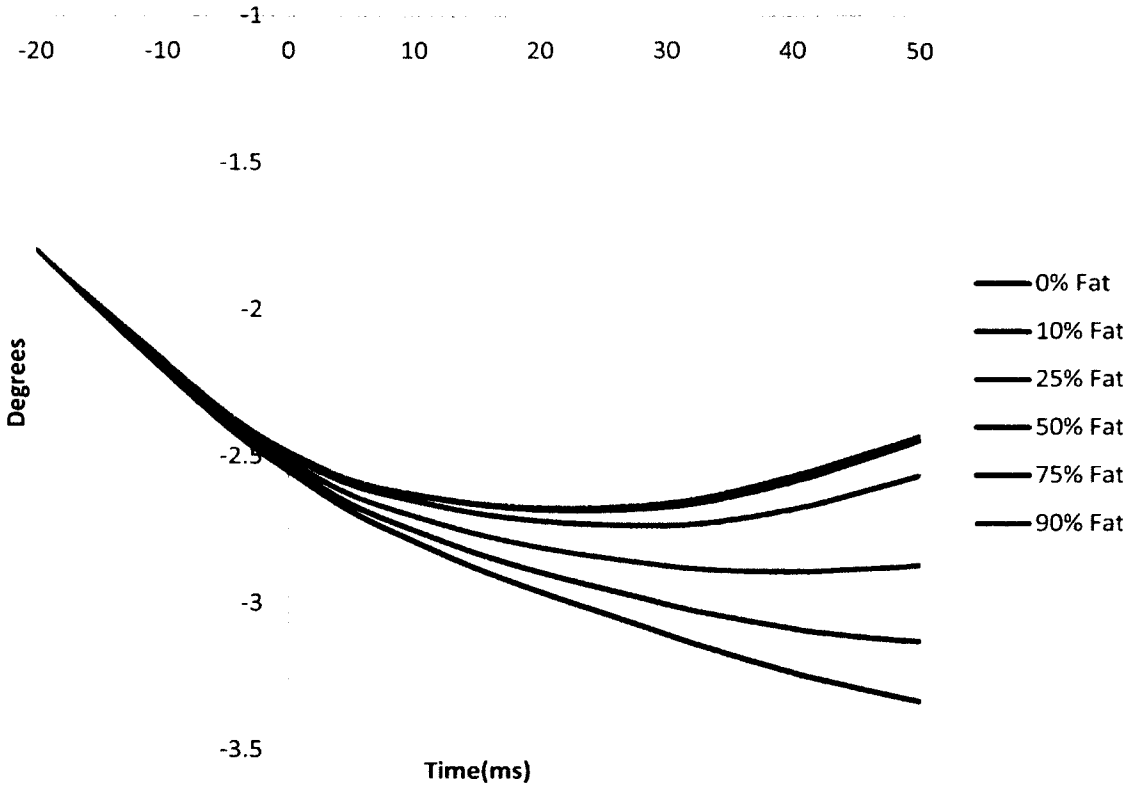

Figure H-5: Knee frontal plane rotation, where positive and negative values indicate knee adduction and abduction, respectively.

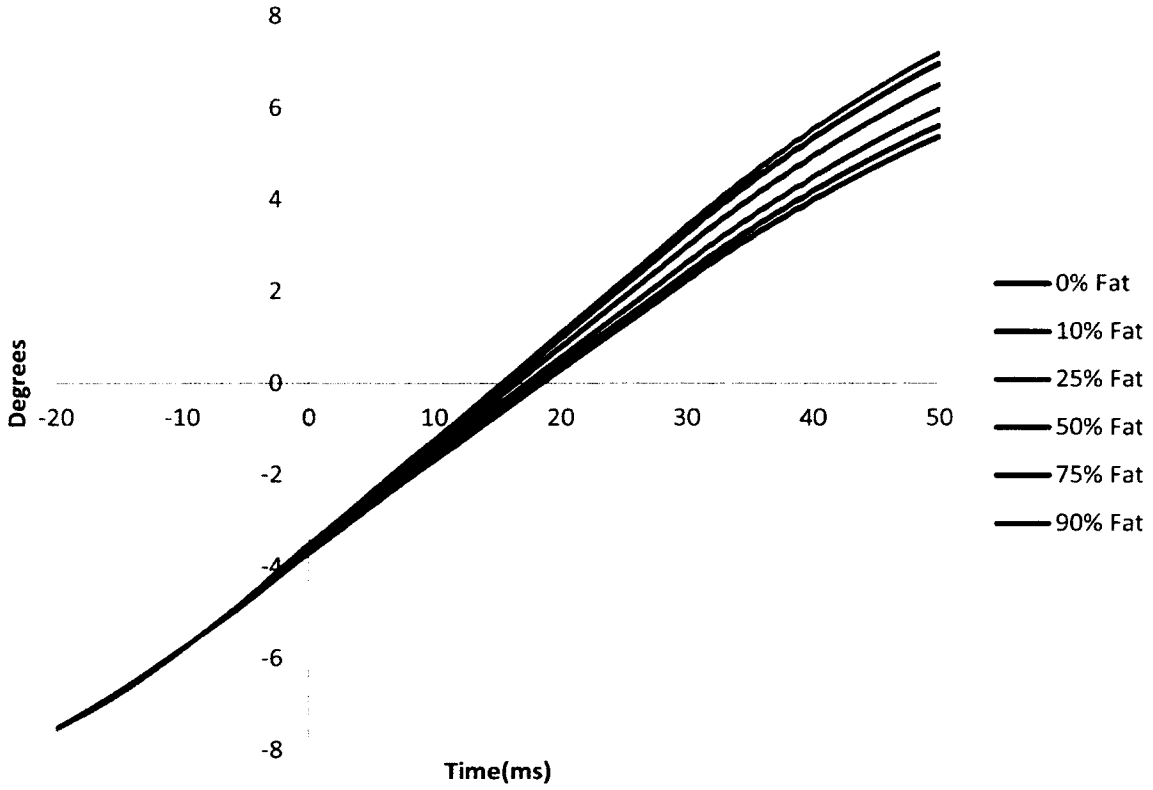

Figure H-6: Knee transverse plane rotation, where positive and negative values indicate knee internal and external rotation, respectively.

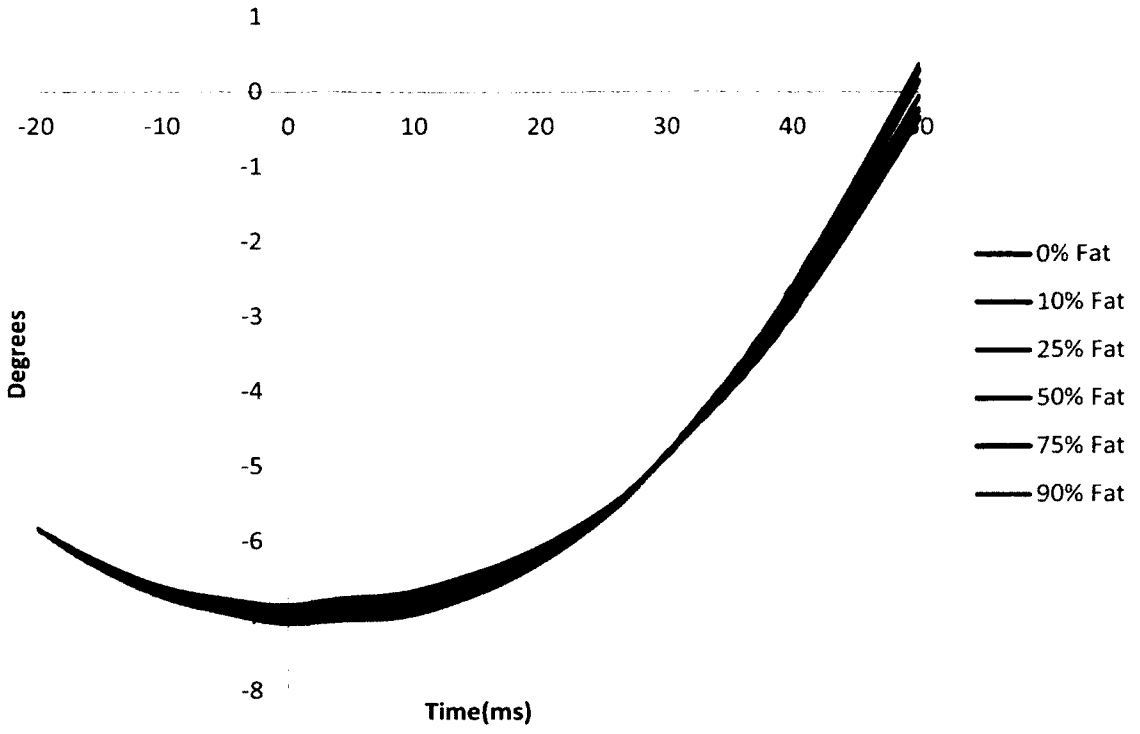

Figure H-7: Ankle sagittal plane rotation, where positive and negative values indicate ankle dorsiflexion and plantarflexion, respectively.

Appendix I: Upper Extremity Marker Plates

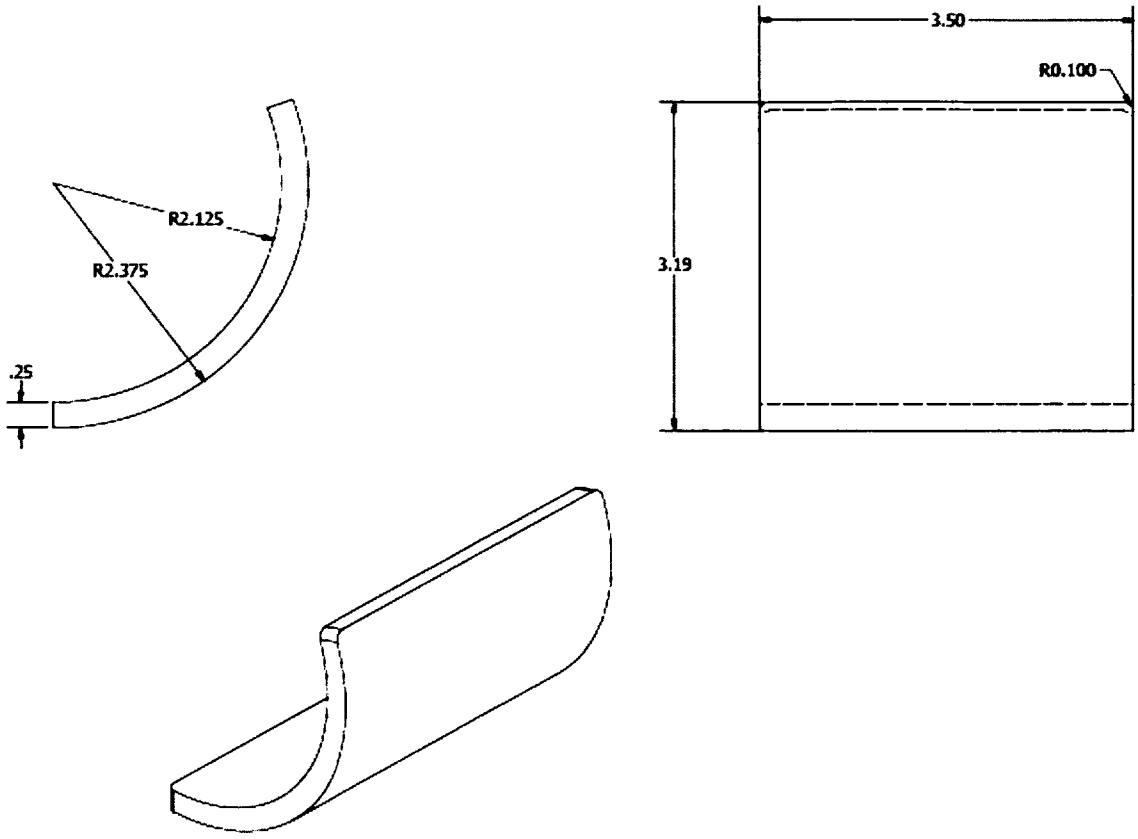

Figure I-1: Custom designed rigid marker plates for the humerus, where the listed dimensions are in inches.

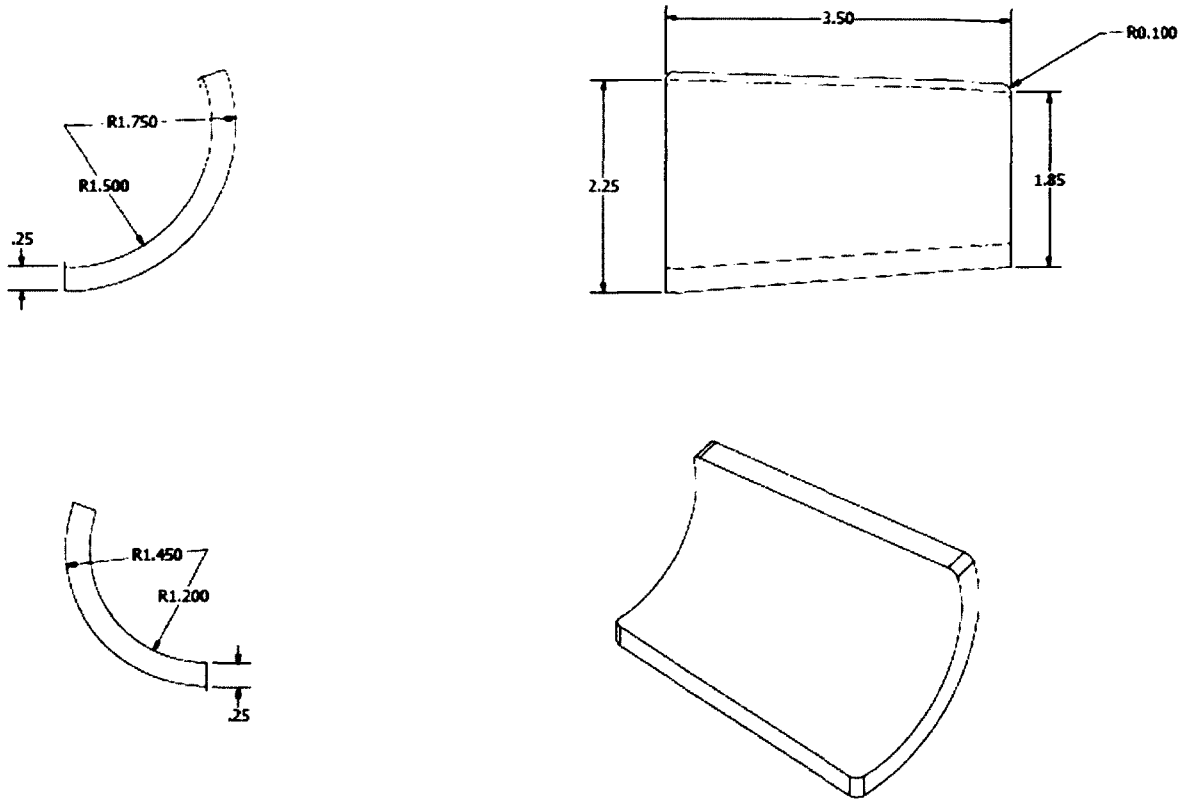

Figure I-2: Custom designed rigid marker plates for the forearm, where the listed dimensions are in inches.

Appendix J: Musculoskeletal Modeling Workflow

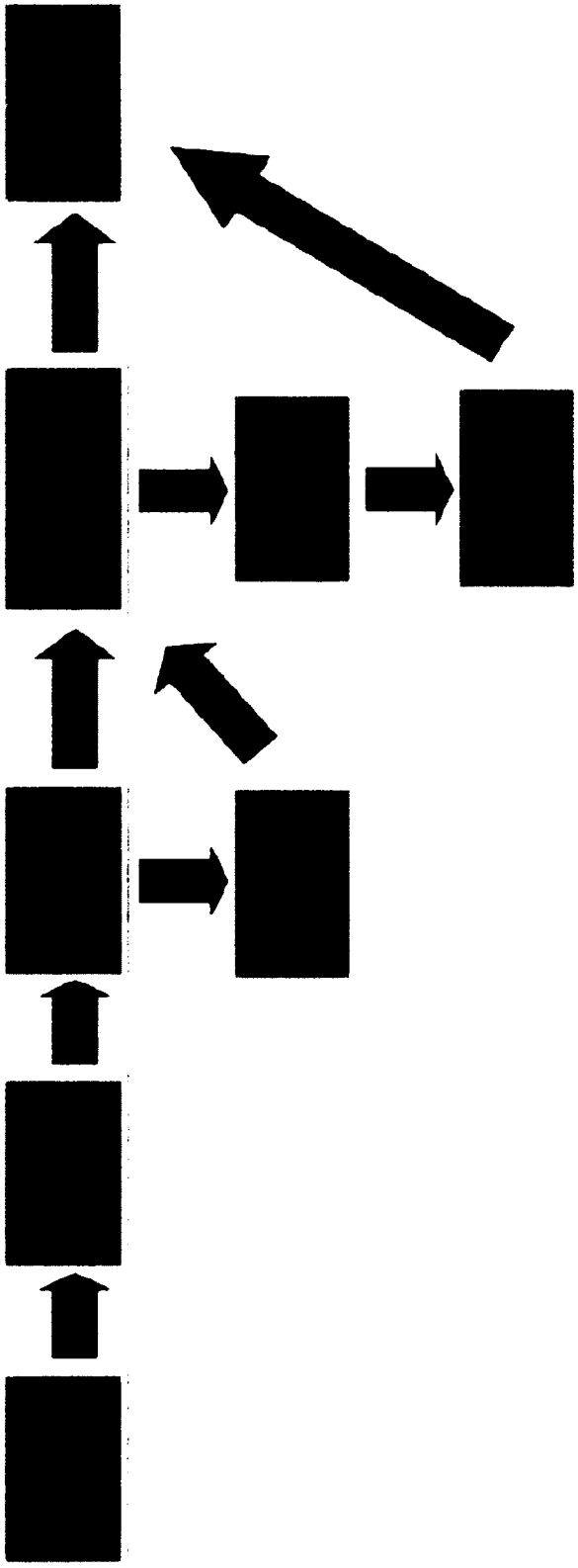

Figure J-1: Workflow used to produce musculoskeletal models

Appendix K: ACL Loading of Each Participant

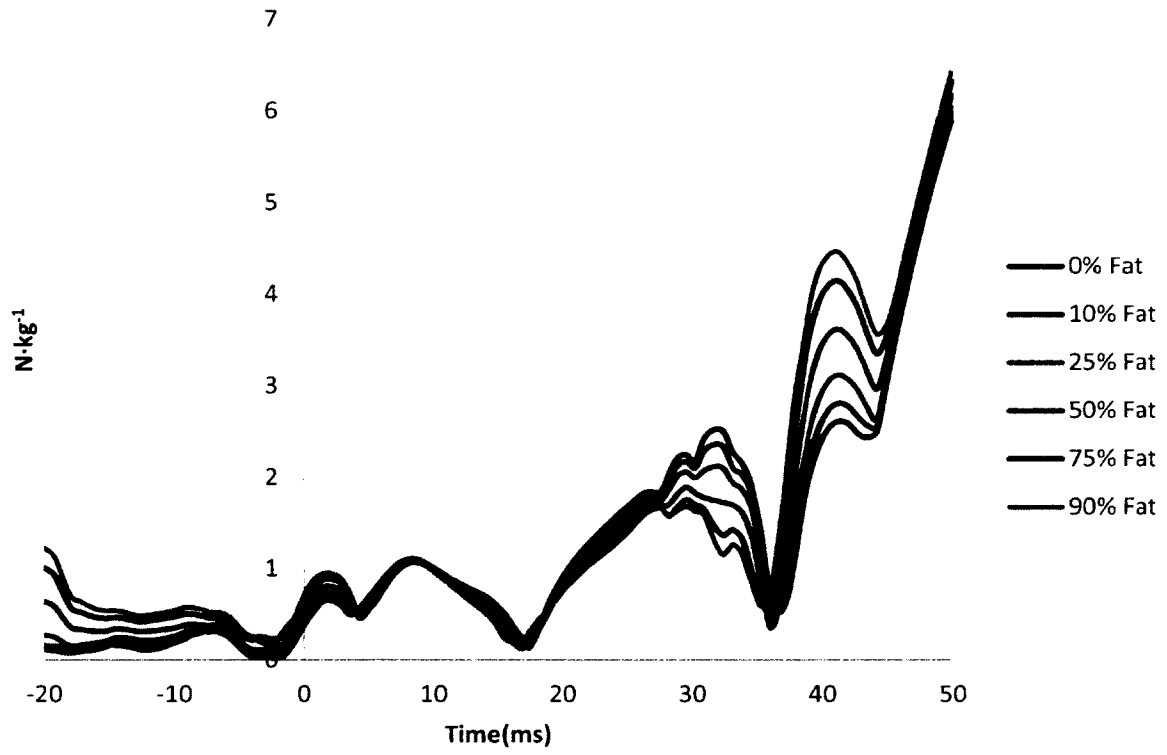

Figure K-1: Total ACL loading for participant one

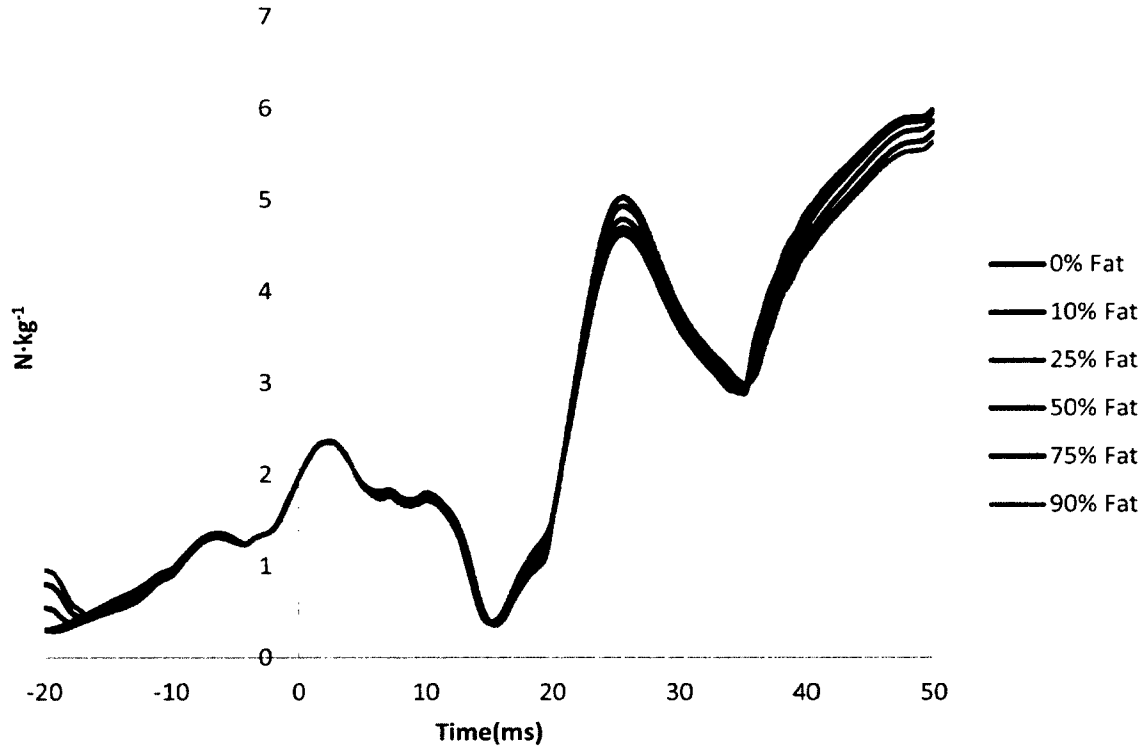

Figure K-2: Total ACL loading for participant two

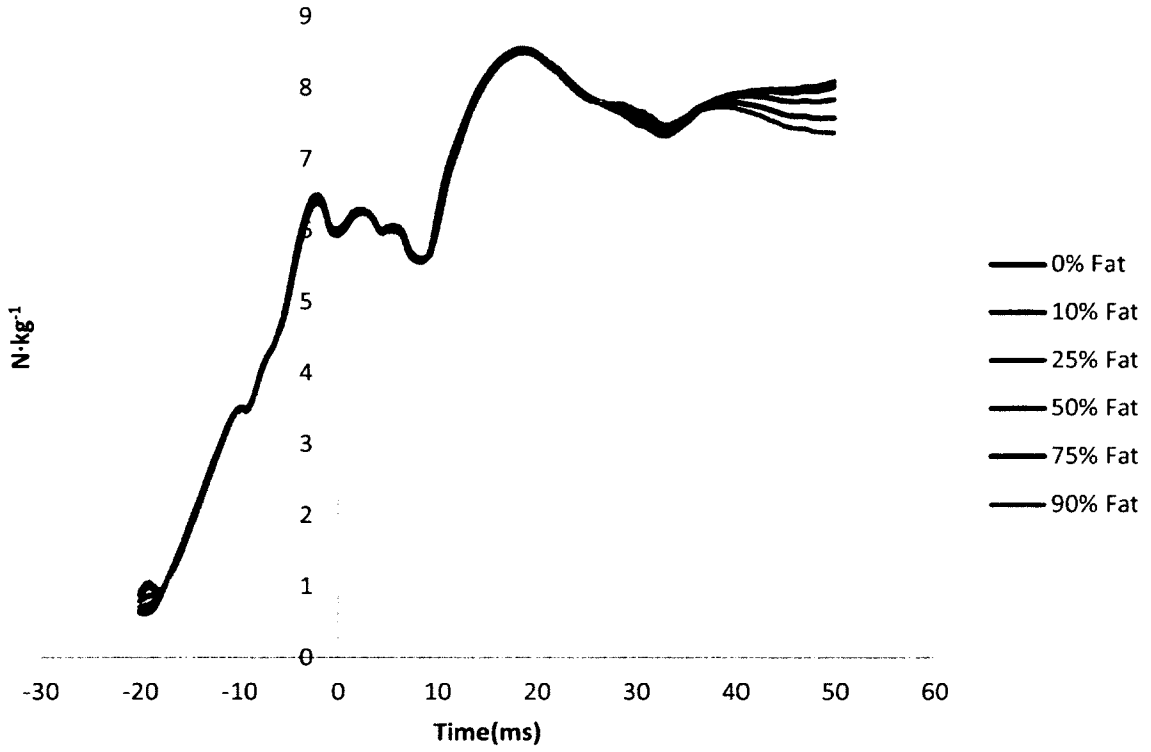

Figure K-3: Total ACL loading for participant three

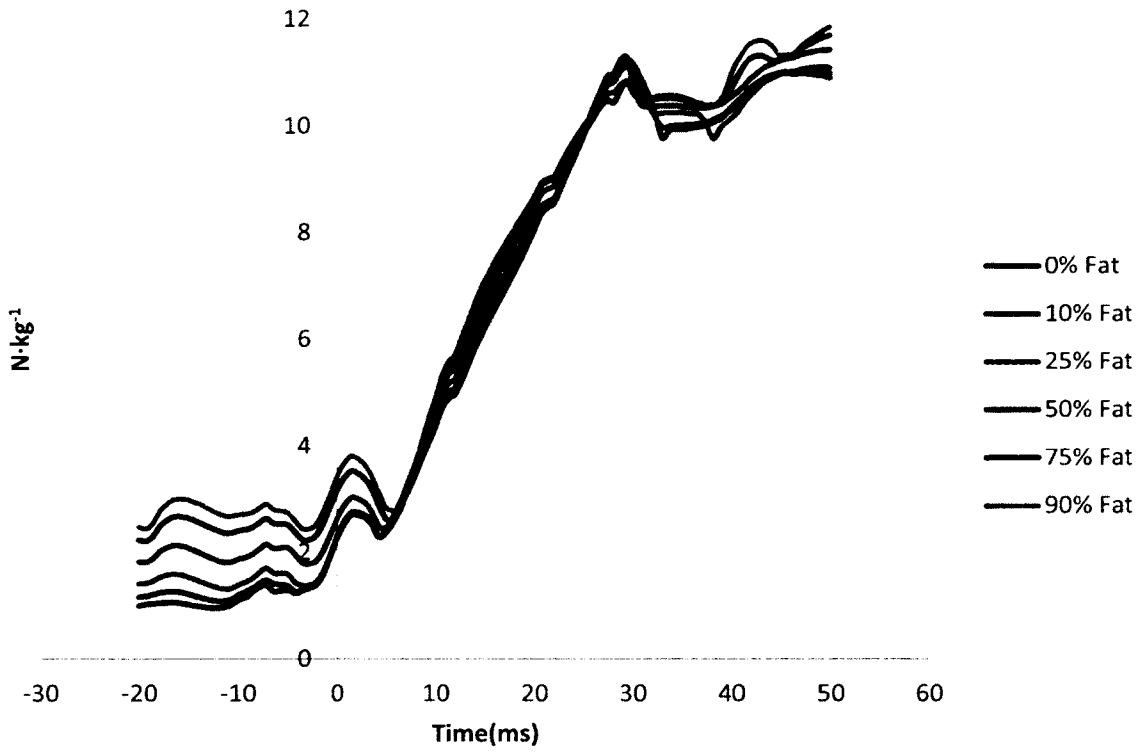

Figure K-4: Total ACL loading for participant four

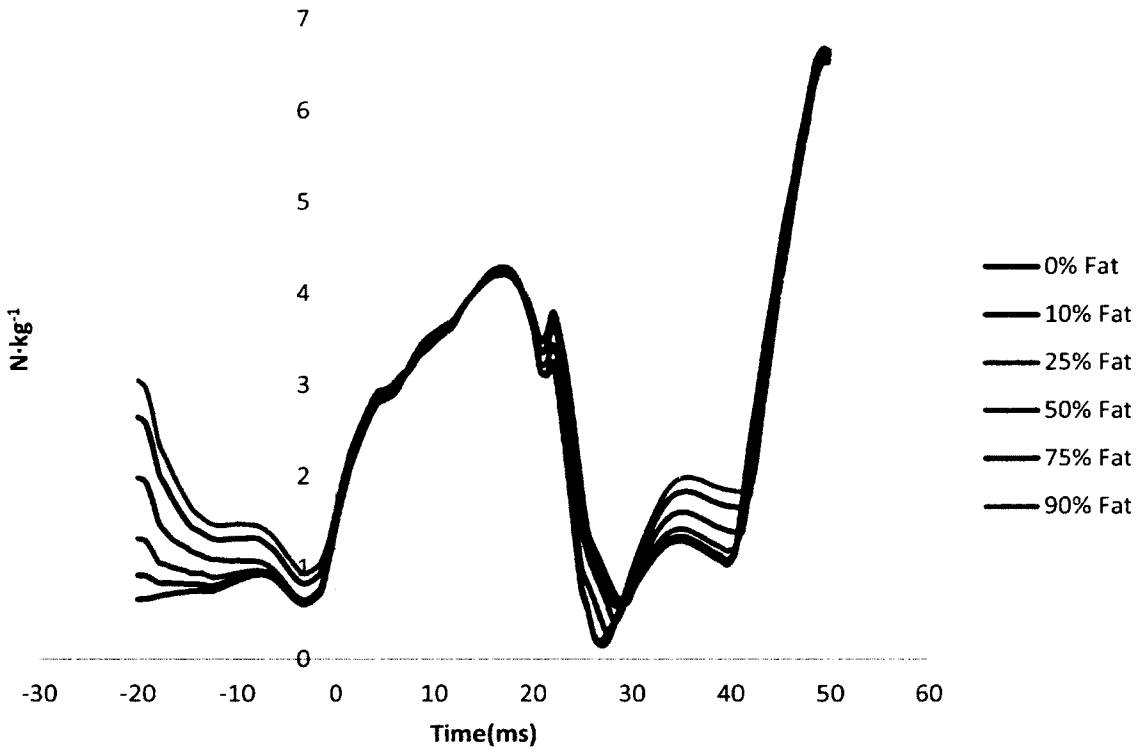

Figure K-5: Total ACL loading for participant five

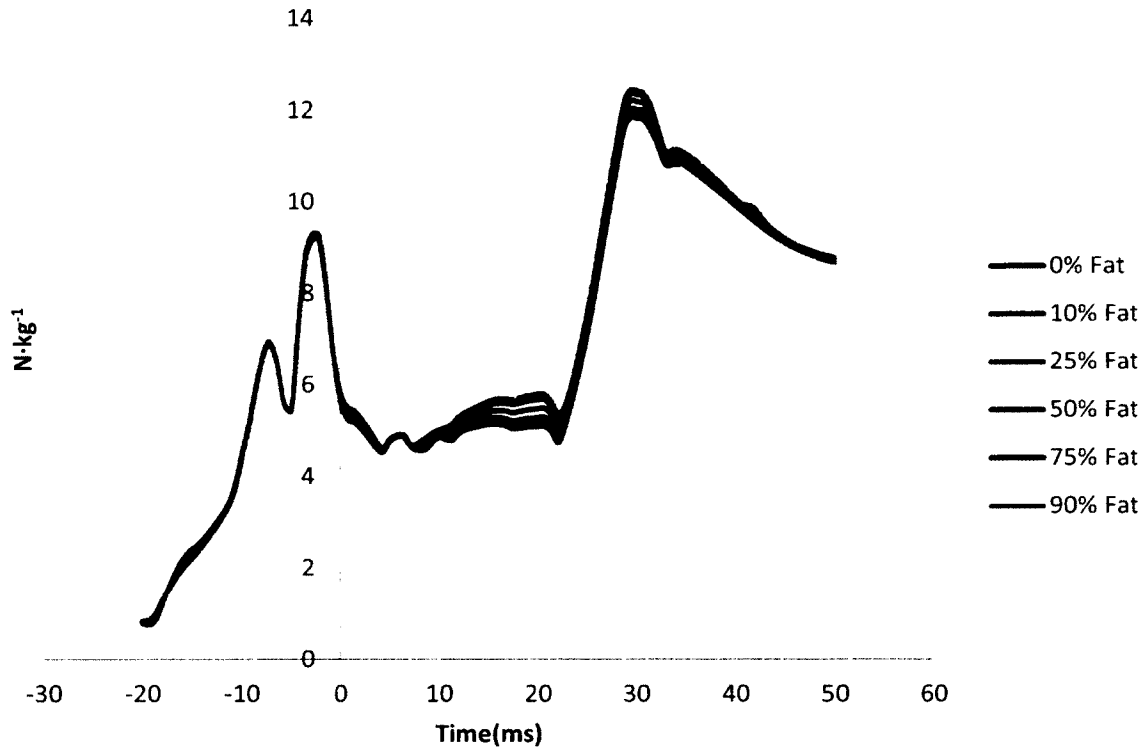

Figure K-6: Total ACL loading for participant six

Appendix L: Informed Consent Document

INFORMED CONSENT DOCUMENT

OLD DOMINION UNIVERSITY

PROJECT TITLE: The effects of isolated hamstrings fatigue on the lower extremity

INTRODUCTION
The purposes of this form are to give you information that may affect your decision whether to say YES or NO to participation in this research, and to record the consent of those who say YES. This study will take place in the Motion Analysis Laboratory at Old Dominion University in the Student Recreation Center in room 1007.

RESEARCHERS

Responsible Principal Investigator:
Stacie I. Ringleb, PhD, Dept. of Mechanical and Aerospace Engineering, Frank Batten College of Engineering

Investigators:
Michael Samaan, MS and Sebastian Bawab, PhD, Department of Mechanical and Aerospace Engineering
Joshua Weinhandl, PhD, Department of Human Movement Sciences
Matthew Hoch, PhD, School of Physical Therapy and Athletic Training

DESCRIPTION OF RESEARCH STUDY
Several studies have been conducted looking into the effects of neuromuscular fatigue on the knee joint. There are various explanations as to the differences in the motion of the knee caused by fatigue but no conclusions have been made.

If you decide to participate, then you will join a study involving research of the motion of the knee and how fatigue affects the motion of the joint. If you say YES, then you will be asked to participate in 3 separate sessions each lasting approximately 2 hours at the Neuromechanics Laboratory in the Student Recreation Center (room 1007). Approximately 40 subjects will be participating in this study.

The first testing session will occur in the Neuromechanics Laboratory. During the first session, you will undergo a protocol that will fatigue your hamstring muscles. Prior to engaging in the fatigue protocol, you will be allowed a 10-minute warm-up on the stationary bike followed by self-directed stretching. After the fatigue protocol is completed, you will be asked to produce a maximal voluntary contraction at the following time points: 0 minutes (immediately after fatigue), 2 minutes, 5 minutes, 10 minutes, 15 minutes and 20 minutes. After explanation of the sidestep cutting task, you will also be allowed to practice the sidestep cutting task using your right leg, until you are comfortable with the maneuver. The sidestep cutting task will consist of a running approach, step with one foot on the force plate and cut to the opposite side of the foot touching the force plate.

You will report to the Neuromechanics Laboratory for the second testing session. You will be asked to be perform 5 anticipated sidestep cuts using the right leg. Prior to testing, you will be allowed a 10-minute warm-up on the stationary bike followed by self-directed stretching. Next, reflective balls will be attached to both of your legs to measure the motion of your bones and sensors will be placed over some of your leg muscles to record their activity. After explanation of the sidestep cut, you will have another opportunity to practice the sidestep cut until you feel comfortable with the maneuver. Next, you will undergo the same fatigue protocol, as was completed in the first testing session, in order to fatigue your hamstring muscles. Upon completion of the fatigue task, you will be asked to perform an additional 5 anticipated sidestep cuts using the right leg.

The third testing session will take place in the Neuromechanics Laboratory at least 48 hours after and at the same time as the second testing session. You will be asked perform maximal voluntary contractions at the hip, knee and ankle joints in order to determine lower limb strength values. You will be asked to complete 3 sets of 3 repetitions for each strength test for a total of 24 sets.

EXCLUSIONARY CRITERIA
You will not be eligible to participate if you have had any lower extremity injuries in the past 6 months. To the best of your knowledge, you should not have any other lower limb injuries that would keep you from participating in this study.

RISKS AND BENEFITS
RISKS: If you decide to participate in this study, then you may face a risk of temporary skin irritation due to the tape and glue that is used to affix the markers and electrodes to the body. The potential risks to the subjects in this study include muscle pain and muscle soreness from the cutting task and fatigue protocol. There is also a risk of ankle sprains and

knee injury during the cutting task, which is similar to the risk you would experience if playing a soccer game. Muscle pain and muscle soreness can be compared as the same sensation you might have after workout.

Also, all personal information provided for the study will be kept confidential. The researcher tried to reduce these risks by removing all linking identifiers. And, as with any research, there is some possibility that you may be subject to risks that have not yet been identified.

BENEFITS. There are no main benefits to you for participating in this study. Your benefit to others, for participating in this study, will allow the researchers to understand the effects of hamstrings fatigue on the motion of the knee. This knowledge will be used to better understand the causes of non-contact ACL injury.

COSTS AND PAYMENTS
You will be placed in a drawing for a $50 gift card for participating in this study.

NEW INFORMATION
If the researchers find new information during this study that would reasonably change your decision about participating, then they will give it to you.

CONFIDENTIALITY
The researchers will take reasonable steps to keep private information, such as questionnaires, medical history, and laboratory findings, confidential. If applicable, the researchers will remove identifiers from the information prior to its processing. The results of this study may be used in reports, presentations, and publications, but the researcher will not identify you. Of course, your records may be subpoenaed by court order or inspected by government bodies with oversight authority.

WITHDRAWAL PRIVILEGE
It is OK for you to say NO. Even if you say YES now, you are free to say NO later, and walk away or withdraw from the study -- at any time. Your decision will not affect your relationship with Old Dominion University, or otherwise cause a loss of benefits to which you might otherwise be entitled.

COMPENSATION FOR ILLNESS AND INJURY
If you say YES, then your consent in this document does not waive any of your legal rights. However, in the event of harm or injury arising from this study, neither Old Dominion University nor the researchers are able to give you any money, insurance coverage, free medical care, or any other compensation for such injury. In the event that you suffer injury as a result of participation in any research project, you may contact Dr. Stacie Ringleb at 757-683-5934 or Dr. George Maihafer the current IRB chair at 757-683-4520 at Old Dominion University, who will be glad to review the matter with you.

VOLUNTARY CONSENT
By signing this form, you are saying several things. You are saying that you have read this form or have had it read to you, that you are satisfied that you understand this form, the research study, and its risks and benefits. The researchers should have answered any questions you may have had about the research. If you have any questions later on, then the researchers should be able to answer them.

Dr. Stacie Ringleb 757-683-5934

If at any time you feel pressured to participate, or if you have any questions about your rights or this form, then you should call Dr. George Maihafer, the current IRB chair, at 757-683-4520, or the Old Dominion University Office of Research, at 757-683-3460.

And importantly, by signing below, you are telling the researcher YES, that you agree to participate in this study. The researcher should give you a copy of this form for your records.

Subject's Printed Name & Signature	Date

INVESTIGATOR'S STATEMENT
I certify that I have explained to this subject the nature and purpose of this research, including benefits, risks, costs, and any experimental procedures. I have described the rights and protections afforded to human subjects and have done nothing to pressure, coerce, or falsely entice this subject into participating. I am aware of my obligations under state and federal laws, and promise compliance. I have answered the subject's questions and have encouraged him/her to ask additional questions at any time during the course of this study. I have witnessed the above signature(s) on this consent form.

Investigator's Printed Name & Signature	Date

VITA

Education

M.S. University of Texas at San Antonio — December 2009
Biomedical Engineering

B.S. Rutgers University — May 2008
Biomedical Engineering

Professional Experience

Instructor, Exploring Engineering Technology (ENGN 110) — 2013 – 2014

Graduate Teaching Assistant, Project Management II (MAE 435) — 2012 – 2014

Instructor, Solid Mechanics Laboratory (MAE 225) — 2010 – 2014

Graduate Teaching Assistant, Solid Mechanics (MAE 220) — 2010 – 2011

Honors and Awards

Batten College Faculty Award in Mechanical Engineering — 2014

Opensim Workshop Travel Award ($2000) — 2013

Tiwari Endowed Graduate Scholarship, Old Dominion University ($4,000) — 2013

Graduate Student Travel Award, Old Dominion University ($500) — 2010

Research

Articles – Published

Choisne, J., Ringleb, S.I., **Samaan, M.A.**, *et al.* (2012) "Influence of Kinematic Analysis Methods on Detecting Ankle and Subtalar Joint Instability." Journal of Biomechanics **45**(1): 46-52.

Articles – In Review

Samaan, M.A., Hoch, M.C., Ringleb, S.I., *et al.* "Isolated Hamstrings Fatigue Alters Joint Coordination During a Cutting Maneuver". Journal of Applied Biomechanics.

Samaan, M.A., Greska, E.K., Hoch, M.C., *et al.* "Dynamic Postural Control Two Years Following Anterior Cruciate Ligament Reconstruction in a Female Collegiate Soccer Player". International Journal of Athletic Therapy & Training